GEORGIA INSTITUTE OF TECHNOLOGY
Engineering Experiment Station

PROJECT INITIATION

Date: July 15, 1968

Project Title: Study for Improved Microwave Cavities for Polymer and Biological ESR Measurements

Project No.: A-1107-001

Project Director: R. G. Checkelford

Sponsor: National Aeronautics and Space Administration

Effective . . . . June 21, 1968 . . . . . Estimated to run until: . . June 20, 1969 . . . . . .

Type Agreement: . . . NAS2-5016 . . . . . Amount: $. 21,423* . . . . . .

Reports: Quarterly Report
Final Report

Contact Person: Mr. H. Matthews
Contract Administrator
NASA
Ames Research Center
Moffett Field, California 94035
(for administrative matters)

Dr. Ronald Reinisch
same address as Mr. Matthews
(for technical matters)

*Contract provides $23,493 which is allocated in the following manner:

Electronics	$21,423
Nuclear Sciences	2,070

Assigned to . . Electronics . . . . . Division

COPIES TO:

- ☐ Project Director
- ☐ Director
- ☐ Associate Director
- ☐ Assistant Director(s)
- ☐ Division Chiefs
- ☐ Branch Head
- ☐ General Office Services
- ☐ Engineering Design Services
- ☐ Photographic Laboratory
- ☐ Research Security Officer
- ☐ Accounting
- ☐ Purchasing
- ☐ Report Section
- ☑ Library
- ☐ Rich Electronic Computer Center
- ☐ _____

GEORGIA INSTITUTE OF TECHNOLOGY
Engineering Experiment Station

PROJECT INITIATION

Date: July 15, 1968

Project Title: Study for Improved Microwave Cavities for Polymer and Biological ESR Measurement

Project No.: A-1107-002

Project Director: Dr. John J. Heise

Sponsor: National Aeronautics and Space Administration

Effective . . . June 21, 1968 . . . . . Estimated to run until: . . . June 20, 1969 . . . . . .

Type Agreement: . NAS2-5016 . . . . . Amount: $ 2,070* . . . . . .

Reports: Quarterly Report
Final Report

Contact Person: Mr. H. Matthews
Contract Administrator
NASA
Ames Research Center
Moffett Field, California 94035
(for administrative matters)

Dr. Ronald Reinisch
same address as Mr. Matthews
(for technical matters)

*Contract provides $23,493 which is allocated in the following manner:

Electronics	$21,423
Nuclear Sciences	2,070

Assigned to . . . . Nuclear Sciences . . . . . Division

COPIES TO:

- ☐ Project Director
- ☐ Director
- ☐ Associate Director
- ☐ Assistant Director(s)
- ☐ Division Chiefs
- ☐ Branch Head
- ☐ General Office Services
- ☐ Engineering Design Services
- ☐ Photographic Laboratory
- ☐ Research Security Officer
- ☐ Accounting
- ☐ Purchasing
- ☐ Report Section
- ☒ Library
- ☐ Rich Electronic Computer Center
- ☐

RA-62(12-66)

GEORGIA INSTITUTE OF TECHNOLOGY
Engineering Experiment Station

PROJECT TERMINATION

Date January 14, 1970

PROJECT TITLE: Study for Improved Microwave Cavities for Polymer & Biological ESR Measurements

PROJECT NO: A-1107-001 & 002

PROJECT DIRECTOR: Mr. R. C. Shackelford & Dr. John J. Heise

SPONSOR: NASA - Ames Research Center

TERMINATION EFFECTIVE: December 15, 1969

CHARGES SHOULD CLEAR ACCOUNTING BY: December 31, 1969*

*Except possibly some charges connected with Magnet rental.

Contract Closeout Items Remaining: Final Contract Modification (tie up loose ends)
Final Invoice & Closing Documents
Final Report of Inventions
Gov't. Property Inventory & Cert. of Proper Usage .... Gov't. Prop.

Electronics Division (Special Techniques)

COPIES TO:

Project Directors (2)
Director
Associate Director
Assistant Directors
Division Chief
Branch Head
Accounting
Engineering Design Services
General Office Services
Photographic Laboratory
Purchasing
Report Section
Library
Security
Rich Electronic Computer Center

Form EES 402 (R10-62)

GEORGIA INSTITUTE OF TECHNOLOGY
EXPERIMENT STATION

225 North Avenue, Northwest · Atlanta, Georgia 30332

2 October 1968

Dr. R. F. Reinisch
N-240-1
NASA/Ames Research Center
Moffet Field, California 94035

Title: Study for Improved Microwave Cavities for Polymer and Biological ESR Measurements

Subject: Quarterly Progress Report on Contract No. NAS2-5016 for the Period 21 June 1968 through 20 September 1968

Dear Sir:

This letter reports progress of research on the subject contract during the period 21 June 1968 through 20 September 1968. The first quarter's research has been concentrated on the calculation of design curves for the fabrication of a dielectric ESR cavity at the frequency of 9.5 GHz. The candidate materials considered were Sapphire, Spectrosil--a high purity synthetic fused quartz, and Lucalox--a polycrystalline alumina which is closely related to Sapphire. The initial dielectric cavity will be fabricated from Spectrosil because of its avilability, high purity, and low cost. If favorable results are obtained in the measurement of loaded Q and ESR lines of aqueous samples, a second cavity will be constructed of either Sapphire or Lucalox which will provide about a factor of three increase in loaded Q.

The configuration of the dielectric cavity is shown in Figure 1. It consists of a dielectric tube capped with two metal end plates. Microwave energy is coupled to the resonant structure through a circular iris located over the wall of the dielectric tube in the end plate. For ESR studies, the sample may be placed in the bore of the tube or just adjacent to the outside surface thereby providing a high degree of flexibility on sample shape and volume which can be accommodated. Such cavities constructed of various low loss dielectrics commonly exhibit loaded Q's as high as 5000.

The characteristic equation relating the velocity of propagation (V_p), the relative dielectric constant (ε_r) and the resonant frequency (ν) for a given mode can be derived from the electromagnetic boundary problem. The cavity will support a number of modes which are designated by the three subscripts, l, m, n, where l represents variation in an angular direction about the cavity centerline, m specified the root for which the characteristic

equation is solved, and n gives the electrical length of the cavity in terms of the number of resonant wavelengths. The characteristic equations for the two simplest modes, TE_{0mn} and TM_{0mn} are given below[1]

$$\frac{CJ_0(k_2a')I_1(k_1a') - J_1(k_2a')I_0(k_1a')}{CN_0(k_2a')I_1(k_1a') - N_1(k_2a')I_0(k_1a')} = \frac{CJ_0(k_2b')K_1(k_1b') + J_1(k_2b')K_0(k_1b')}{CN_0(k_2b')K_1(k_1b') + N_1(k_2b')K_0(k_1b')} \quad (1)$$

where $J_i(x)$ and $N_i(x)$ are the ordinary Bessel Functions of the first and second kind respectively, $I_i(x)$ and $K_i(x)$ are the modified Bessel functions, $a' = a/\lambda$, $b' = b/\lambda$, a is the inner radius of the dielectric tube, b is the outer radius of the dielectric tube, λ is the free space wavelength, $k_1 = 2\pi[(c/v_p)^2 - 1]^{\frac{1}{2}}$, $k_2 = 2\pi[\epsilon_r - (c/v_p)^2]^{\frac{1}{2}}$, for TE_{0mn} modes $C = k_2/k_1$, and for TM_{0mn} modes $C = k_2/\epsilon_r k_1$.

A computer program was written in Fortran IV to calculate appropriate solutions to Equation (1) for the TE_{01n} mode, and for $(\epsilon_r)^{-\frac{1}{2}} \leq V_p/c \leq 1$.

For a given value of ϵ_r and V_p/c, appropriate values of a' and b' were found to satisfy Equation (1). In this manner, a commercially available dielectric tubing was selected to satisfy Equation (1) for a given wavelength. There are several ways to present this data in graphical form. Figure 2 shows the variation in a/λ versus the ratio of inner to outer radius a/b for a given value of V_p/c and three values of relative dielectric constant corresponding to Spectrosil, Lucalox, and Sapphire. These data were computed for values of V_p/c ranging from 0.7 to 0.95 in steps of 0.05. Since the data showed that the appropriate solutions for the range of tubing sizes available would satisfy the design wavelength for a restricted range of V_p/c, additional calculations were made over the range $0.9 \leq V_p/c \leq 0.95$ in 0.01 steps. These calculations are shown in Figure 3. Here the presentation has been changed to show the variation of V_p/c as a function of frequency for a given ratio of a/b. Two values of a/b are shown representing the two extreme values for which

---

1. F. J. Rosebaum, Review of Scientific Instruments, Vol. 35, No. 11, 1550, (1964).

legitimate solutions are found. In this figure we have presented only the calculations for Spectrosil since considerations of availability, cost, and electrical properties made it a first choice for the initial cavity design.

Once the proper value of V_p/c has been determined for a given ratio a/b and a given design wavelength λ, the length L, of the cavity is calculated from the resonance condition

$$L = \left(\frac{n}{2}\right) \left(\frac{V_p}{c}\right) \lambda$$

The ratio of cavity length to order number, L/n, is shown in Figure 4 as a function of frequency for the two values of a/b considered in Figure 2.

From these design curves the tubing size and cavity length have been chosen for Spectrosil with $\varepsilon_r = 3.78$. For the TE_{014} mode, and a design frequency of 9.5 GHz, the cavity length L for a/b = 0.9016 is 5.792 cm and for a/b = 0.8920, L = 4.880 cm. Machining of the metal end plates has been completed, and fabrication of the cavity will be completed as soon as the dielectric tubing is received.

The research program for the next quarter will include testing of the dielectric cavity and the initial design of a Fabry Perot structure. Tests for the dielectric cavity will be concentrated on determining the effect of aqueous samples on the loaded Q at the frequency of 9.5 GHz. Various sample loading configurations will be employed to optimize the total sample volume and placement for maximum sensitivity in the detection of ESR lines. In general, one would expect an increase in sensitivity resulting from an increase in the volume of spins, and a corresponding decrease resulting from dielectric heating in the additional volume. The relative magnitude of the two effects depends on the electric and magnetic field configuration in the cavity. Since the electric field decreases to zero at the cavity centerline, it is likely that symmetric loading about the axis of the dielectric tube will be the optimum loading configuration.

Negotiations for leasing the six-inch Varian magnet are completed, and delivery of the magnet is expected during the quarter.

Respectfully submitted,

R. G. Shackelford, and

J. J. Heise
Project Directors

Approved:

A. P. Sheppard, Head
Special Techniques Branch
Electronics Division

Attachments (4)

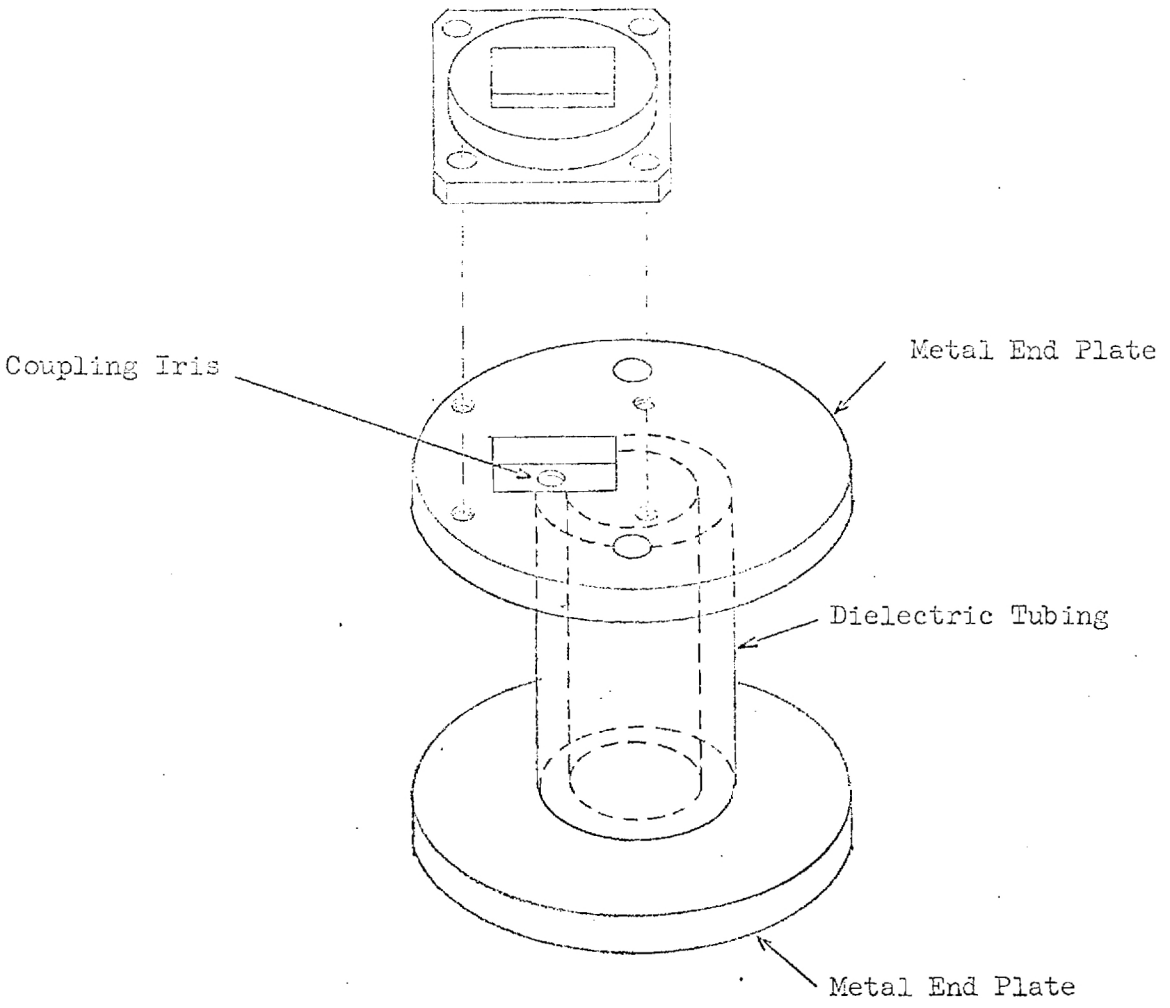

Figure 1. Dielectric Cavity

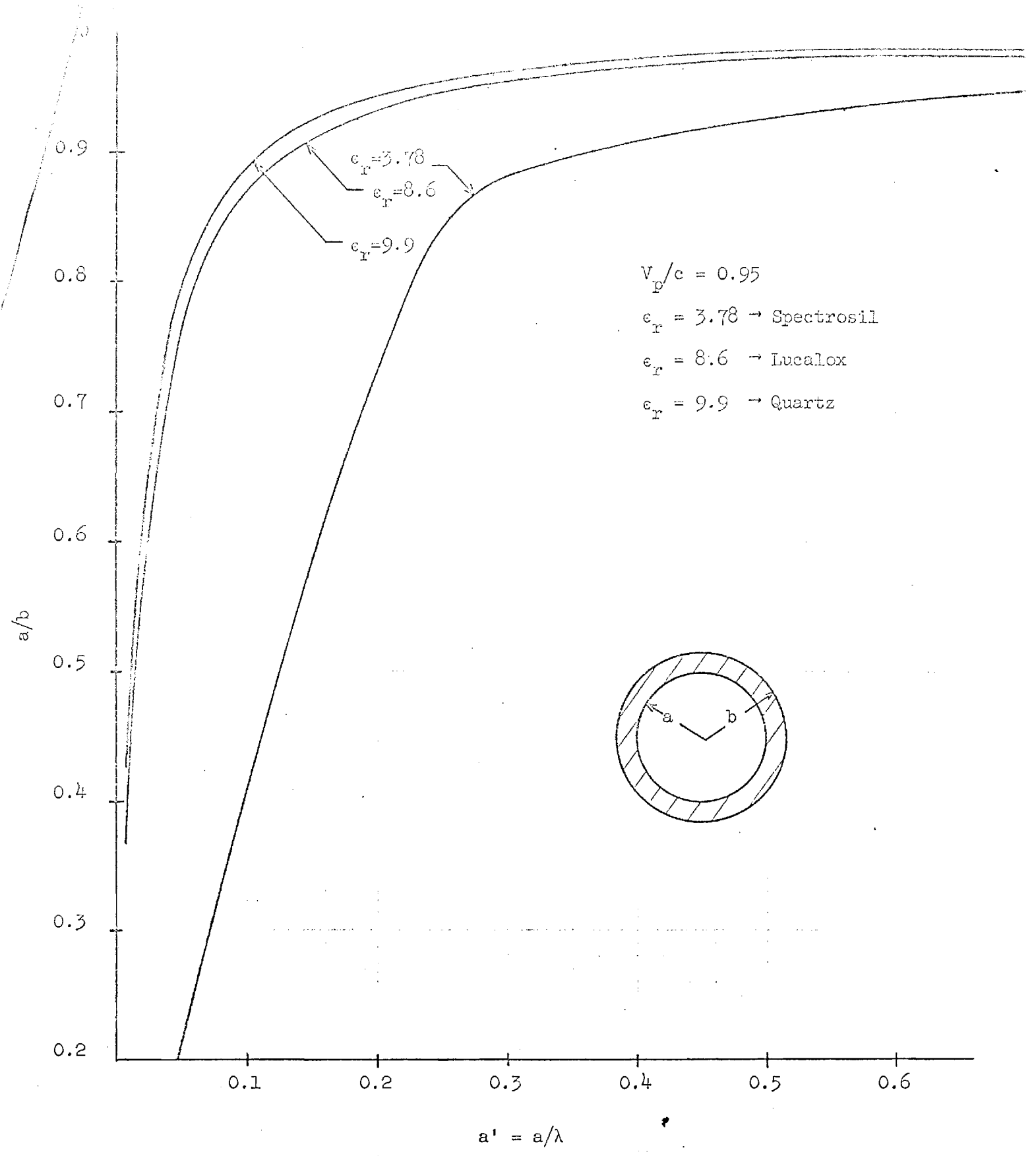

Figure 2. Solution of the Characteristic Equation for the TE_{0ln} mode for Spectrosil, Lucalox, and Quartz

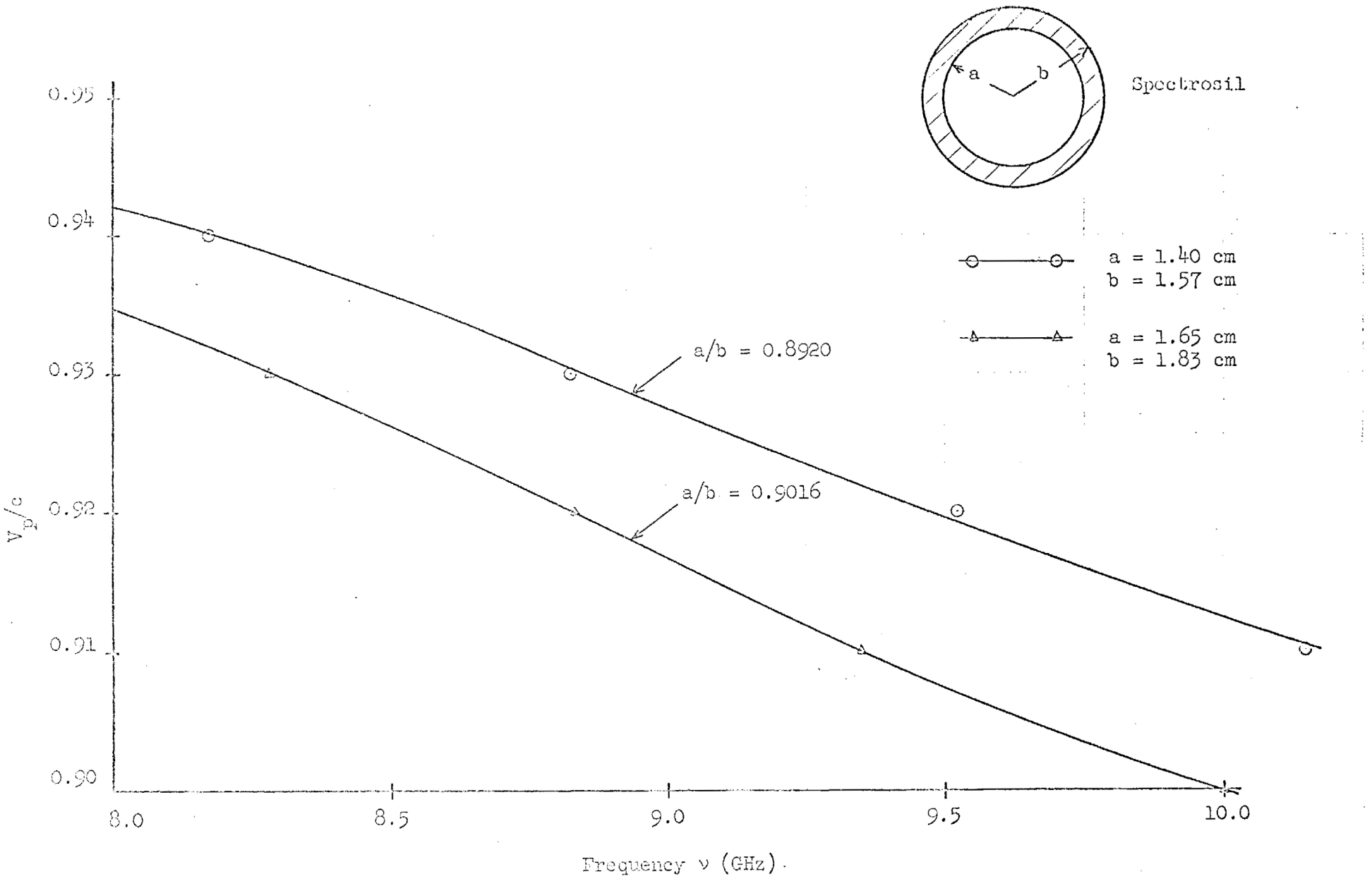

Figure 3. Relative Velocity of Propagation as a Function of Frequency for Spectrosil

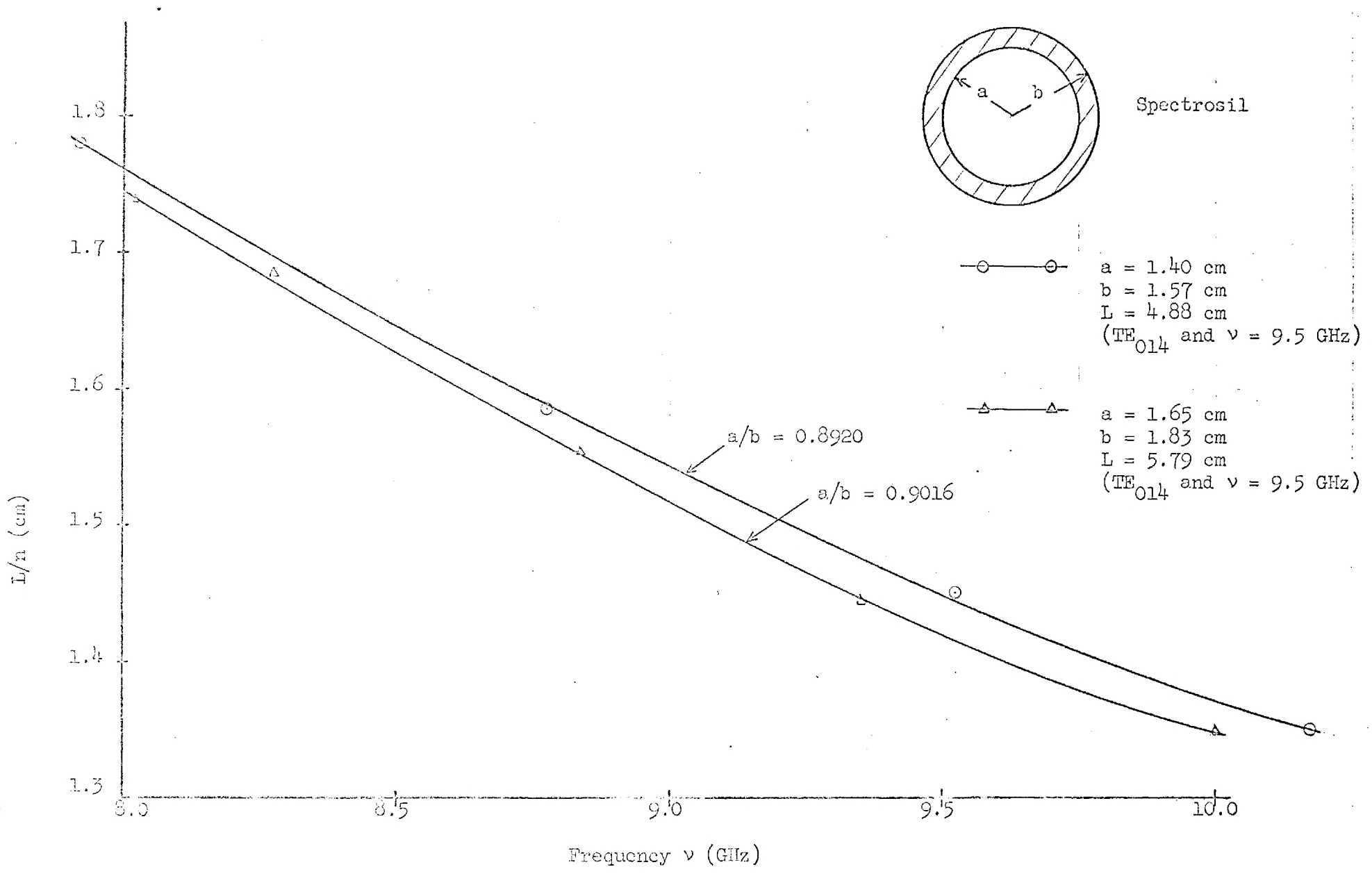

Figure 4. Ratio of Resonant Length to Order Number as a Function of Frequency for Spectrosil

GEORGIA INSTITUTE OF TECHNOLOGY
EXPERIMENT STATION 225 North Avenue, Northwest · Atlanta, Georgia 30332

31 December 1968

Dr. R. F. Reinisch
N-240-1
NASA/Ames Research Center
Moffett Field, California 94035

Title: Study for Improved Microwave Cavities for Polymer and Biological ESR Measurements

Subject: Quarterly Progress Report on Contract No. NAS2-5016 for the Period 21 September 1968 through 20 December 1968

Dear Sir:

This letter reports progress of research on the subject contract during the period 21 September 1968 through 20 December 1968. Construction of two dielectric cavities employing Spectrosil® has been completed. Preliminary measurements have been made to determine the resonant frequency and loaded Q for each cavity. The effects of aqueous sample loading were investigated by measuring the Q of the cavity with a water-filled teflon tube placed at the cavity centerline. A Fabry-Perot resonator has also been constructed and preliminary measurements made to determine its mode structure and loaded Q.

The measurement of loaded Q and coupling coefficient, β, was accomplished using two different techniques. While the two techniques are somewhat similar, one involves the calculation of Q from static measurements while the other allows a direct measurement of Q by using a signal source whose output frequency can be swept linearly across the cavity response characteristic. In the first technique, the loaded Q is calculated from measurements of the voltage standing wave ratio (VSWR) as a function of frequency about resonance. By noting the shift in position of the standing wave null from its value at resonance to its value at some frequency far removed from resonance, one can determine whether the cavity is overcoupled or undercoupled. For the undercoupled case,

$$\beta = \frac{1}{(VSWR)_0} \quad ,$$

where $(VSWR)_0$ is the voltage standing wave ratio at resonance. In the experimental procedure, (VSWR) is measured as a function of frequency and the loaded Q is calculated by determining the two frequencies f_1 and f_2 corresponding to the half power (VSWR) which for the undercoupled case is given by

$$(VSWR)_{\frac{1}{2}} = \frac{1 + \beta + \beta^2 + (1 + \beta)\sqrt{1 + \beta^2}}{\beta}$$

Figures 1 and 2 show the variation of (VSWR) with frequency for the two dielectric cavities. The loaded Q is calculated from

$$Q_L = \frac{Q_0}{1 + \beta} \quad .$$

The effects of aqueous sample loading were investigated by placing a 5/8" diameter water-filled teflon tube on the cavity centerline. Figure 3 shows the change in resonant frequency and Q caused by the teflon tube alone, while Figure 4 shows the change caused by the teflon tube filled with water.

The results of the measurements obtained with the (VSWR) technique are summarized in Table I. The resonant frequency of the TE_{014} mode was found to be approximately 9.7 GHz for both tubing sizes. Using the calculations presented in the first quarterly report, the design frequency was 9.5 GHz. The small difference between the design frequency and the measured resonant frequency could be the result of a small variation in the length of the dielectric tube, or a small variation in the assumed dielectric constant of 3.78. Data are also presented for the TE_{015} mode whose resonant frequency was found to be approximately 11.7 GHz. The values of loaded Q measured are lower than one would expect for a low loss dielectric such as Spectrosil®. The loaded Q of several commercial cavities was measured using the same technique and excellent correlation was obtained between the measured Q and the manufacturer's specified value of Q. The losses in the dielectric cavity are a function primarily of the losses in the dielectric tubing and the metal end plates. The cavity is relatively insensitive to alignment of the end plates since it is a guided wave structure. For a loss tangent of 5.8×10^{-4} (approximately equal to that of Quartz), Becker and Coleman[1] predict a loaded Q of about 700 for the equivalent size tube in the TE_{011} mode. However, since the total loss depends on both the losses in

[1] R. C. Becker and P. D. Coleman, Proceedings of the Symposium on Millimeter Waves, Vol. 9, pp. 191-222, New York, 1959.

the dielectric tube and the end plates, one cannot be sure without making the actual calculation how this figure would scale for the TE_{014} case. To verify that alignment was not critical, thin metal shims were inserted between the dielectric tube and the metal end plate at various positions and the Q was again measured. No significant change in Q was noted. A simple experiment to determine the predominant loss factor will be to construct another cavity of significantly shorter length. For example, if we construct a TE_{012} cavity the Q would increase by a factor of two over the TE_{014} cavity if the dielectric losses are the predominant ones. These tests will be performed during the next quarter.

The effects of water loading on the dielectric cavity were severe for the water column diameter chosen in the preliminary tests. Table I shows that the loaded Q was reduced to approximately 75 with the water-filled teflon tube inserted on the cavity centerline. It remains to be seen what aqueous sample column diameter increases losses sufficiently to prohibit detection of esr lines in an aqueous sample. The magnet system leased from Varian Associates has not arrived as yet; however, every effort is being made to expedite its shipment since the above measurements are critical to the question of whether a lower loss cavity employing a high cost dielectric such as sapphire should be constructed.

Figure 5 shows the cavity response characteristic as measured by the second technique. A swept frequency generator was employed to produce a dynamic cavity response curve. The source frequency is swept linearly over a preselected bandwidth about a preselected center frequency and the reflected power from the cavity is displayed on an oscilloscope whose horizontal sweep is derived from the sweep generator. The response curve is calibrated in amplitude by an attenuator placed between the sweep generator and the cavity, and the frequency is calibrated directly from the dial readings on the source. Although this technique is much faster than the (VSWR) method, it is not as accurate since the bandwidth cannot be determined closer than ± 20 percent from the sweep generator. Its chief merit is that the high sweep range, 8.0 to 12.4 GHz, allows one to quickly determine the approximate frequency of several resonant modes. Figure 6

is a photograph of the swept frequency measurement apparatus, and Figure 7 shows the dielectric cavity employing Spectrosil® under test.

Construction of a prototype Fabry-Perot cavity was also completed during the quarter and preliminary measurements made to determine its mode structure and loaded Q. Resonant frequencies were found to occur from 8.0 to 12.4 GHz on the sweep generator at 0.5 GHz intervals. The regular spacing corresponds to axial modes and no off-axis modes were observed. The loaded Q was found to be approximately 25,000 although this figure may well be somewhat low since the fm sidebands of the source oscillator could be seen superimposed on the cavity response on the lower sweep ranges. The cavity response is shown in Figure 5, and a photograph of the prototype cavity shown in Figure 8.

Research efforts during the next quarter will be directed toward improving the Q of the dielectric cavity employing Spectrosil®, beginning measurements to determine the sensitivity of esr samples in the dielectric cavity, and continuing measurements on the Fabry-Perot cavity. The importance of testing the prototype cavities in an ESR spectrometer is of primary concern, and continued efforts are being made to secure delivery of the leased system from the vendor.

Respectfully submitted.

J. J. Heise, and

R. G. Shackelford
Project Directors

Approved:

A. P. Sheppard, Head
Special Techniques Branch
Electronics Division

Attachments (2)

Table I

a/b	Mode	f_0(GHz)	β	$(VSWR)^{\frac{1}{2}}$	Δf(MHz)	Q_L	Q_0
.9016 T*	TE_{015}	12.001	0.357	8.20	50.87	236	320
.9016 W**	TE_{015}	11.994	0.159	14.83	181.2	66	77
.9016 W**	TE_{014}	10.117	0.079	28.60	162.0	69	74
.9016	TE_{014}	9.696	0.244	10.80	31.30	300	374
.9016	TE_{015}	11.623	0.714	6.35	52.0	224	386
.8920	TE_{014}	9.697	0.193	12.50	37.7	257	307
.8920	TE_{015}	11.710	0.550	6.80	49.5	236	366
Fabry-Perot	TE_{018}	$\approx$ 9.5			$\approx$ 0.32		$\approx$ 25,000

*5/8" Diameter Teflon Tube placed on Cavity Centerline

**5/8" Diameter Water-Filled Teflon Tube placed on Cavity Centerline

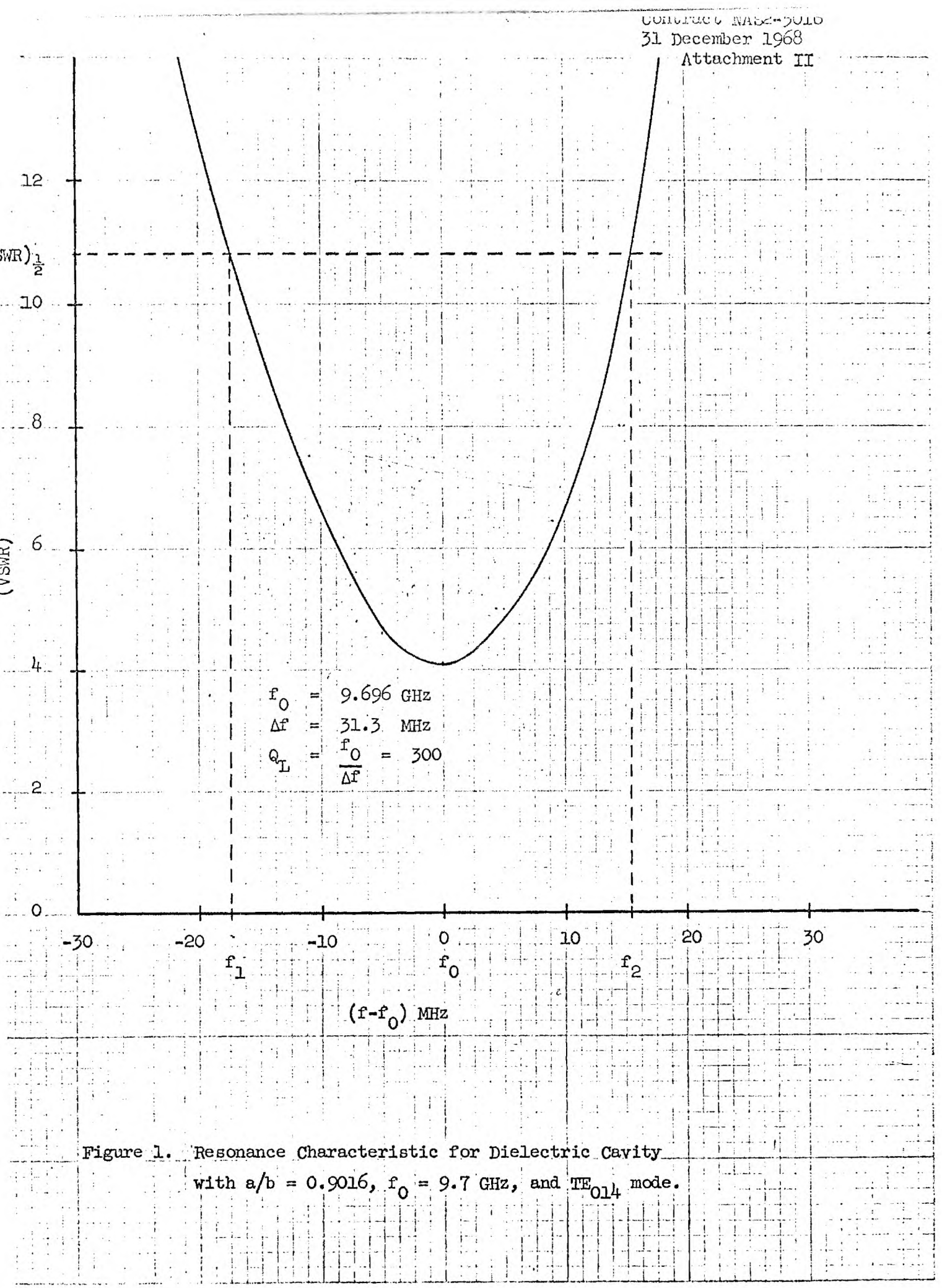

Figure 1. Resonance Characteristic for Dielectric Cavity with a/b = 0.9016, f_0 = 9.7 GHz, and TE_{014} mode.

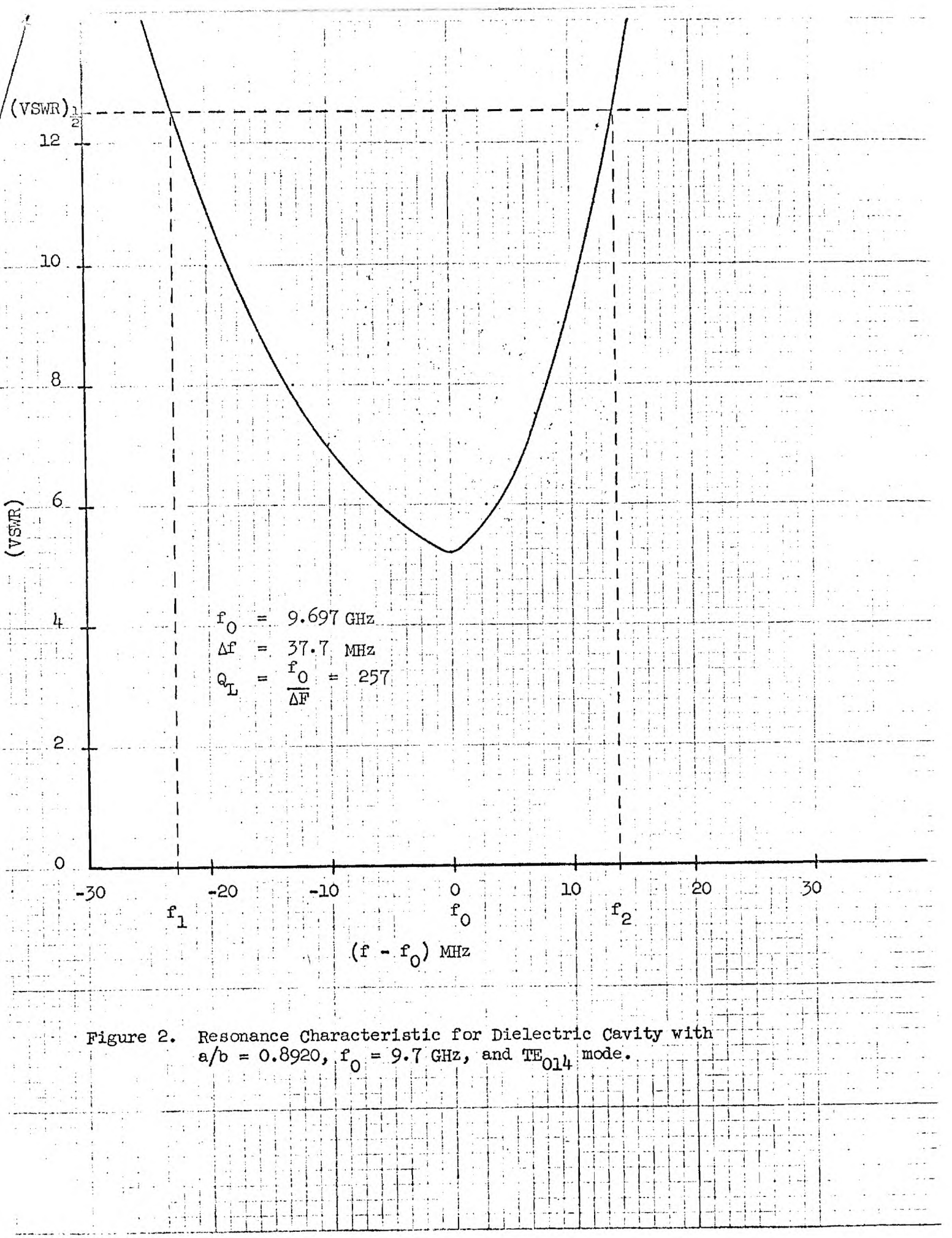

Figure 2. Resonance Characteristic for Dielectric Cavity with $a/b = 0.8920$, $f_0 = 9.7$ GHz, and TE_{014} mode.

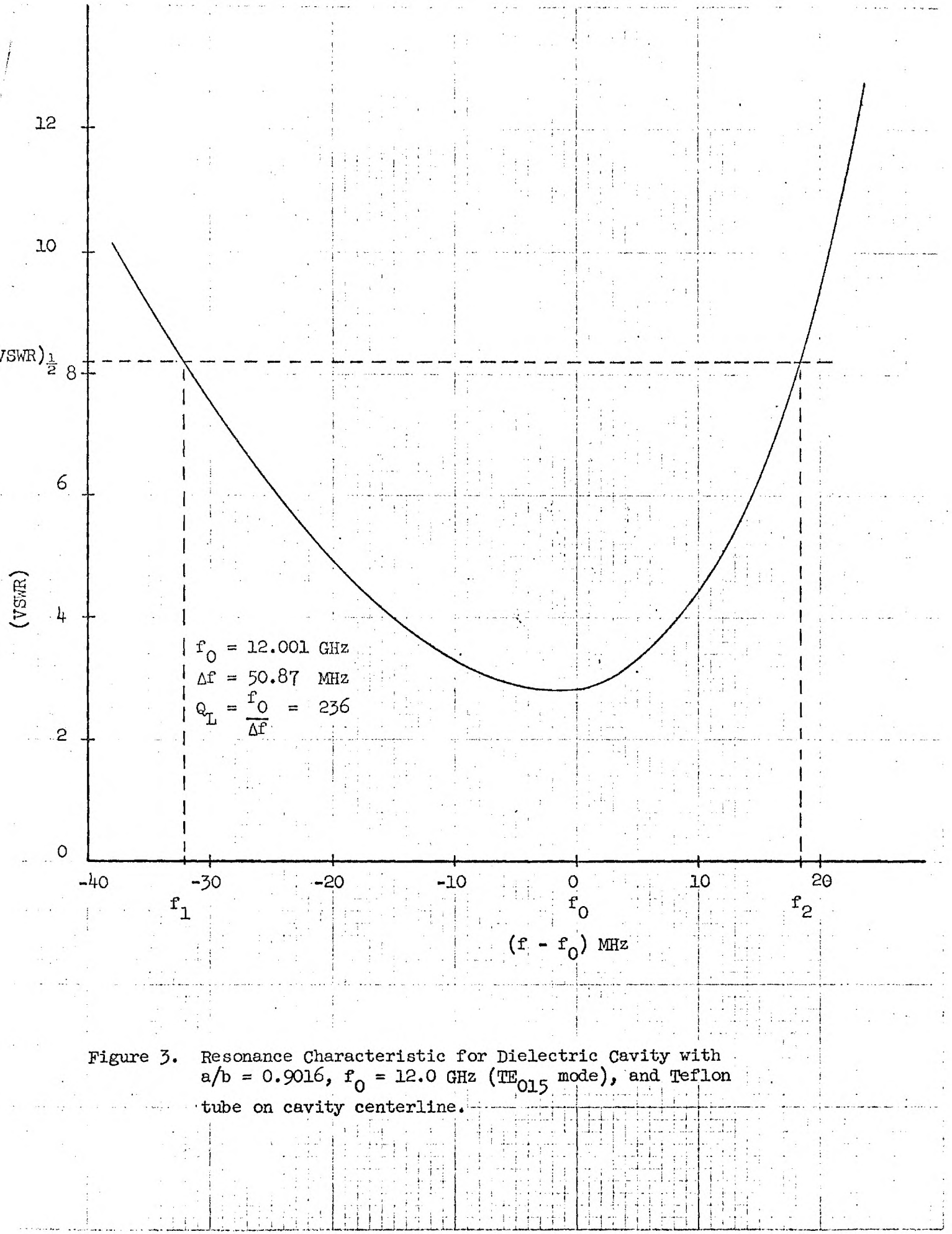

Figure 3. Resonance Characteristic for Dielectric Cavity with a/b = 0.9016, f_0 = 12.0 GHz (TE_{015} mode), and Teflon tube on cavity centerline.

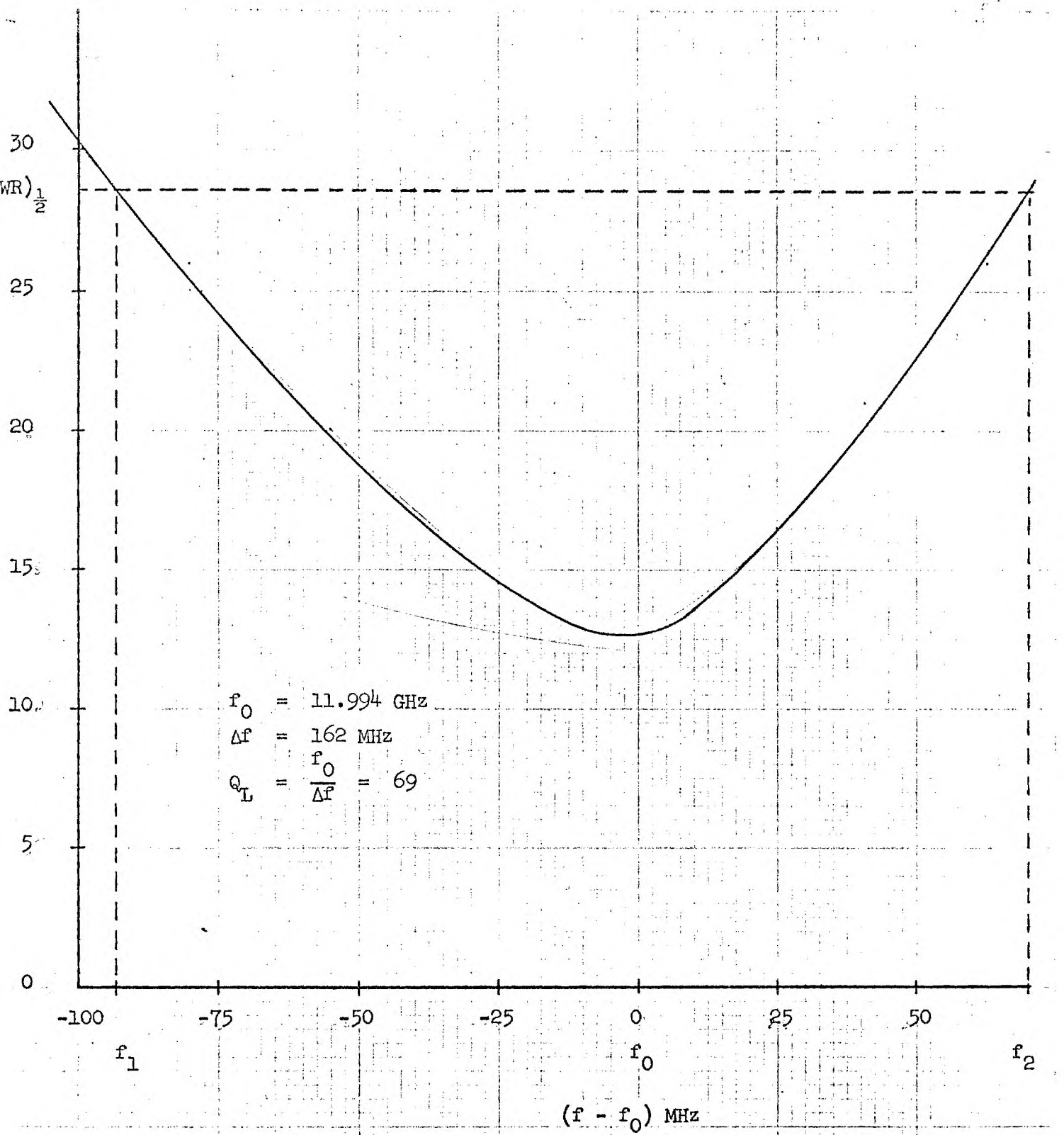

Figure 4. Resonance Characteristic for Dielectric Cavity with a/b = 0.9016, f_0 = 12.0 GHz (TE_{015} mode), and water filled Teflon Tube on cavity centerline.

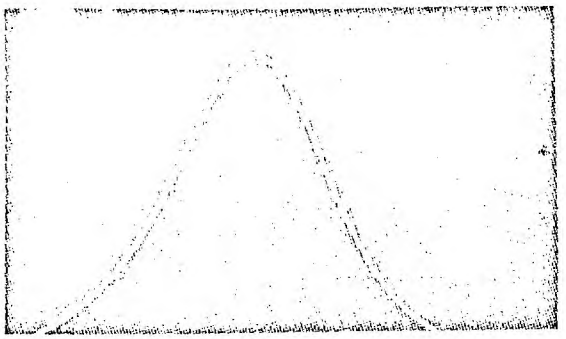

(1) a/b = 0.8920; f_0 = 9.7 GHz(TE_{014})
Horizontal Scale: 6 MHz/div.

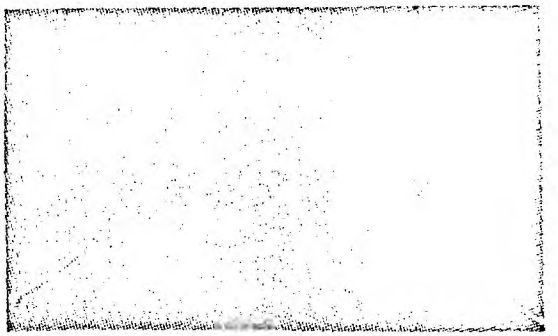

(2) a/b = 0.8920; f_0 = 11.7 GHz(TE_{015})
Horizontal Scale: 6 MHz/div.

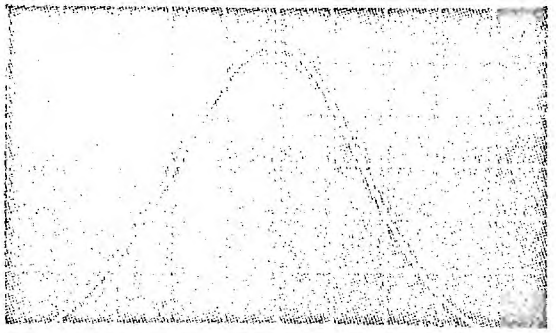

(3) a/b = 0.9016; f_0 = 9.7 GHz(TE_{014})
Horizontal Scale: 6 MHz/div.

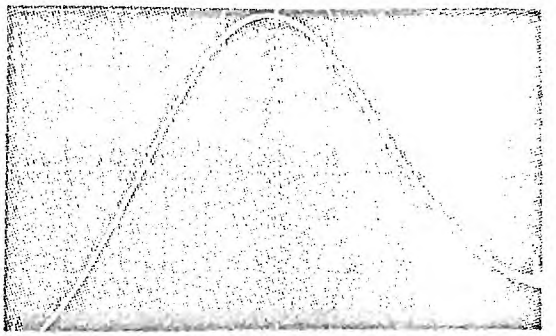

(4) a/b = 0.9016; f_0 = 11.7 GHz(TE_{015})
Horizontal Scale: 6 MHz/div.

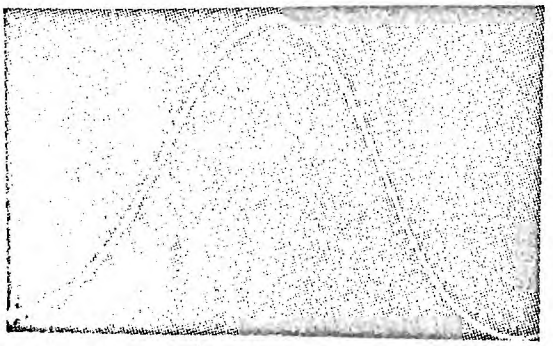

(5) a/b = 0.9016: Water filled Teflon Tube on Centerline; f_0 = 10.117 GHz (TE_{014})
Horizontal Scale: 25 MHz/div.

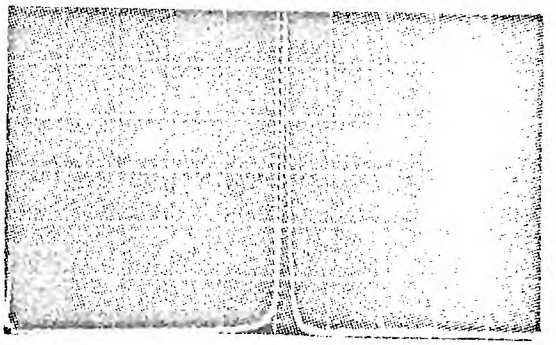

(6) Fabry-Perot Resonator
f_0 = 8.0 GHz
Horizontal Scale: 1 MHz/div.

Figure 5. Resonance Characteristic for Dielectric Cavities (1) - (5), and Fabry-Perot Resonator (6) Obtained with Sweep Generator Technique.

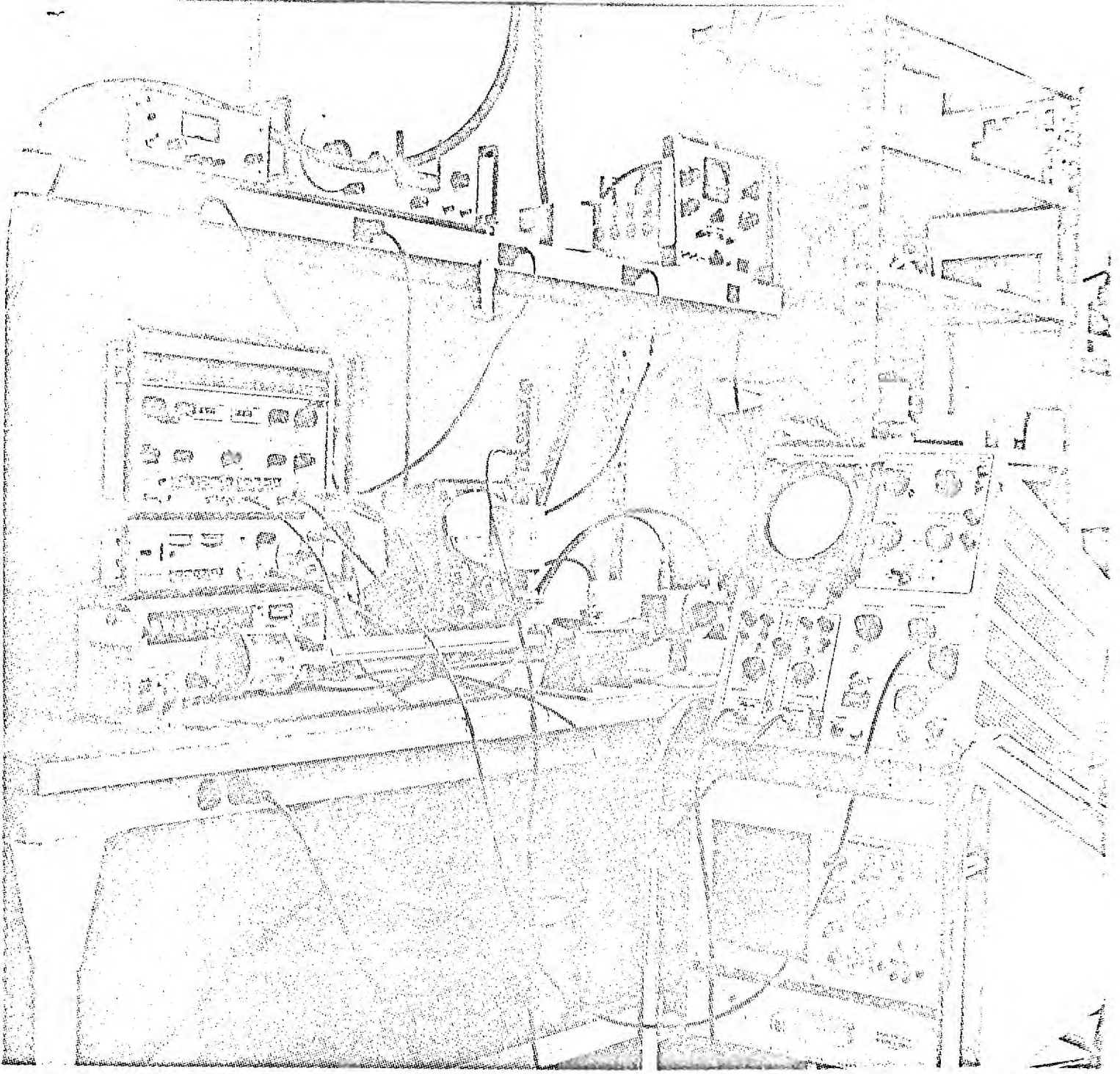

Figure 6. Experimental Apparatus Employed in the Sweep Generator Technique for Measuring the Resonance Characteristic of the Dielectric Cavity.

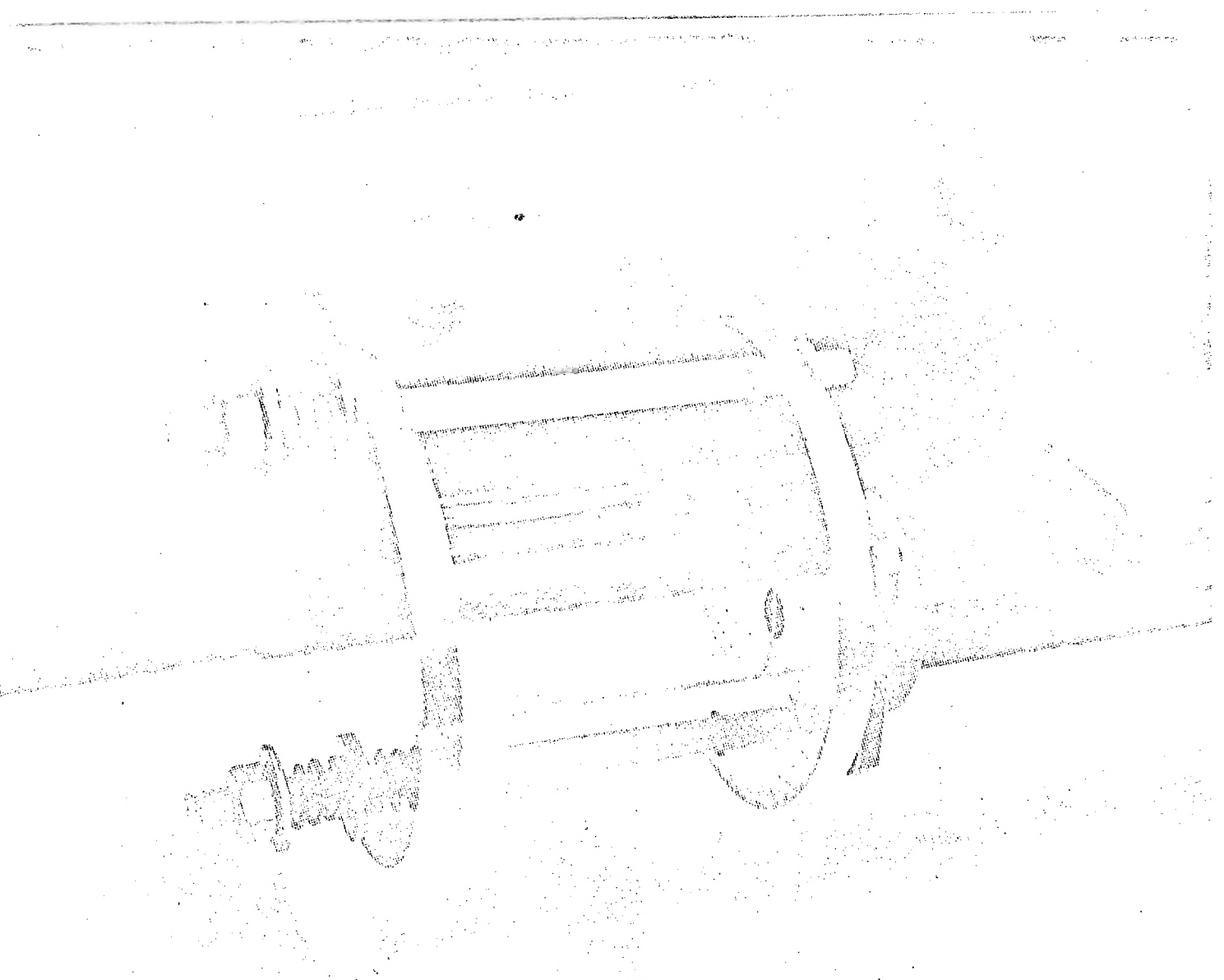

Figure 7. Dielectric Cavity under Test.

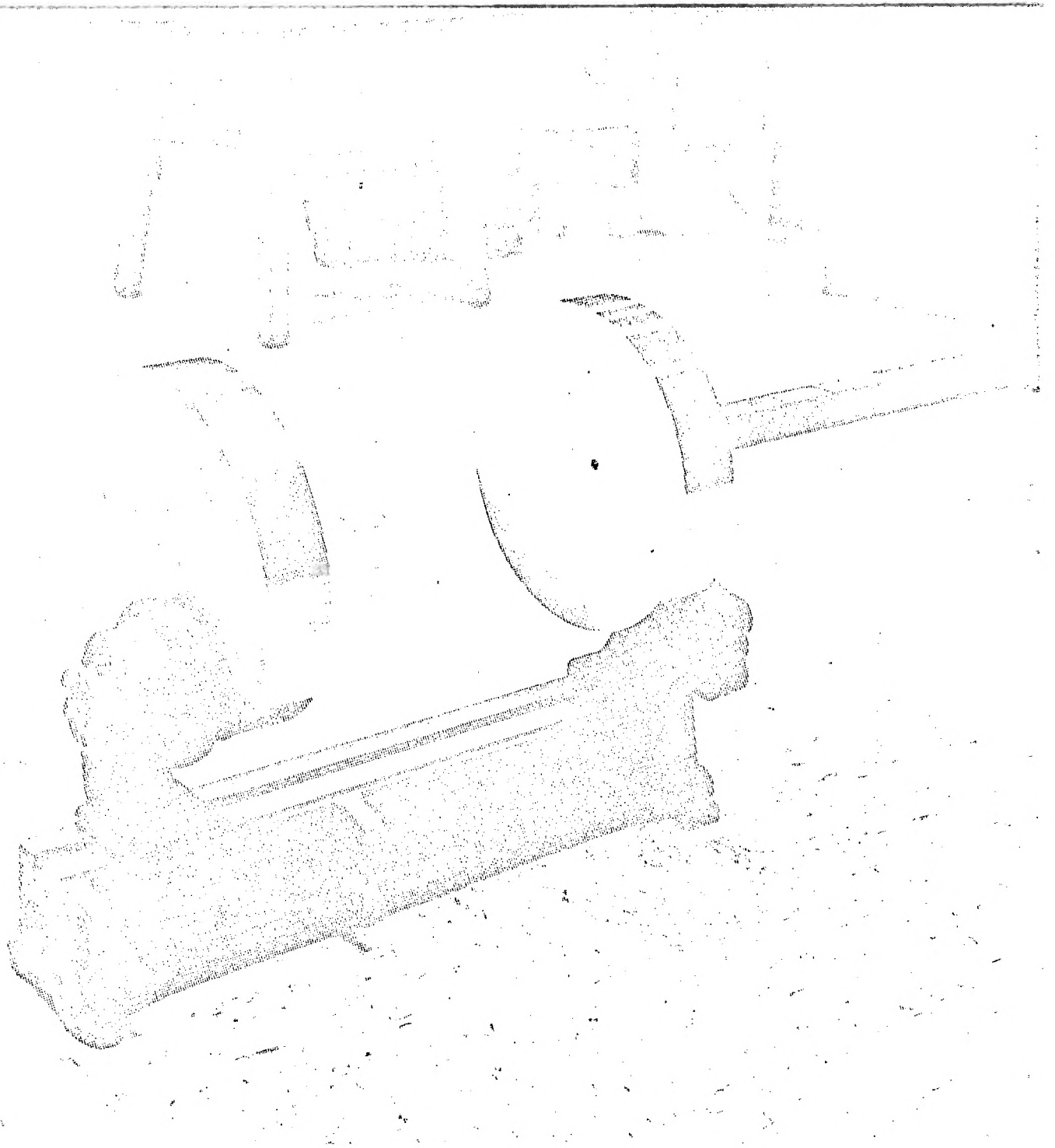

Figure 8. Prototype Fabry-Perot Resonator.

GEORGIA INSTITUTE OF TECHNOLOGY
ENGINEERING EXPERIMENT STATION

225 North Avenue, Northwest · Atlanta, Georgia 30332

2 April 1969

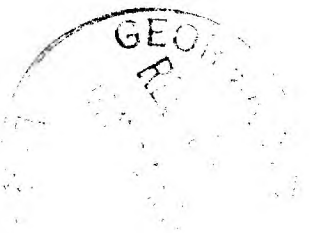

Dr. R. F. Reinisch
N-240-1
NASA/Ames Research Center
Moffett Field, California 94035

Title: Study for Improved Microwave Cavities for Polymer and Biological ESR Measurements

Subject: Quarterly Progress Report on Contract No. NAS2-5016 for the Period 21 December 1968 through 20 March 1969

Dear Sir:

This letter reports progress of research on the subject contract during the period 21 December 1968 through 20 March 1969. This quarter's research has been devoted to a thorough study of factors affecting the Q of a dielectric cavity. Among those factors investigated were coupling mechanisms, surface preparation of the metal end plates, degree of polish on the ends of the dielectric tube, and perturbation of the field by the cavity supporting structure. As yet no ESR studies have been conducted because of repeated delays by Varian Associates in delivery of the six inch magnet system.

The low values of unloaded Q exhibited by the first dielectric cavity, which employed Spectrosil® tubing, prompted a thorough investigation of those factors which were thought likely to contribute to the loss mechanisms. The first experiment performed was the testing of a dielectric cavity in the TE_{012} mode which was constructed using the same techniques for cutting the Spectrosil® tubing to its correct length, and employing the same end plates used on the TE_{014} cavity. The purpose of this experiment was to determine whether the losses were being incurred primarily in the tubing or in some other mechanism. As expected, in view of the low loss tangent of Spectrosil®, it was found that the Q values were almost identical for the two cavities.

The next step involved the investigation of those loss mechanisms which might be traced to construction techniques. The most likely candidates were

the surface finish of the aluminum end plates and smoothness of the ends of the dielectric tubing which together would affect the field configuration by modifying the boundary conditions at any point for which an air gap existed on the plane of intersection.

The initial technique for cutting the Spectrosil® tubing to length involved the use of a diamond wheel cutting saw followed by a grinding process to insure parallelism of the two ends. This process resulted in some chipping at the ends of the tubing. A new process was evolved which greatly reduced the chipping and resulted in smooth glazed finish on the ends of the tubing. In this process, a more accurate cutting saw was used thereby eliminating the grinding step used in the original process, and the ends of the tubing were fire polished to produce the glazed finish. The metal end plates were also lapped and repolished to provide a much smoother surface than was originally thought to be necessary. The results of the measurement of Q_L and Q_0 for this cavity are shown in Table I. Both a circular iris and a slit iris were employed with variable widths to obtain the optimum coupling coefficient. These measurements showed that an unloaded Q of 1100 could be obtained in the TE_{015} mode, and a value of 485 could be obtained for the TE_{014} mode with an optimum coupling coefficient. The maximum Q_0 obtained for the original cavity was 386 in the TE_{015} mode, and 374 in the TE_{014} mode. Attempts to critically couple either mode resulted in lower values of unloaded Q. This would suggest the possibility of losses being introduced by the slide screw tuner in the form of secondary resonances which were observed between the coupling iris and the tuner.

The relatively low value of Q_0 obtained for the TE_{014} mode is puzzling in view of the significant improvement obtained for the TE_{015} mode. The possibility of field perturbations caused by the nylon rod supporting structure was investigated since Becker and Coleman's[1] paper shows the E_θ field to fall off as r/λ_0. Hence the radial extent of the E_θ field is

---

[1] R. C. Becker and P. D. Coleman, "The Dielectric Tube Resonator: A Device For The Generation and Measurement of Millimeter and Submillimeter Waves," Proceedings of the Symposium on Millimeter Waves, Vol. 9, pp 191-222, (1959).

greater for the TE_{014} than the TE_{015} mode. A plexiglass yoke assembly was contructed to press the end plate firmly against the dielectric tubing, while removing the supporting structure several inches outside the radius of the end plates. As shown in Table I, no improvement in Q_0 was seen for either mode.

Plans for the last quarter include final construction of a high Q dielectric cavity employing sapphire tubing. Calculations have been completed for the tubing dimensions and quotations have been received from several suppliers of sapphire stock. All machining of the sapphire tubing will be handled by the manufacturer since our glass blowing laboratory is not equipped to efficiently handle this material. The delay in receiving the magnet system from Varian has caused much concern since ESR studies will be extremely difficult to implement in the short time remaining for experimental work on the present contract. Repeated calls to Varian Associates have produced promises of shipment but as yet no magnet system has been delivered.

A Fabry Perot cavity will also be constructed during the quarter. The prototype cavity constructed earlier has revealed extremely high Q ($\sim$ 25,000), but final evaluation of its applicability as an open boundary ESR cavity will not be possible without experiments designed to determine the optimum sample loading configuration and coupling to the magnetic field.

A proposal for continuation of this research is currently being prepared, and it is possible that the project goals will be modified to compensate for late delivery of the magnet system and the desirability of performing ESR studies on both cavity configurations. It is our desire to deliver the cavities in a condition which would provide maximum usefulness for NASA personnel. We feel that this can be accomplished only through complete testing of the cavities while incorporated into an ESR spectrometer.

Respectfully submitted,

Approved:

J. F. Heise, and

R. G. Shackelford
Project Directors

A. P. Sheppard, Head
Special Techniques Branch
Electronics Division

Attachment (1)

TABLE I

a/b	Mode	f_0(GHz)	Iris	β	Q_L	Q_0
0.9016	TE_{015}	11.684	C^1 - 3/16"	0.06	1021	1021
0.9016	TE_{015}	11.680	C^1 - 1/4"	0.162	946	1103
0.9016	TE_{015}	11.669	C^1 - 5/16"	0.270	684	868
0.9016	TE_{015}	11.676	S^2 - 3/16"	0.389	633	879
0.9016	TE_{015}	11.676	S^2 - 3/16"	0.970*	285	570
0.9016	TE_{014}	9.704	C^1 - 1/4"	0.08	485	485
0.9016	TE_{014}	9.696	C^1 - 5/16"	0.278	313	397
0.9016	TE_{014}	9.646	S^2 - 3/16"	0.05	459	482
0.9016	TE_{014}	9.644	S^2 - 3/16"	0.625*	292	475
0.9016**	TE_{014}	9.704	C^1 - 5/16"	0.295	313	405
0.9016	TE_{012}	9.883	C^1 - 5/16"	0.526	170	324

C^1 - Circular Iris

S^2 - Slit Iris

* - Cavity Matched with Slide Screw Tuner

** - Plexiglass Yoke Support

GEORGIA INSTITUTE OF TECHNOLOGY
EXPERIMENT STATION 225 North Avenue, Northwest · Atlanta, Georgia 30332

20 June 1969

Dr. R. F. Reinisch
N-240-1
NASA/Ames Research Center
Moffett Field, California 94035

Title: Study for Improved Microwave Cavities for Polymer and Biological ESR Measurements

Subject: Quarterly Progress Report on Contract No. NAS2-5016 for the Period 21 March 1969 through 20 June 1969

Dear Sir:

This letter reports progress of research on the subject contract during the period 21 March 1969 through 20 June 1969. The project termination date has been extended to 20 September 1969 with no increase in funds to provide for incorporation of the Varian six-inch magnet and field regulated supply into an ESR spectrometer. This quarter's research has been devoted primarily to laboratory installation of the Varian magnet system, and testing of an ESR spectrometer.

Figure 1 shows a photograph of the magnet installation. A 220 volt three phase breaker panel was installed at the magnet location to provide input power to the magnet power supply and to add back-up fusing against current overload. A pressure regulated water line was also installed to provided cooling for the magnet coil and power supply circuit board. The dielectric cavity was suspended between the pole pieces by means of a plexi-glass bracket which was attached to the magnet yoke. A photograph of this assembly is shown in Figure 2.

The ESR spectrometer was assembled from available components and makes use of the simple heterodyne scheme of Manenkov and Prokhorov.[1] The block diagram of the spectrometer shown in Figure 3 reveals its basic principals of operation. The modulated microwave signal reflected from the test cavity is combined via the circulator with the local oscillator in a balanced mixer. The difference frequency component is passed through an IF amplifier whose bandwidth is made as narrow as possible to obtain the maximum signal-to-noise ratio. The modulation component is detected and amplified to a level which is appropriate to drive the y-axis of an oscilloscope whose sweep is derived from the modulation signal. The resulting oscilloscope trace represents the bandpass characteristic of the ESR material in the cavity.

Several microwave sources have been employed in an effort to establish the necessary system parameters for detection of a known volume of strong pitch in the spectrosil dielectric cavity. Because of its utility, a sweep generator was first investigated. It was found that its FM noise spectrum was too wide for compatible operation with the narrow band IF amplifier. Several unstabilized klystrons were also tried with similar results. Tests are currently underway employing a stabilized klystron, and preliminary results are favorable.

Calibration of the system will be attempted by comparing a known volume of dpph in the dielectric tube resonator and a rectangular Varian ESR cavity.

---

1 A. A. Manenkov and A. M. Prokhorov, Radiotekh. i Elektron., 1 469, (1956).

The measurements on the dielectric tube resonator will be concentrated on determining its performance with aqueous biological samples.

The program of research for the last quarter will include final assembly of the two prototype cavities and such ESR testing as time permits. In view of the comparatively high Q exhibited by the Fabry-Perot resonator, as much time as possible will be devoted to determining its applicability as an ESR cavity. Small diameter spectrosil tubing placed on axis will serve as a sample holder for the sapphire dielectric cavity. The optimum sample placement for the Fabry-Perot cavity will be a planar configuration with the sample material sandwiched between two thin low-loss dielectric sheets.

Respectfully submitted,

J. J. Heise, and

R. G. Shackelford
Project Directors

Approved:

A. P. Sheppard, Head
Special Techniques Branch
Electronics Division

Attachments (3)

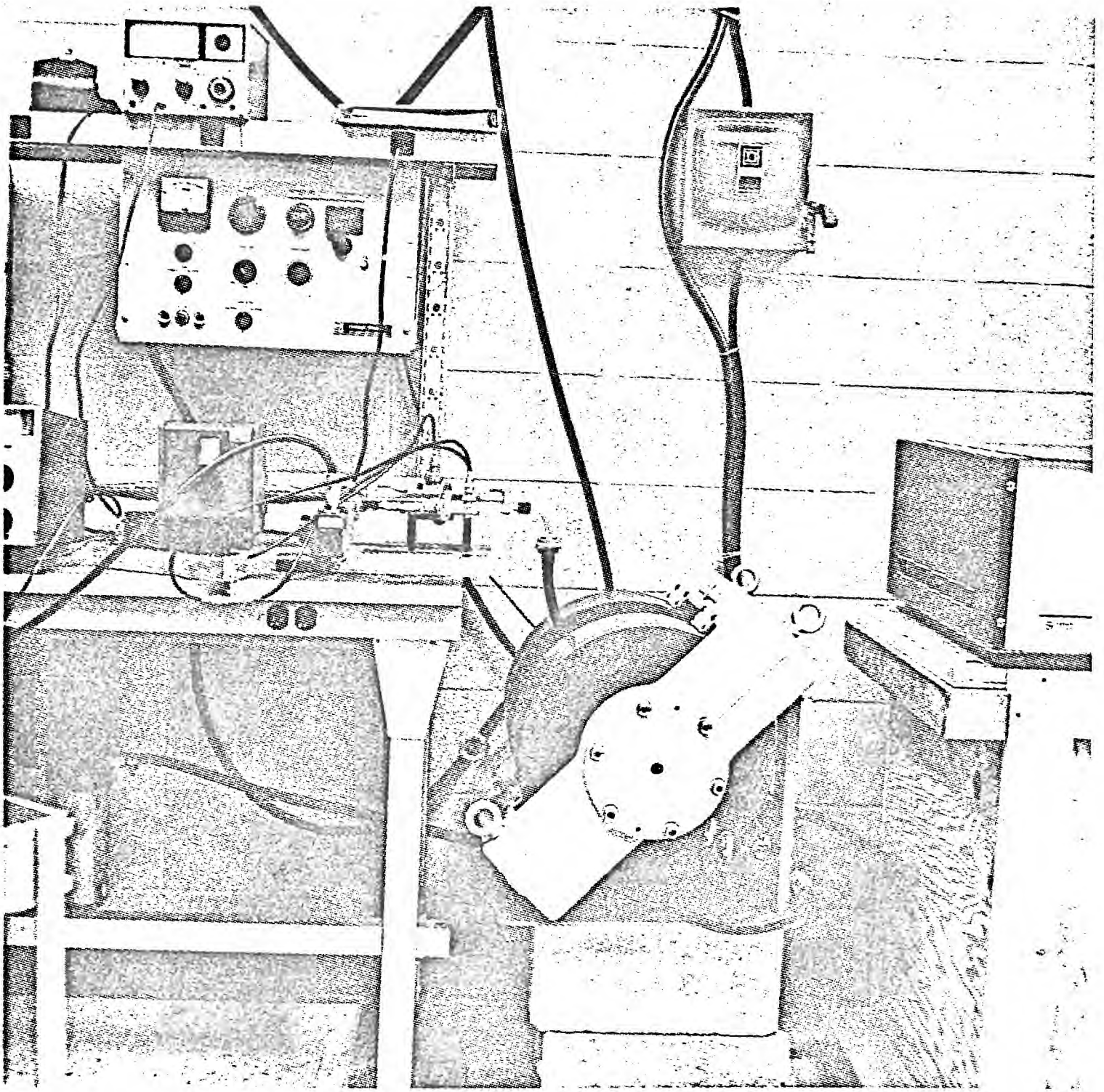

Figure 1. Varian Magnet Installation

Figure 2. Mounting Structure for Dielectric Cavity

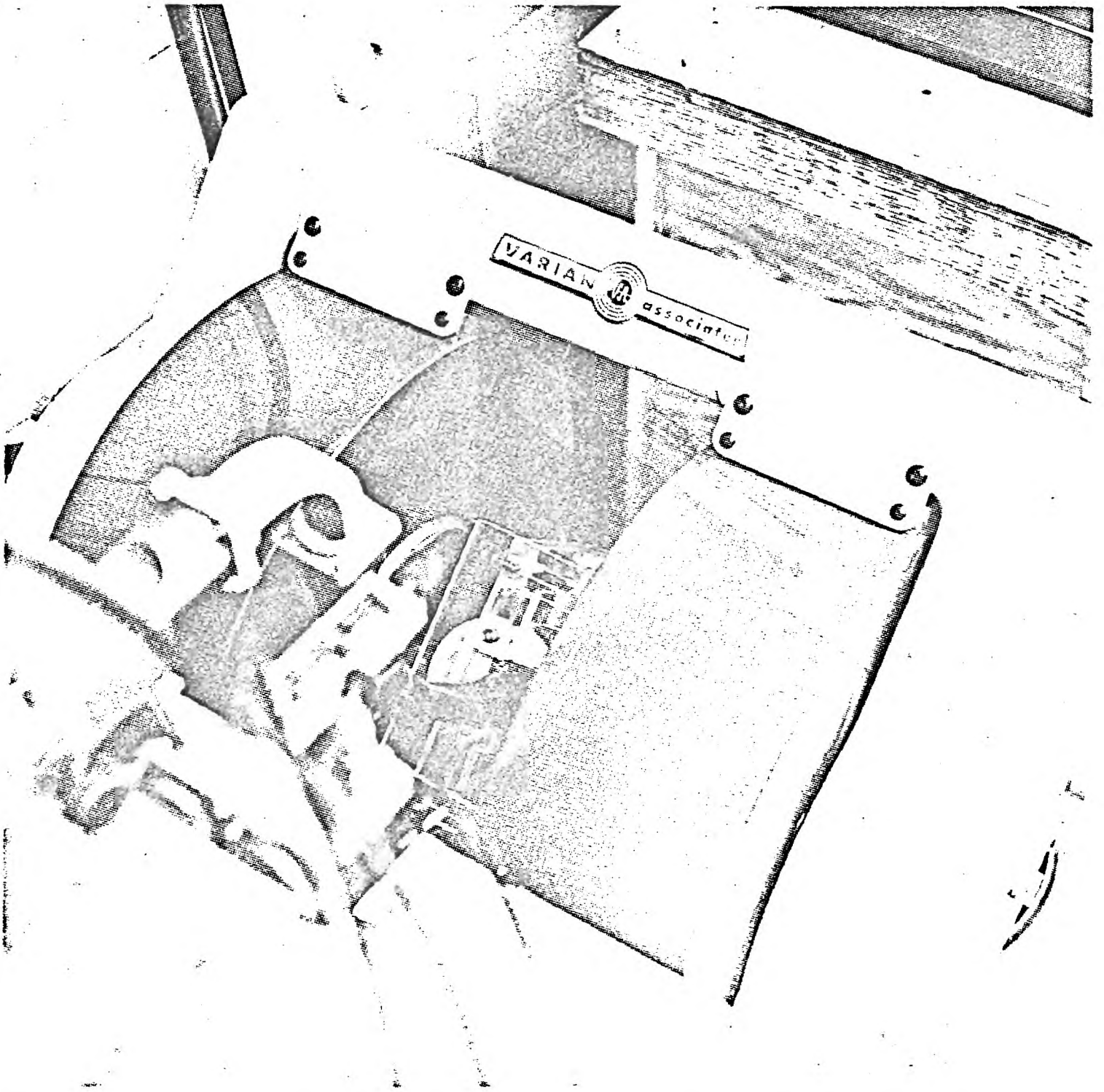

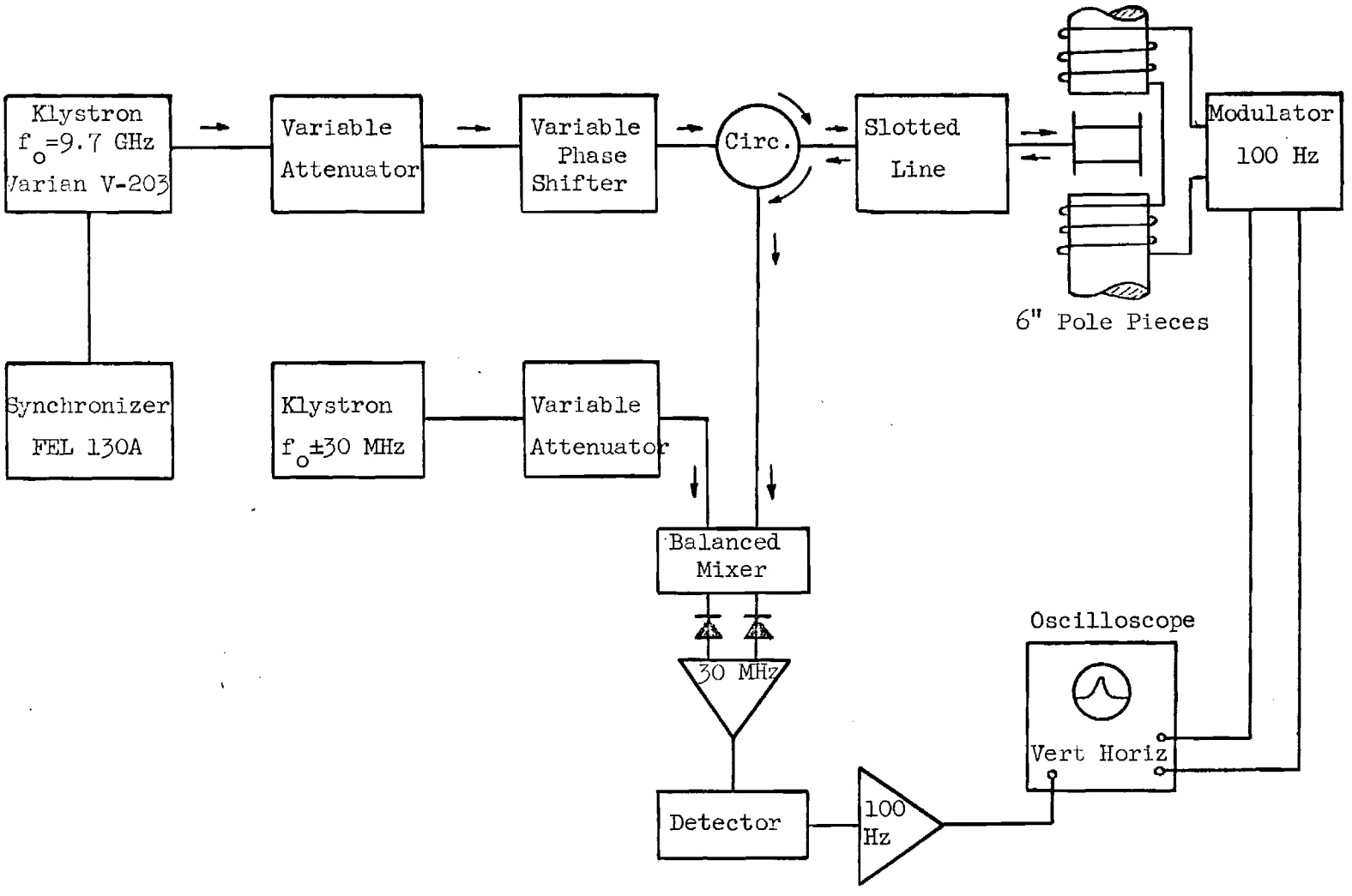

Figure 3. Block Diagram of Heterodyne ESR Spectrometer

GEORGIA INSTITUTE OF TECHNOLOGY
Engineering Experiment Station
Atlanta, Georgia 30332

FINAL REPORT

PROJECT NO. A-1107

STUDY FOR IMPROVED MICROWAVE CAVITIES FOR POLYMER AND BIOLOGICAL ESR MEASUREMENTS

By

R. G. SHACKELFORD

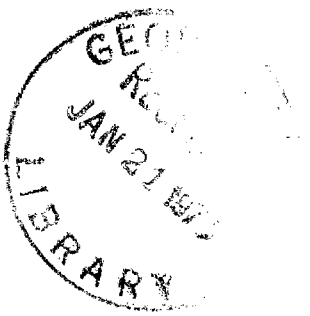

RESEARCH CONTRACT NAS2-5016

21 June 1968 to 20 September 1969

Performed for

NATIONAL AERONAUTICS AND SPACE ADMINISTRATION
WASHINGTON, D. C. 20546

GEORGIA INSTITUTE OF TECHNOLOGY
Engineering Experiment Station
Atlanta, Georgia 30332

FINAL REPORT

PROJECT NO. A-1107

STUDY FOR IMPROVED MICROWAVE CAVITIES FOR POLYMER AND BIOLOGICAL ESR MEASUREMENTS

By

R. G. SHACKELFORD

RESEARCH CONTRACT NAS2-5016

21 June 1968 to 20 September 1969

Performed for

NATIONAL AERONAUTICS AND SPACE ADMINISTRATION
WASHINGTON, D. C. 20546

ABSTRACT

The objective of this research program was to determine the applicability of the open boundary resonator to electron spin resonance (ESR) instrumentation. Measurements were made to determine the resonator quality factor and the optimum geometry for coupling to the electron spin configuration in solid and liquid state samples. The design and construction of both a dielectric cavity resonator and a Fabry-Perot resonator are discussed. Characteristic microwave measurements at the frequency 9.5 GHz are presented for both open boundary resonator types. In addition, an ESR spectrometer was constructed and measurements were made using free radical 2, 2 diphenyl-1-picrylhydrazyl (DPPH) to determine the performance of the open boundary resonator relative to a standard Varian Model E3 waveguide cavity equipped with a radiation window.

The microwave tests demonstrated the high Q properties of both the dielectric cavity resonator (DCR) and the Fabry-Perot resonator (FPR). Unloaded Q's greater than 5000 were achieved with a single crystal sapphire tube DCR and a confocal FPR with 5.5 inch diameter reflectors. It was found that lossy samples such as organic solvents could be placed in the DCR with the geometry providing maximum spin coupling without serious degradation of the cavity Q. Comparative ESR measurements performed with the sapphire DCR revealed a 10 dB improvement in signal-to-noise ratio in ESR detection over the Varian waveguide cavity. It was found, however, that perturbations by the ESR magnet pole pieces, which had a gap spacing of four inches, prevented ESR testing of the FPR.

The interest in the open boundary resonator and its applicability to ESR instrumentation stems from a geometrical configuration which allows illumination of the ESR sample with electromagnetic radiation extending into the near-ultraviolet wavelength region. The results obtained during this one year research program have shown the dielectric tube resonator to be competitive with the standard waveguide cavity and have demonstrated several desirable properties of the Fabry-Perot resonator which could be exploited by employing an ESR magnet with sufficiently wide pole gap. The favorable results obtained with the DCR employing single crystal sapphire suggest the need for further research to optimize ESR sample placement and to provide a technique for sample cooling.

TABLE OF CONTENTS

LIST OF FIGURES

LIST OF FIGURES (continued)

LIST OF TABLES

I. INTRODUCTION

In the two decades since its inception by Zavoisky[1], the technique of electron spin resonance spectroscopy has been extended from the applications in crystal physics and concentrated solution chemistry into the realm of free-radical initiated polymers and biological applications. Early efforts were limited to systems which exhibited high concentrations of free electron spin states because of a lack of sensitivity. The first biological applications[2] over a dozen years ago were confined to solid state derivatives because the presence of water, with its high dissipation factor, reduces the sensitivity of ESR spectrometers. Many ESR investigators continue to freeze water-containing samples and thereby realize greater sensitivity in the detection of electron spins.[3] However, dependence on frozen samples excludes information relevant to reaction mechanisms dominant at higher temperatures.

In the last few years, ESR has been effective in the detection of transient oxidation-reduction reactions in normally operating biological and biochemical systems.[4] ESR has provided new information about valence states of metals and parameters of metal binding to biochemical compounds. Changes in ESR spectra have also been observed in the results of abnormal metabolic conditions.[5] Recent reviews[6,7] attest to the applicability of ESR as a means for making non-destructive measurements in relation to the biological cells and their constituents. Little attention has been given to optimizing the ESR microwave cavity in terms of handling large samples, reducing the deleterious effects of water dissipation, or in providing complete illumination of the sample by optical and ultraviolet sources.

The standard microwave ESR cavity is a closed boundary metallic cavity whose geometrical configuration is determined by the application of electromagnetic boundary conditions to Maxwell's equations. The configuration of the standard ESR cavity is generally rectangular, cylindrical, or coaxial. Solution of the electromagnetic wave equation in rectangular coordinates leads to sinusoidal functions for the standing wave field components, while cylindrical coordinates lead to Bessel function solutions for the stationary fields.

An important parameter for the microwave cavity is its quality factor, Q, which gives the ratio of energy stored in the cavity volume to energy dissipated in the metallic walls or lost by radiation through imperfections in the boundary structure. The mechanism for ESR detection of a sample located in the cavity depends on the change in Q which is caused by microwave power absorption in the sample spin system at resonance.

A thorough knowledge of the microwave field configuration of an ESR cavity is necessary for optimum sample location. In order to achieve maximum sensitivity in an ESR cavity, the power absorbed by the sample's electron spin system must be maximized, while power absorbed in the sample by other mechanisms must be minimized. The power absorbed by the sample spin system at resonance, P_s, is proportional to the mean square value of the microwave magnetic field over the sample volume. Only the component of rf field which is perpendicular to the static field, $H_\perp$, is capable of coupling power into the spin system; hence,

$$P_s \propto \langle H_\perp^2 \rangle = \frac{1}{V} \int_{\text{sample}} H_\perp^2 \, dV, \qquad (1)$$

where the integral is carried out over the entire sample volume, V_s, which is exposed to the microwave and static magnetic fields.

The power absorbed and converted to heat in the sample can be represented by a complex propagation constant γ which depends on the microwave frequency, the permeability, and the dielectric constant of the sample. Any heat producing mechanism (finite conductivity of the sample, dipole absorption in liquid, crystalline defects, etc.) can be thought of in terms of a complex dielectric constant $\epsilon^* = \epsilon' - j\epsilon''$ and a loss tangent defined by $\tan \delta = \epsilon''/\epsilon'$. Power absorbed in the sample, P_D, may then be given in terms of the dielectric constant ϵ', the microwave frequency ν, and the microwave electric field $\mathcal{E}$ by

$$P_D = 2\pi\nu\epsilon' \tan \delta \int_{\text{sample}} \mathcal{E}^2 \, dV \quad . \tag{2}$$

It is apparent from the discussion above, and the expressions (1) and (2), that the desired sample location for maximum sensitivity is a volume within the cavity which has a high average value of magnetic field and a low average value of electric field.

A relative figure of merit for ESR cavities is the filling factor η which is defined by

$$\eta = \frac{\int_{\text{sample}} H_\perp^2 \, dV}{\int_{\text{cavity}} H_\perp^2 \, dV} \quad . \tag{3}$$

The filling factor is proportional to the ratio of the power absorbed in the sample spin system to the power stored in the cavity volume. Since the ESR detection mechanism is based on the absorption of microwave power in the sample, the sensitivity of an ESR spectrometer is inversely proportional

to the filling factor. A knowledge of the filling factor η, the magnetic susceptibility X'', and the cavity geometry is sufficient for the calculation of the minimum detectable spins in a given sample.

Two promising possibilities for achieving improved capability in biological applications of electron spin resonance, particularly for illumination of a sample with optical and ultraviolet radiation, are the dielectric cavity[8] and the Fabry-Perot cavity.[9] The dielectric cavity employs a dielectric rod or tube between two flat, parallel plates. This cavity offers the option of inserting an aqueous sample either on the cavity centerline or just outside the dielectric tube. Inside the dielectric tube the electric field for the TE modes has zero magnitude along the cavity centerline and hence losses should be minimized by placing the sample at this position. Efficient sample irradiation is possible if a transparent dielectric is chosen. The sample can also be inserted at a position outside the dielectric tube where it can be more efficiently illuminated with ultraviolet radiation although electric field losses are greater. High purity synthetic quartz or sapphire tubing is a good choice electrically and at the same time has a high transmission coefficient to near-ultraviolet radiation.

As the ratio of reflector diameter to wavelength increases, the confocal Fabry-Perot cavity offers increased Q over the dielectric cavity and hence greater sensitivity for non-lossy samples since it eliminates the dissipative loss associated with the dielectric tube. This cavity, however, for X-band microwave operation, and the same reflector size, has a Q which is comparable with the DCR since the increased loss incurred by placing the dielectric tube in the cavity volume is offset by the reduced diffraction losses that result

from the microwave energy being confined to a region near the dielectric tube.

Although the microwave electric and magnetic fields are in space quadrature along the Fabry-Perot cavity axis, the stored energy tends to fill the cavity cross section more uniformly than in a rectangular waveguide cavity. The most promising sample configuration takes the form of a thin sheet placed perpendicular to the cavity axis at a point along the axis where the transverse magnetic field is a maximum and the transverse electric field is a minimum. Sample illumination is easily accomplished over a wide range of wavelengths since the walls of the cavity are completely open.

This report describes the design and construction of a dielectric tube resonator and a Fabry-Perot resonator, and the results of measurements made to determine their applicability to ESR spectroscopy. The emphasis has been placed on determining the cavity quality factor Q, and the effects of loading with various solvents which could be employed in biologically oriented ESR applications.

The dielectric tube resonator has been compared with a commercially developed rectangular waveguide cavity to provide a relative figure of merit for its evaluation in detection of radiation induced transient radicals. Considerable effort has been expended in determining the complex mode structure and field configuration of the dielectric tube resonator for the purpose of providing a basis for evaluating the feasibility of using more complex sample holding assemblies for cryogenic measurements.

II. DESIGN OF THE DIELECTRIC CAVITY AND FABRY-PEROT OPEN BOUNDARY RESONATORS

A. The Dielectric Cavity Resonator

The dielectric cavity resonator (DCR) consists of a dielectric tube capped with two metal end plates. A small hole located over or adjacent to the wall of the dielectric tube serves to couple the microwave energy into the cavity from a waveguide which is butted to one of the end plates. The details of this assembly are shown in Figure 1. The DCR is a slow wave structure in which the microwave energy is confined to a region very close to the dielectric cylinder. This structure will support both transverse electric (TE), transverse magnetic (TM), and hybrid (HE or HM) modes. The various modes are designated by three subscripts, k, m, n, where k represents variation in an angular direction about the cavity centerline, m represents species variation along the radial direction, and n gives the length of the cavity in terms of the number of resonant half wavelengths. The axially symmetric modes (k = 0) can only be TE_{0mn} or TM_{0mn}, and hence symmetrical coupling of microwave energy into the DCR is usually sufficient to eliminate the hybrid mode.

The electromagnetic boundary value problem for the DCR has been solved by Becker and Coleman[10] for the transverse modes. The characteristic equation relating the velocity of propagation (V_p), the relative dielectric constant (ϵ_r), and the resonant frequency (ν_o) for the TE_{0mn} and TM_{0mn} modes is:

$$\frac{CJ_0(k_2a')I_1(k_1a') - J_1(k_2a')I_0(k_1a')}{CN_0(k_2a')I_1(k_1a') - N_1(k_2a')I_0(k_1a')} = \frac{CJ_0(k_2b')K_1(k_1b') + J_1(k_2b')K_0(k_1b')}{CN_0(k_2b')K_1(k_1b') + N_1(k_2b')K_0(k_1b')} \quad (4)$$

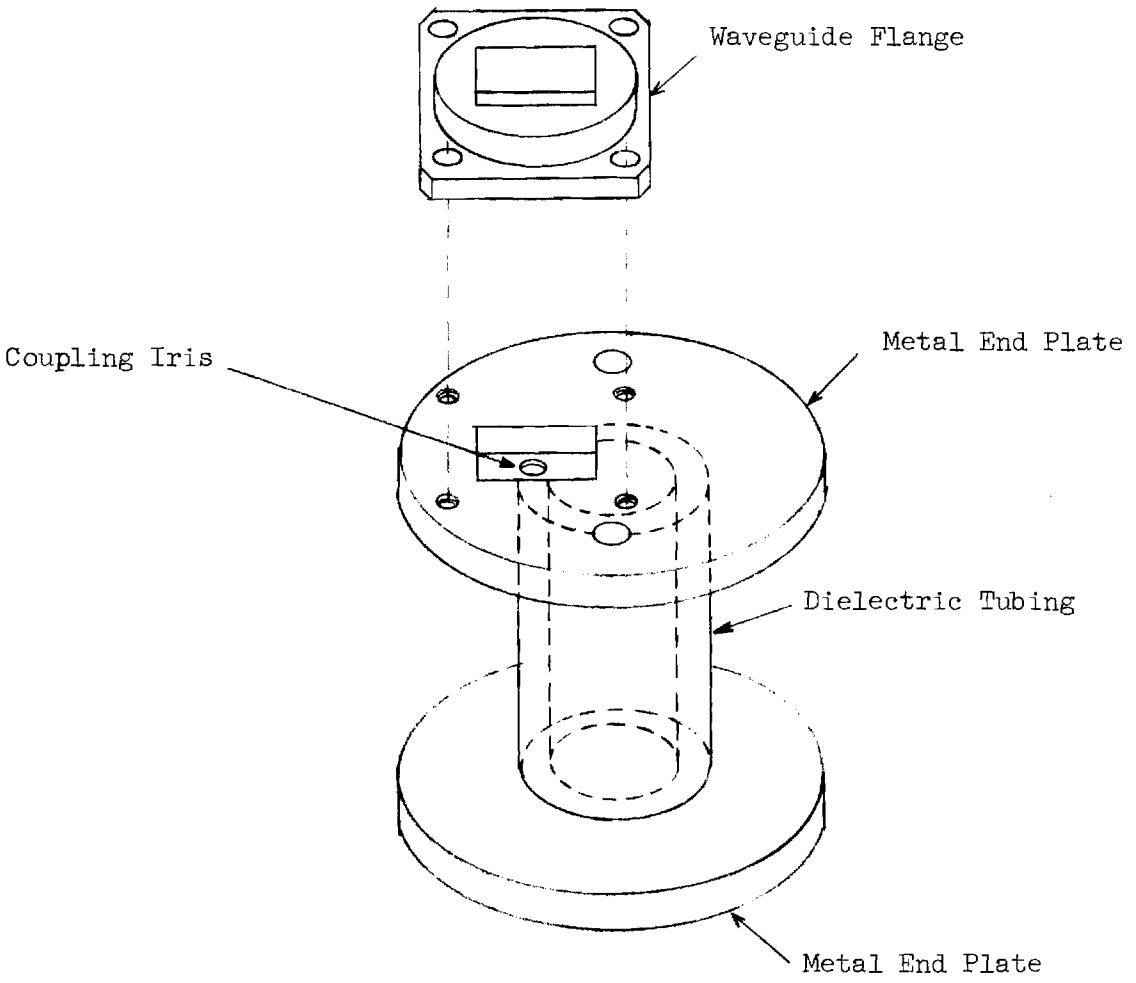

Figure 1. Dielectric Cavity Resonator

where $J_i(x)$ and $N_i(x)$ are the ordinary Bessel functions of the first and second kind respectively, $I_i(x)$ and $K_i(x)$ are the modified Bessel functions, $a' = a/\lambda$, $b' = b/\lambda$, a is the inner radius of the dielectric tube, b is the outer radius of the dielectric tube, λ is the free space wavelength, $k_1 = 2\pi \left[(c/V_p)^2 - 1\right]^{\frac{1}{2}}$, $k_2 = 2\pi \left[\epsilon_r - (c/V_p)^2\right]^{\frac{1}{2}}$, c is the velocity of light, for TE_{0mn} modes $c = k_2/k_1$, and for TM_{0mn} modes $c = k_2/\epsilon_r k_1$.

Two cavities were constructed and tested during this research program. The dielectric materials chosen were Spectrosil®, a high purity synthetic fused quartz, and synthetic sapphire, a high purity rhombohedral single crystal. These materials were selected because they possess low values of loss tangent at the design microwave frequency and high values of transmission coefficient from the optical through near-ultraviolet wavelengths.

The desired mode for ESR operation is the TE_{01n} mode which has an axial and radial component of magnetic field (H_r and H_z) and a circumferential electrical field (E_θ). On the cavity centerline, E_θ is equal to zero while H_z has fallen off slightly from its maximum value at the wall of the dielectric tube. A typical field distribution for Spectrosil is shown in Figure 2. A computer program was written in Fortran IV to numerically calculate solutions to Equation (4) for the TE_{01n} mode. A print-out of this program is contained in Appendix I.

For a given value of the parameters of ϵ_r and V_p/c, the quantities a/λ and b/λ were found to satisfy Equation (4). These calculations were repeated over a range of the parameter V_p/c defined by: $(\epsilon_r)^{-\frac{1}{2}} \leq V_p/c \leq 1$. A typical calculation is presented graphically in Figure 3. Here the ratio a/b has

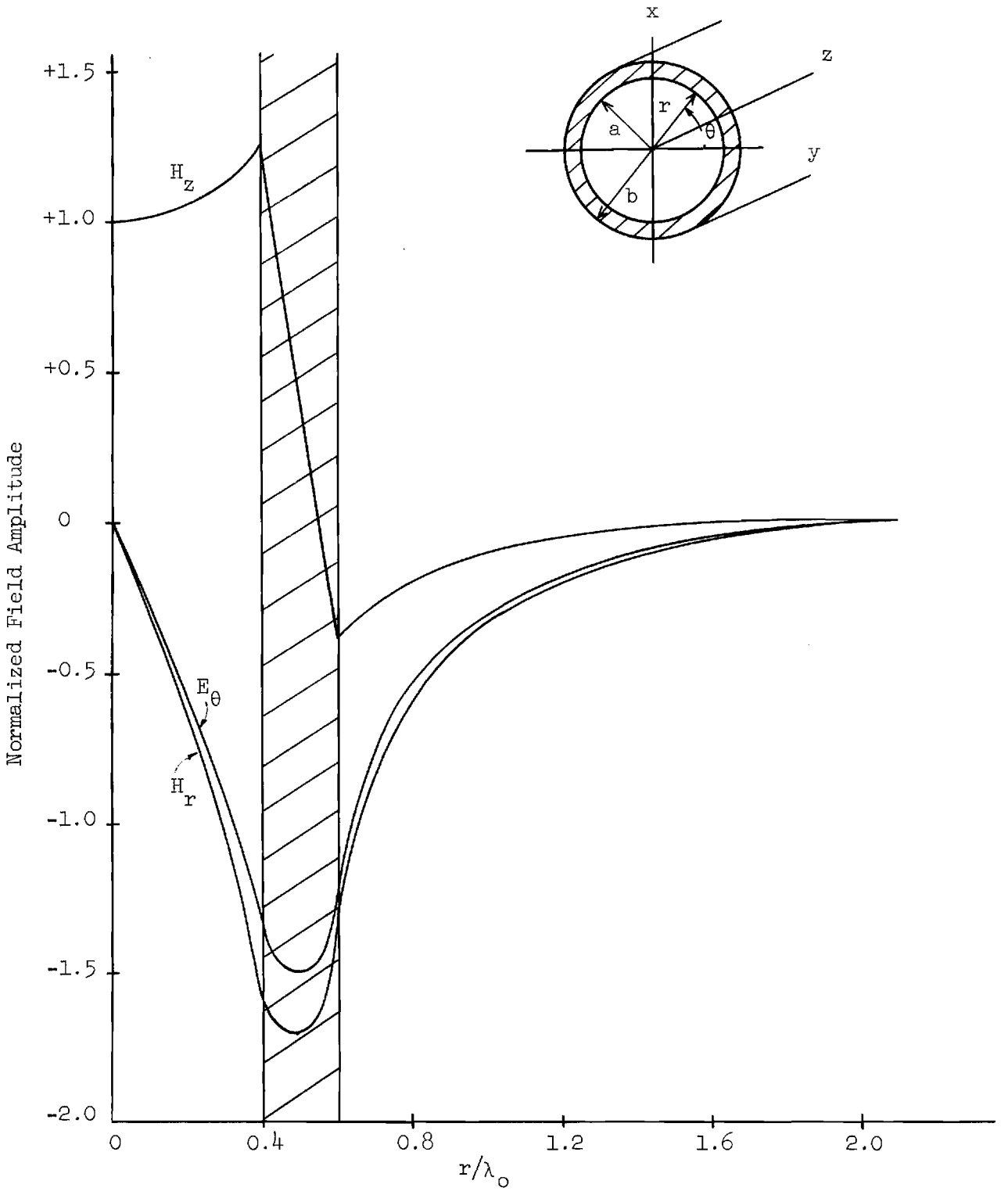

Figure 2. Electric and Magnetic Field Distribution for a Quartz Dielectric Cavity Resonator in the TE_{0ln} Mode

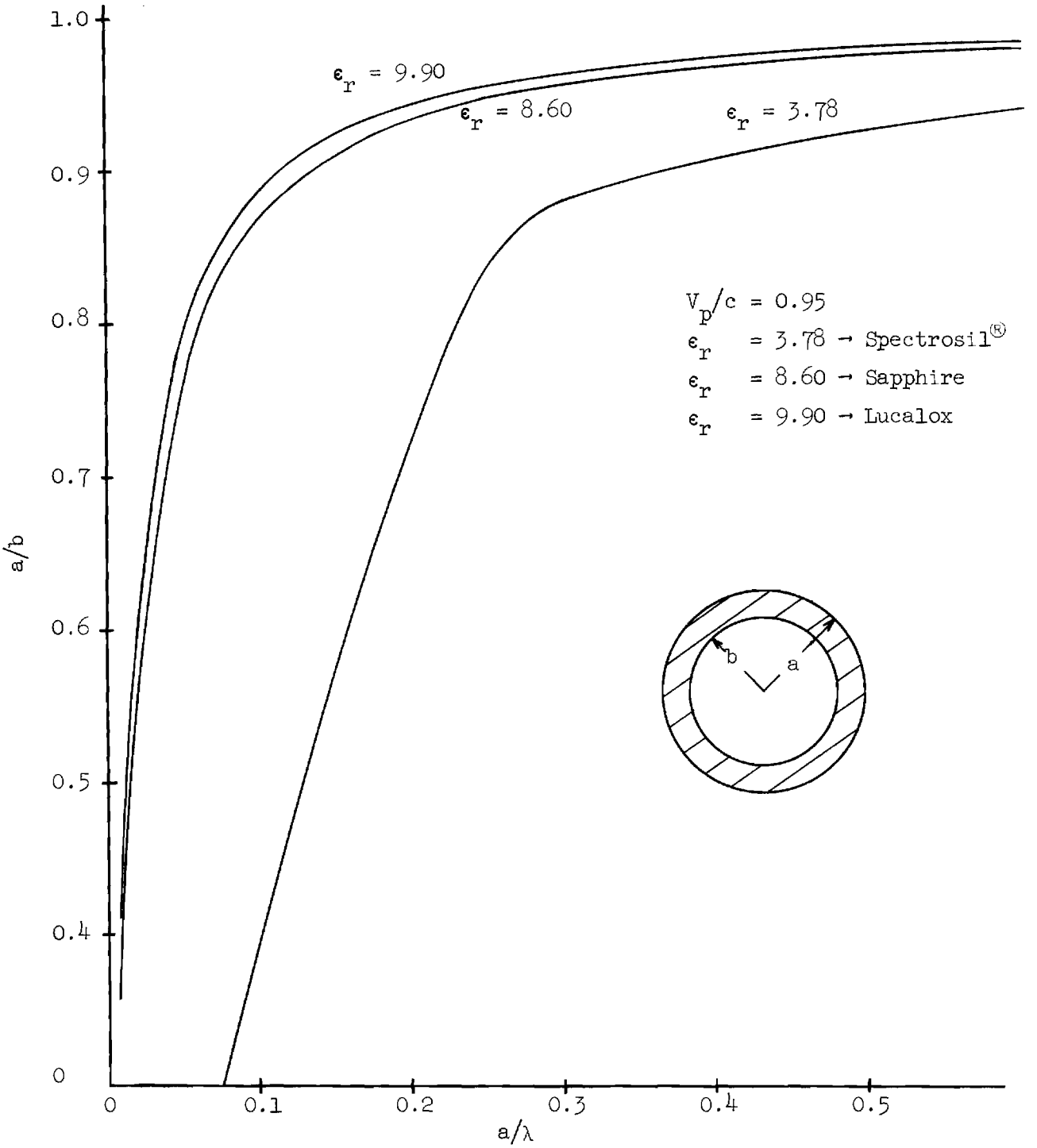

Figure 3. Solution of the Characteristic Equation for the Dielectric Cavity Resonator in the TE_{01n} Mode

been plotted as a function of a/λ for $\epsilon_r = 3.78$ (Spectrosil®), $\epsilon_r = 8.60$ (sapphire), $\epsilon_r = 9.90$ (Lucalox®), and $V_p/c = 0.95$. It is apparent from Figure 3 that the resonant frequency is much less sensitive to variations in the cavity dimensions if the ratio a/b is such that the solution to the characteristic equation falls on the straight line portion of the curve with the highest slope. This consideration alone would place a maximum value on a/b of about 0.85 for Spectrosil tubing, and about 0.90 for sapphire tubing, and, the dependence of cavity Q on the tubing dimensions would indicate that operation close to the maximum a/b is desirable. Becker[11] has shown that for Teflon® ($\tan \delta = 5.8 \times 10^{-4}$) the resonator Q increases as the ratios a/b and a/λ_o increase. For example, his calculations predict a Q of 2400 for a TE_{011} Teflon cavity with a/b = 0.9 and a Q of 2050 for the same cavity with a/b = 0.7. This trend is to be expected since the energy stored in the cavity increases as the cavity volume increases, and the energy dissipated in the dielectric rod decreases as the volume of the dielectric decreases.

The design procedure for the Spectrosil cavity involved selection of a commercially available tubing diameter and wall thickness which would satisfy the characteristic equation for the TE_{01n} mode at a specified microwave frequency. The microwave frequency was chosen to be identical to the Varian Model E-3 ESR spectrometer operating frequency (9.5 GHz) so that the Varian rectangular waveguide ESR cavity could be used as a standard for comparison. Computations were first performed over the range $0.6 \leq V_p/c \leq 0.95$ in 0.05 steps. These results showed that the range of available commercial tubing sizes would provide solutions to the characteristic equation at the design

wavelength only for values of V_p/c between 0.9 and 0.95. The outside tubing radius was selected to satisfy the requirement $b/\lambda_o \leqq 0.6$ to assure a low value of electric field at the edge of the metal end plate. Final computations over the restricted range of V_p/c was performed in 0.01 unit steps, and the results of these calculations are shown in Figure 4. In this figure the presentation has been changed to show the variation of V_p/c as a function of frequency for a given value of a/b. The values of a/b shown represent the two commercially available values closest to a/b = 0.85 for which solutions to the characteristic equation were found.

Once the proper value of V_p/c has been determined for a given ratio a/b and a given design wavelength λ_o, the length, L, of the cavity is calculated from the resonance condition:

$$L = (\frac{n}{2})(\frac{V_p}{c})\lambda_o \quad , \tag{5}$$

where n is the axial mode order number. The ratio of cavity length to order number, L/n, is shown in Figure 5 as a function of frequency for the two selected values of a/b. Table I gives the cavity dimensions for the TE_{014} mode as determined from Figures 4 and 5 at the design frequency of 9.5 GHz. The diameter of the metal end plate was limited by the nominal four-inch magnet pole spacing employed in the ESR spectrometer used in this research program.

Design of the sapphire cavity required only a single calculation to determine the desired value of a/b for selected values of V_p/c and b/λ_o. This simplification resulted from the decision to have the sapphire tube machined to specifications rather than attempting to select a tube from available sizes. In this manner, a near optimum value of a/b was found to

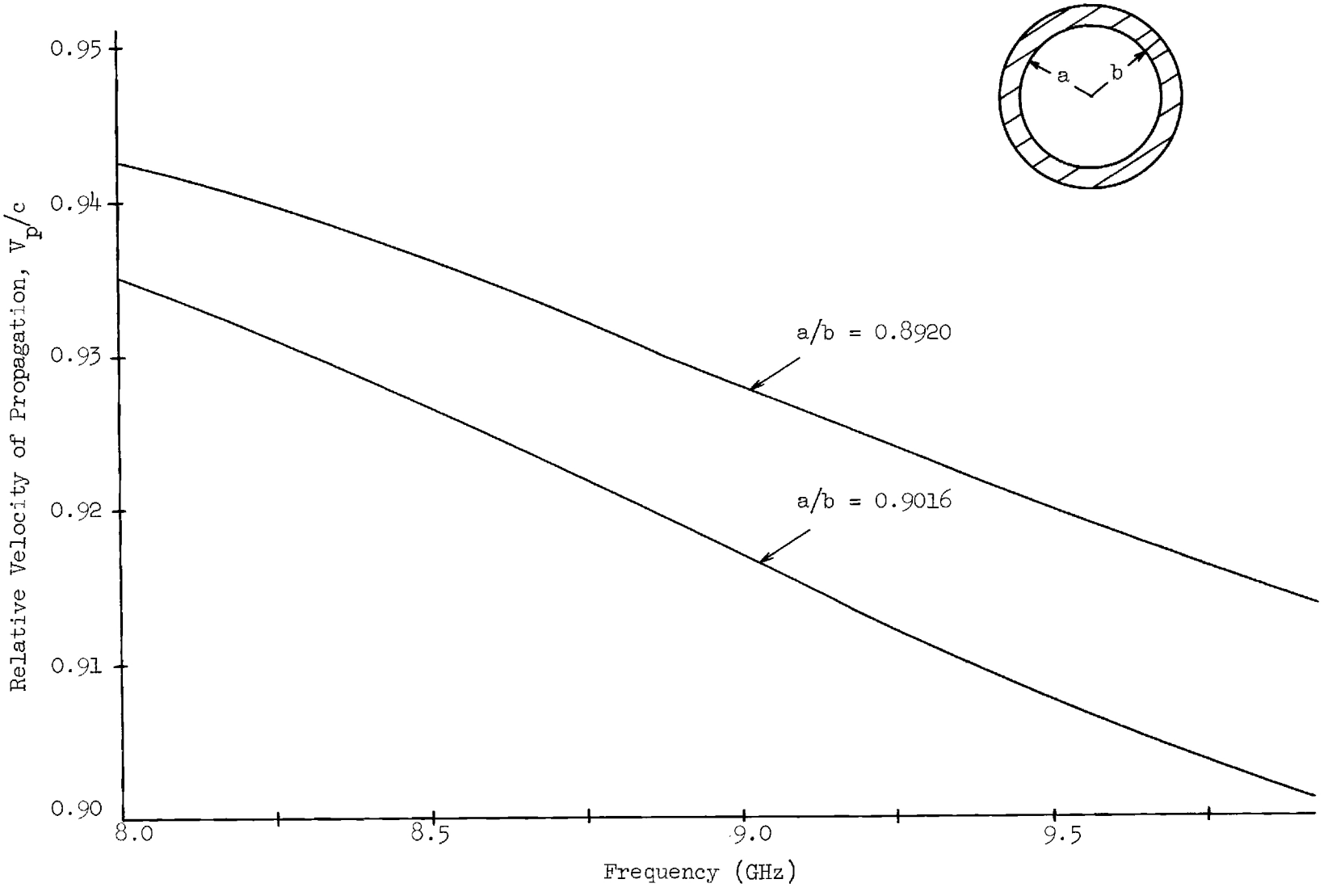

Figure 4. Relative Velocity of Propagation as a Function of a Frequency for the Spectrosil DCR in the TE_{0ln} Mode

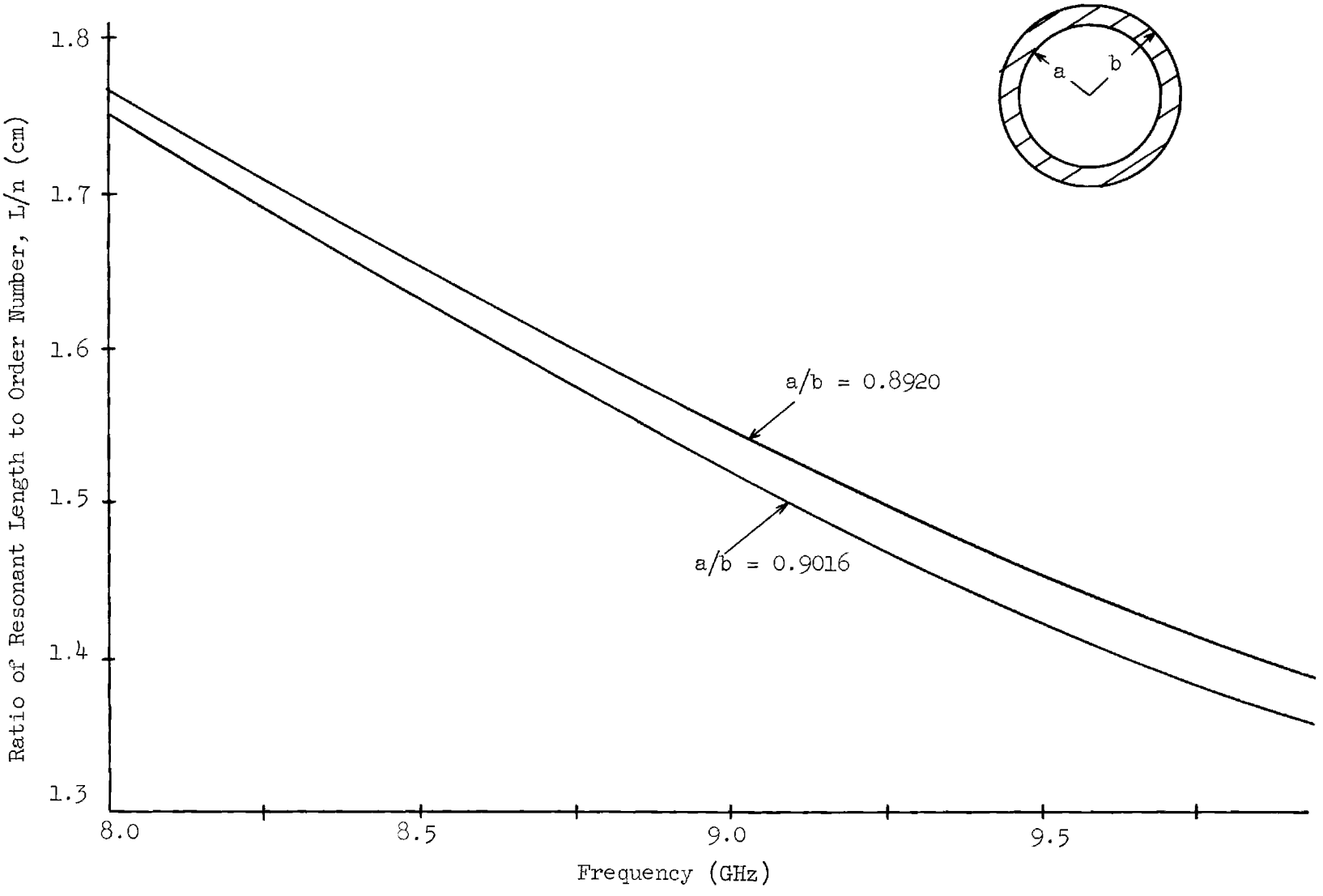

Figure 5. Ratio of Resonant Length to Order Number as a Function of Frequency for the Spectrosil DCR in the TE_{01n} Mode

TABLE I. CALCULATED DIMENSIONS OF DIELECTRIC CAVITY RESONATORS WITH ν_o = 9.5 GHz

Material	a/b	2b (cm)	b/λ_o	R^*/λ_o	L (cm)	Mode
Spectrosil	0.892	3.140	0.497	1.510	5.792	TE_{014}
Spectrosil	0.902	3.660	0.579	1.510	5.680	TE_{014}
Sapphire	0.878	2.530	0.400	1.510	4.420	TE_{014}

R* - Radius of Metal End Plate

satisfy the characteristic equation. Since a Q of 4000 or higher was expected for the sapphire DCR (for sapphire, $\tan \delta = 2 \times 10^{-4}$), b/λ_o was conservatively fixed at the value 0.4 to prevent non-zero electric fields at the edges of the metal boundary planes from contributing to the resonator losses.

B. The Fabry-Perot Resonator

The Fabry-Perot resonator (FPR) consists of two plane parallel reflecting plates separated by a dielectric medium, usually air. Coupling to this resonator may be accomplished by transmission through partially reflecting end plates or by coupling through an aperture cut in a totally reflecting end plate. A similar resonator can be formed by two spherical reflectors of equal curvature separated by their common radius of curvature. This resonator is known as the confocal Fabry-Perot or Connes resonator. A family of resonators with identical reflectors can be parametrically defined by the relation:

$$g = 1 - d/R \quad , \tag{6}$$

where d is the separation between the reflectors and R is the radius of curvature of the reflectors. Using this convention, a plane-parallel Fabry-Perot resonator is defined by g = 1, and a confocal Fabry-Perot resonator is defined by g = 0.

The approximate Q of the Fabry-Perot resonator is given by

$$Q = \frac{2\pi d}{\alpha \lambda_o} \quad , \tag{7}$$

where d is the spacing between the reflectors (cavity length), λ_o is the resonant wavelength, and α is the fractional power loss per bounce from a reflector. The loss term, α, is the sum of diffraction and reflection losses, and may be written as

$$\alpha = \tfrac{1}{2}(\alpha_{D1} + \alpha_{D2}) + \alpha_R \quad , \tag{8}$$

where α_{D1} and α_{D2} are the diffraction losses at each reflector, and α_R is the reflection loss per bounce plus any absorption or scattering loss incurred in the dielectric medium on a single pass.

The diffraction losses for the generalized Fabry-Perot interferometer have been computed by Boyd and Gordon[9] and Li[12]. Although their calculations were based on the approximation that all cavity dimensions are large with respect to a wavelength (a requirement which is not strictly met at X-band with reasonable sized cavities), the general trend of their results is applicable to the present cavity design. If the diffraction losses are small compared with reflection losses, the resonator Q is proportional to the spacing between reflectors. As the spacing is increased, the resonator Q will continue to increase slowly until a point is reached where the diffraction losses are equal to the reflector losses. Any further increases in reflector spacing will then result in a rapid decrease in the Q.

For the generalized Fabry-Perot resonator, the diffraction losses can be characterized in terms of the Fresnel number, N, which is defined by

$$N = \frac{a^2}{d\lambda_o} \quad , \tag{9}$$

where a is the reflector radius. The diffraction losses decrease with increasing Fresnel number and a family of curves can be formed by allowing the parameter g to assume discrete values between zero and one. For Fresnel numbers greater than 1.0, the diffraction loss of the plane-parallel resonator ($g = 1.0$) is much greater than that of the confocal resonator ($g = 0$). For example, $\alpha = 0.08$ for $g = 0$ and $N = 1$, whereas $\alpha = 18$ for $g = 1$ and $N = 1$.

The design considerations for the FPR are the same as those for the DCR. Namely, one desires to design the resonator for high Q and optimum field configuration to minimize losses in the ESR sample. The field configuration for the Fabry-Perot resonator results from a quasi-TEM mode structure. This mode is characterized by nearly transverse electric and magnetic field components which are in quadrature along the cavity axis. A solution to the electromagnetic boundary value problem in cylindrical coordinates leads to TEM_{pkq} modes where the mode numbers p and k are coupled through the Laguerre polynomial solution to the radial equation, k is associated with the angular dependence via the function $e^{ik\Phi}$, and q gives the number of half wavelength variations along the cavity axis. The resonance condition for the confocal resonator is given by

$$\frac{4d}{\lambda} = 2q + 2p + k + 1 \quad . \tag{10}$$

The desirable mode for ESR operation is the TEM_{00q} mode which fills a large volume in the cavity and has a symmetrical gaussian amplitude distribution in the radial direction across a plane perpendicular to the cavity axis. The electric field is virtually zero at the reflector surfaces and in planes perpendicular to the cavity axis at intervals of one half wavelength along the axis.

Thus the optimum sample configuration and location is in the form of a thin sheet of sample material placed perpendicular to the cavity axis at a position for which the electric field is at a minimum.

Although the diffraction losses for the confocal resonator are much smaller than for any other cavity configuration, it can be seen from Equation (10) that the confocal resonator is highly degenerate for large axial mode numbers. Note, for example, that increasing $(2p + k)$ by two and decreasing the axial mode number q by one gives the same frequency. Thus great care must be taken in coupling to such a structure in order to prevent exciting higher order modes which degrade the cavity Q.

It is sometimes desirable to separate the reflectors slightly less than the confocal spacing in order to spoil the mode degeneracy. Goubau and Schwering[13] have shown that the resonance condition for reflectors of equal radius of curvature and arbitrary spacing is given by

$$\frac{2d}{\lambda} = q + \frac{1}{\pi}(2p + k + 1)\cos^{-1}\left(1 - \frac{d}{r_c}\right) \tag{11}$$

For $d \neq r_c$, Equation (11) does not predict degeneracy of modes. Note that for the TEM_{00q} axial mode, both Equation (10) and Equation (11) reduce to the resonance condition:

$$d = \frac{q\lambda}{2} \tag{12}$$

If size were not a limitation, one could easily optimize the Q of the Fabry-Perot resonator for any given design frequency and surface reflectivity. However, for ESR applications, the maximum reflector diameter is limited by the magnet pole spacing. Thus one must vary the length of the cavity and the

reflector curvature to arrive at the maximum obtainable Q for the chosen microwave frequency. For the confocal or nearly confocal resonator, the half power width of the field at a point half way between the two reflectors is smaller than the half power width at the reflector surface by a factor of $\sqrt{2}$. Thus the reflector diameter could be slightly larger than the magnet pole gap without causing serious perturbation of the cavity fields.

One may arrive at the optimum cavity length by calculating Q as a function of cavity length d or order number q using Equations (7), (8), and (12). The reflection loss α_r is calculated from

$$\alpha_r = \frac{2}{1 + 377\delta\sigma} \tag{13}$$

where δ is the skin depth of the reflector material at the microwave frequency, and σ is the conductivity of the reflector material. For aluminum reflectors at ν_o = 9.5 GHz, $\alpha_r = 1.7 \times 10^{-4}$. The diffraction loss per pass, α_p, has been obtained from the computations of Li[12] for the equivalent Fresnel number as calculated from Equation (9). These data are compiled in Table II. One would thus expect the cavity Q to depend strongly on the diffraction losses. This expected behavior is confirmed in Figure 6 which shows the Q of a nearly confocal resonator as a function of reflector spacing for 5.5 inch diameter aluminum reflectors. Although these calculations will not be exactly applicable to the present design because of the approximations involved in computing the diffraction losses, the general trend is applicable and suggests that, for an initial design, the spacing between reflectors should be made approximately equal to the reflector diameter.

TABLE II. DIFFRACTION LOSS FOR THE TEM_{00q} MODE IN A CONFOCAL RESONATOR AT ν_o = 9.5 GHz

d (inches)	q	N	α_D
3.729	6	1.63	10^{-5}
4.351	7	1.40	7×10^{-5}
4.972	8	1.22	10^{-4}
5.594	9	1.09	4×10^{-4}
6.215	10	0.98	10^{-3}
6.837	11	0.89	2×10^{-3}
7.458	12	0.81	4×10^{-3}
8.080	13	0.75	7×10^{-3}
8.701	14	0.69	10^{-2}
9.323	15	0.65	2×10^{-2}
9.944	16	0.61	3×10^{-2}
10.566	17	0.57	4×10^{-2}
11.187	18	0.54	6×10^{-2}

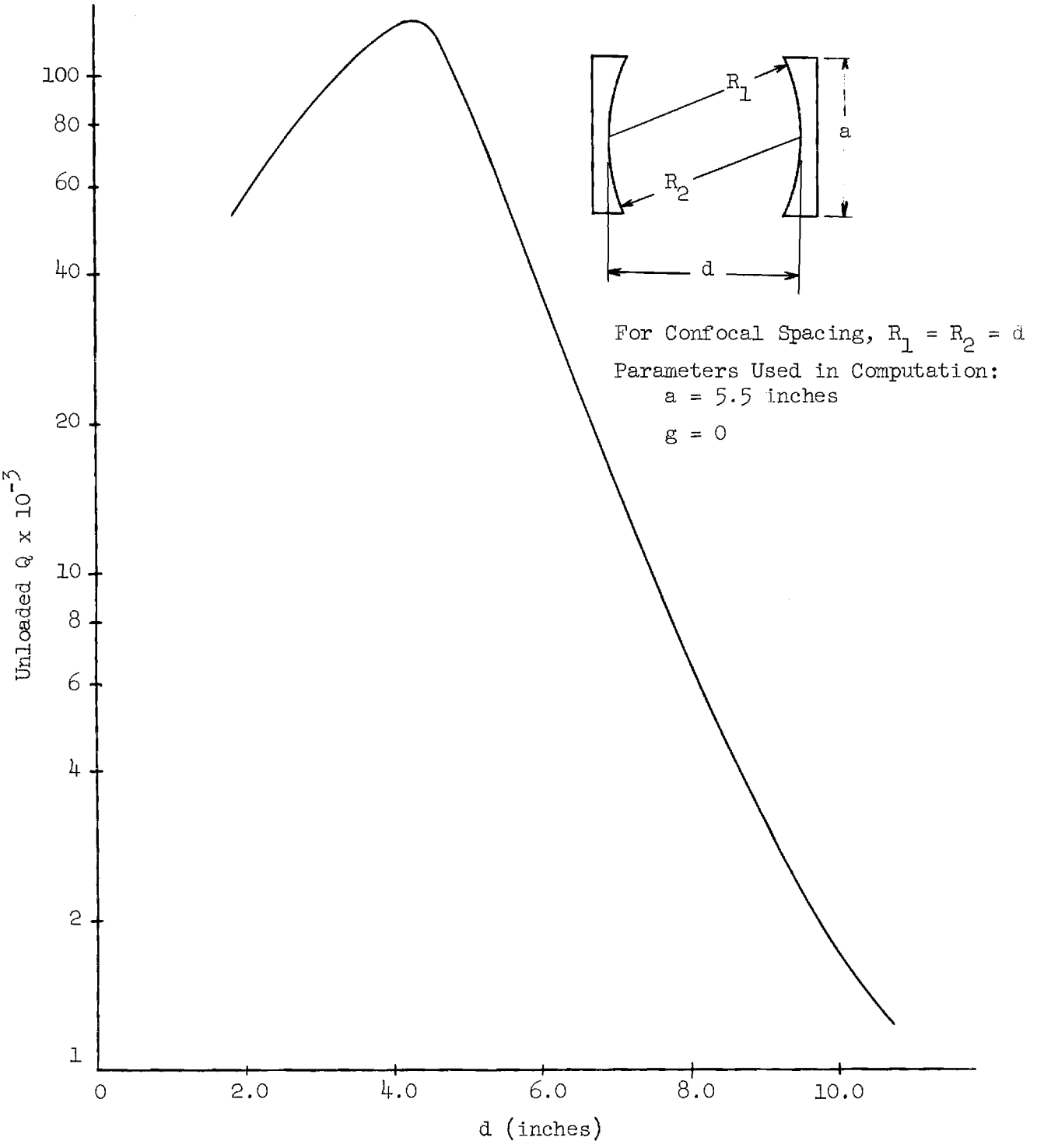

Figure 6. Q of the Confocal Fabry-Perot Resonator as a Function of Reflector Spacing

III. EFFECTS OF SAMPLE LOADING ON THE LOADED Q OF THE OPEN BOUNDARY RESONATOR

The criterion established in Section I for evaluation of the applicability of a resonator structure to ESR measurements depends on a knowledge of three parameters: (1) the resonator quality factor Q, (2) the filling factor η, and (3) the deterioration in Q caused by a lossy ESR sample. Parameters (1) and (3) can be determined by microwave measurements alone, while parameter (2) is more easily determined by employing comparative ESR measurements.

A multipurpose measurement set-up was devised to determine the microwave characteristics of the open boundary resonators constructed during this research program. This set-up, whose block diagram is shown in Figure 7, was used to determine the spectrum of resonance modes between 8.0 and 12.4 GHz, and to accurately measure the Q and center frequency of the individual resonance modes within this broad band. This basic set-up was also used to study the mode configuration of the DCR and comprised the microwave portion of the ESR spectrometer which will be described in Section IV of this report.

The accuracy of frequency measurements made using the sweep generator was improved by superimposing a calibrated cavity wavemeter resonance line on the resonant spectrum of the test cavity. In this manner the resonant frequency of each mode was determined by the wavemeter scale instead of the

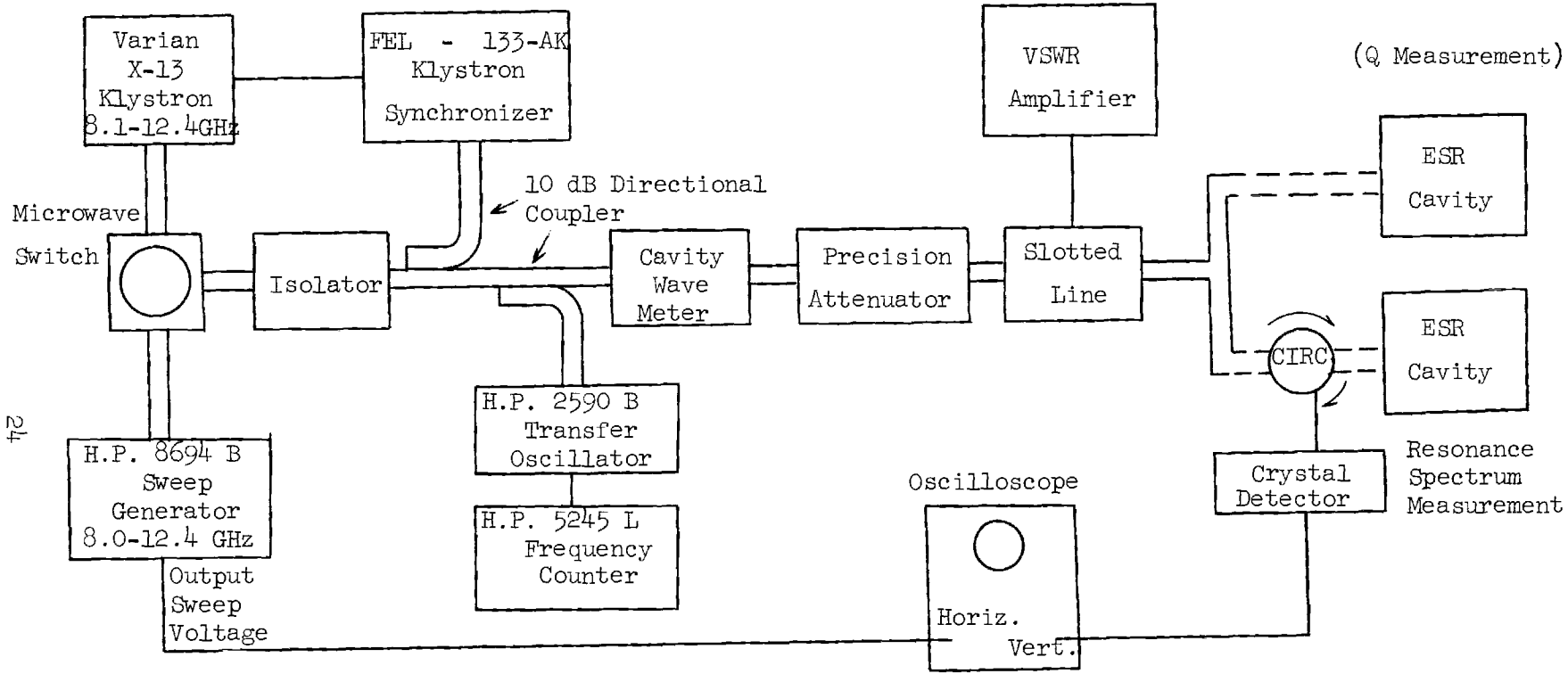

Figure 7. Block Diagram of Microwave Test Set-Up Used in the Measurement of ESR Cavity Characteristics

internal sweep generator frequency marker. The accuracy of frequency measurements using this scheme is estimated to be ± 4 MHz; while frequency measurements performed with the klystron oscillator and electronic frequency counter were estimated to have an accuracy of ± 10 kHz.

A. Microwave Characteristics of the Dielectric Tube Resonator

The Q of the design resonance mode (TE_{014}) was measured using the VSWR technique as outlined by Ginzton[14]. In this technique, the loaded Q, which includes the effects of losses in both the coupling network and the resonator, is calculated from measurements of the voltage standing wave ratio (VSWR) as a function of frequency at resonance. By noting the shift in position of the standing wave null from its value at resonance to its value at some frequency far removed from resonance, one can determine if the cavity is overcoupled or undercoupled. For the undercoupled case,

$$\beta = \frac{1}{(VSWR)_o} \quad , \tag{14}$$

where β is the coupling coefficient and $(VSWR)_o$ is the voltage standing wave ratio at resonance. In the experimental procedure, (VSWR) is measured as a function of frequency and the loaded Q is calculated by determining the two frequencies ν_1 and ν_2 corresponding to the half power voltage standing wave ratio $(VSWR)_{\frac{1}{2}}$ which for the undercoupled case is given by

$$(VSWR)_{\frac{1}{2}} = \frac{1 + \beta + \beta^2 + (1 + \beta)\sqrt{1+ \beta^2}}{\beta} \quad . \tag{15}$$

Figures 8 and 9 show the variation of (VSWR) with frequency for the TE_{014} DCR employing Spectrosil and sapphire respectively. The unloaded

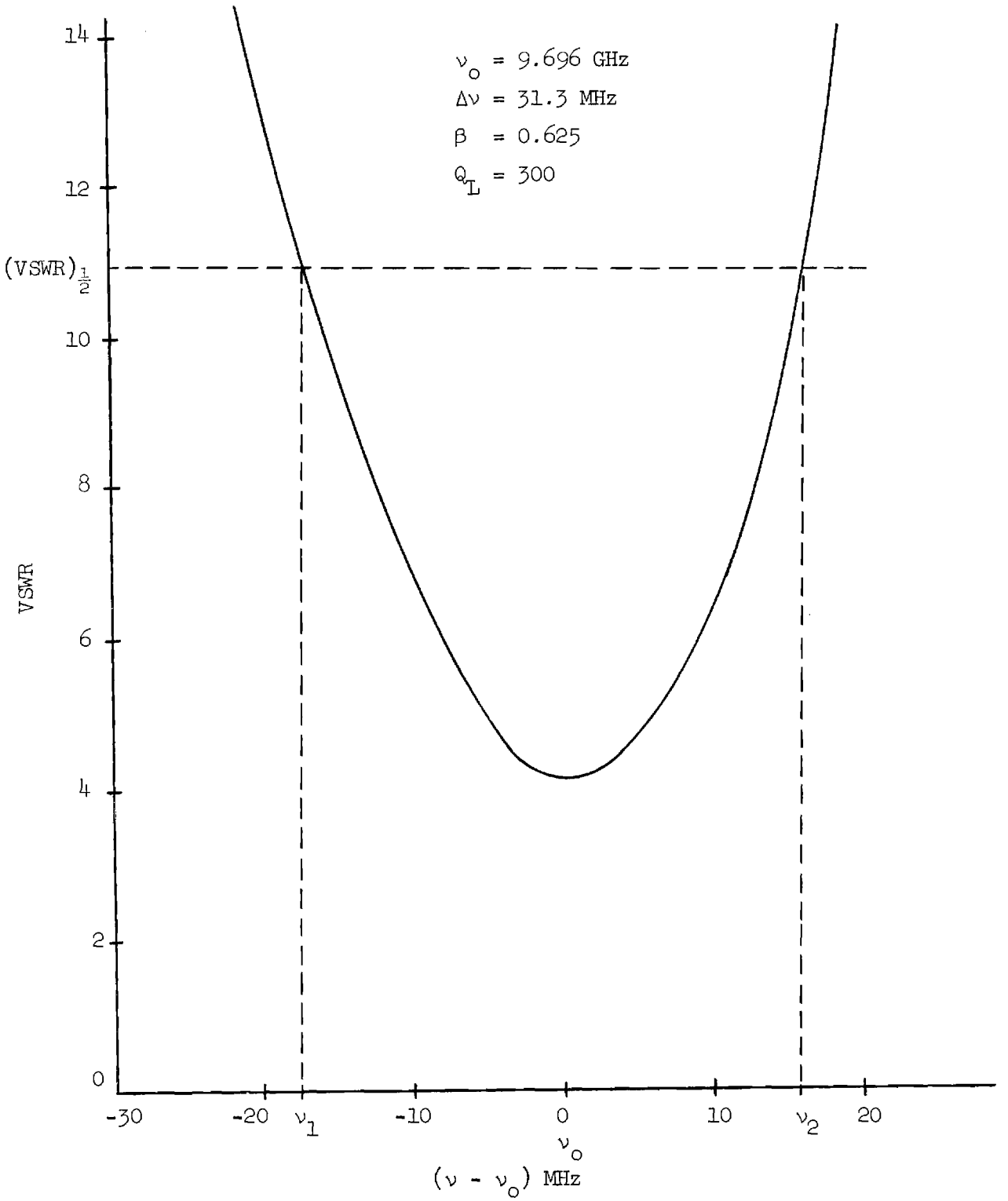

Figure 8. Resonance Characteristic for a Spectrosil DCR in the TE_{014} Mode, with a/b = 0.9016, and ν_o = 9.696 GHz

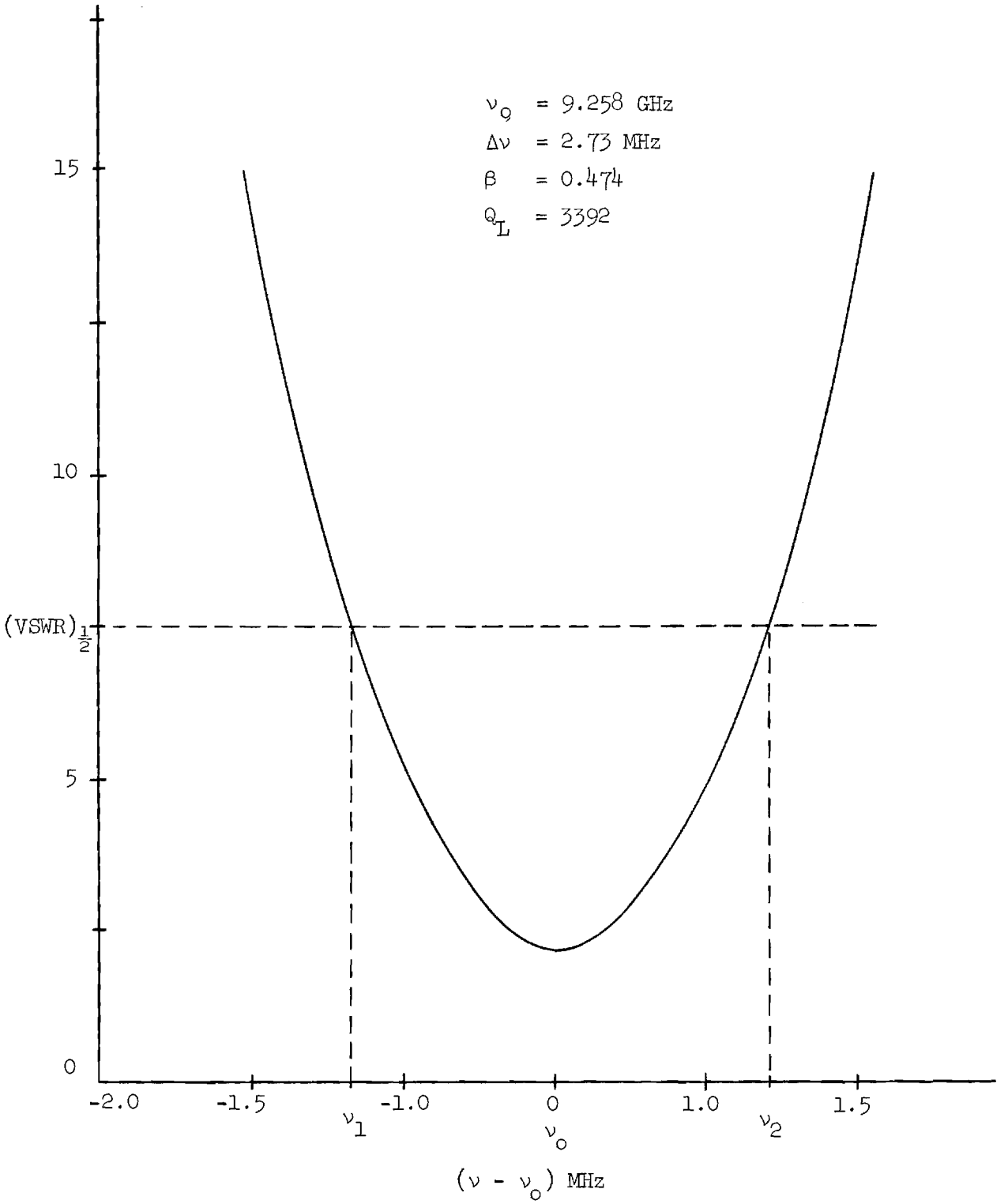

Figure 9. Resonance Characteristic for a Sapphire DCR in the TE_{014} Mode with a/b = 0.878, and ν_o = 9.258 GHz

quality factor Q_O, which is related to the loaded quality factor Q_L by the expression

$$Q_L = \frac{Q_O}{1 + \beta} \quad , \tag{16}$$

represents the effects of internal losses on the cavity resonance, while Q_L represents the effective Q which is "seen" by the microwave transmission line connecting the cavity to the source. The losses represented by Q_L include the cavity losses and the power lost in the coupled resistance. When $\beta = 1$, the coupled resistance is equal to the equivalent cavity series resistance, and the cavity is said to be critically coupled. From Equation (14), it can be seen that $(VSWR)_o = 1$ when the resonator is critically coupled.

The loaded Q of the Spectrosil DCR was found to be lower than one would expect from a high purity quartz. For example, Rosenbaum[8] reported a Q_L of 770 for a quartz DCR operating in the TE_{014} mode. The initial design cavity employing Spectrosil exhibited a Q_L of about 250-300 with β between 0.2 and 0.25. In addition, the resonant frequency was found to be approximately 9.7 GHz for both tubing sizes strongly suggesting that this sample of Spectrosil has a slightly different dielectric constant than that of pure quartz.

Several possibilities were investigated in an effort to determine the loss mechanism responsible for the unexpected low Q. Since the loss tangent of Spectrosil should be comparable to that of pure fused quartz ($\tan \delta = 2.5 \times 10^{-4}$), the initial investigation was focused on those loss mechanisms which might be traced to construction techniques. The most

likely candidates were the surface finish of the aluminum end plates and the finish of the dielectric tubing which together could affect the field configuration by modifying the boundary conditions at any point for which an air gap was found to exist on the plane of intersection.

The initial technique for cutting the Spectrosil tubing to length involved use of a diamond wheel cutting saw followed by a grinding process to insure parallelism of the two ends. This process resulted in some chipping at the ends of the tubing. A new process was evolved which greatly reduced the chipping and resulted in smooth glazed finish on the ends of the tubing. In this process, a more accurate cutting saw was used thereby eliminating the grinding step used in the original process, and the ends of the tubing were fire polished to produce the glazed finish. The metal end plates were also lapped and repolished to provide a much smoother surface than was originally thought to be necessary.

The results of the measurement of Q_L and Q_0 for this improved cavity are shown in Table III. Both a circular iris and a slit iris were employed with variable widths to obtain the optimum coupling coefficient. The optimum coupling coefficient is defined as that value of coupling which yields the maximum change in reflection coefficient for an incremental change in the equivalent cavity resistance. This definition will be related to ESR sensitivity in Section IV. These measurements showed that an unloaded Q of 1100 could be obtained in the TE_{015} mode, and a value of 485 could be obtained for the TE_{014} mode with an optimum coupling coefficient. The maximum Q_0 obtained for the original cavity was 386 in the TE_{015} mode, and 374 in the TE_{014} mode.

TABLE III. MODE CHARACTERISTICS OF A DCR EMPLOYING SPECTROSIL TUBING

a/b	Mode	f_0(GHz)	Iris	β	Q_L	Q_0
0.9016	TE_{015}	11.684	C - 3/16"	0.06	1021	1021
0.9016	TE_{015}	11.680	C - 1/4"	0.162	946	1103
0.9016	TE_{015}	11.669	C - 5/16"	0.270	684	868
0.9016	TE_{015}	11.676	S - 3/16"	0.389	633	879
0.9016	TE_{015}	11.676	S - 3/16"	0.970*	285	570
0.9016	TE_{014}	9.704	C - 1/4"	0.08	485	485
0.9016	TE_{014}	9.696	C - 5/16"	0.278	313	397
0.9016	TE_{014}	9.646	S - 3/16"	0.05	459	482
0.9016	TE_{014}	9.644	S - 3/16"	0.625*	292	475
0.9016**	TE_{014}	9.704	C - 5/16"	0.295	313	405
0.9016	TE_{012}	9.883	C - 5/16"	0.526	170	324

C - Circular Iris

S - Slit Iris

* - Cavity Matched with Slide Screw Tuner

** - Plexiglass Yoke Support

The relatively low value of Q_0 obtained for the TE_{014} mode is puzzling in view of the significant improvement obtained for the TE_{015} mode. The possibility of field perturbations caused by the nylon rod supporting structure was investigated since Becker's[11] paper shows the E_θ field to fall off as r/λ_o, and hence the radial extent of the E_θ field is greater for the TE_{014} than for the TE_{015} mode. A plexiglass yoke assembly was constructed to press the end plates firmly against the dielectric tubing while removing the supporting structure several inches outside the radius of the end plates. As shown in Table III, no improvement in Q_0 was found for either mode. The parallelism of the end plates was investigated although no effects were expected from slight misalignments since the DCR is a slow wave structure. Metal shims were placed between the dielectric tube and the metal end plate to change the alignment of the end plates, and as expected, no significant changes in Q were measured.

The dependence of Q on losses in the dielectric tubing was estimated by constructing a TE_{012} cavity from the Spectrosil tubing with $a/b = 0.9016$. From Equation (2) it is clear that the power dissipated in dielectric losses should decrease by a factor of two if the length of the dielectric tubing is reduced by the same factor. Thus, if the dielectric loss is the dominant factor causing the low value of measured Q, one would expect the Q to be approximately the same for the TE_{012} and TE_{014} cavities since the stored energy is proportional to the mean square value of the magnetic field over the cavity volume. On the other hand, if the dielectric losses are insignificant compared to the other loss mechanisms, then one would expect the Q of the TE_{012} cavity to be about half the Q of the TE_{014} cavity. The results

of this experiment as presented in Table III show that the unloaded Q remained very nearly the same for the two modes. The conclusion drawn from this experiment was that the Spectrosil tubing has a higher loss tangent than the purest form of fused quartz. Further calculations or experiments were not attempted since the maximum Q which could be achieved with the Spectrosil cavity was considered unsuitable for ESR applications.

A final DCR was designed around a synthetic sapphire tube. An optical grade Linde sapphire rod was machined by Insaco Incorporated to the dimensions calculated in Section II for the TE_{014} mode. The dielectric properties of sapphire (Al_2O_3) in the microwave region have been accurately measured and reported by Von Hippel.[15] Sapphire is a rhombohedral hexagonal crystal whose optic axis is along the diagonal of the distorted cubic primitive cell. The dielectric constant at 9.5 GHz for the electric field vector perpendicular to the optic axis is 8.6, while the dielectric constant for the electric field vector parallel to the optic axis is approximately 10.6. The loss tangent for single crystal sapphire is 2×10^{-4} at 9.5 GHz.

When sapphire is grown from the melt, the optic axis is determined by the orientation of the seed crystal and is generally not in the direction along which the boule is pulled from the melt. Thus, for a given sapphire rod the angle of the optic axis may assume a random orientation with respect to the axis of the rod. Unfortunately, this arbitrary relationship between the crystal structure and the axis of the boule was not recognized at the time the tube was machined and the optic axis was not specified in any definite direction. The random direction of the optic axis leads to an interesting interaction between the coupling iris and the orientation of

the sapphire tubing about its own axis. This interaction, while objectionable for the present design, could possibly prove useful in the optimum design of a cavity to accommodate a more exotic sample holding configuration.

Table IV summarizes the properties of a number of modes in the sapphire DCR between 8.9 and 10.3 GHz. For comparison, the properties of the Varian TE_{012} waveguide cavity, equipped with a radiation window, are also presented. Five additional modes were found between 10.3 and 12.4 GHz, but were not investigated because the coupling was not high enough to provide adequate sensitivity in an ESR application. It is immediately obvious from Table IV that the mode structure for the sapphire DCR is much more complex than that of the Spectrosil DCR. The assignment of integer values to the quantum numbers k and m are tentative, whereas the assignment of the axial mode number n was made with a high level of confidence.

The identification of mode type for each resonance was investigated by probing the electric and magnetic fields both inside and outside the dielectric tube. The electric field probe consisted of a small diameter copper rod, and the magnetic field was probed by measuring the ESR coupling of the microwave magnetic field to a 2 mm bore quartz capillary tube filled with DPPH.

Identification of the TE_{0mn} modes was straight forward since all field components possess axial symmetry, and only the E_θ component is zero on the cavity axis. The radial field dependence for the TE_{01q} modes was shown in Figure 2. Hybrid modes are characterized as those modes having axial components of both the electric and magnet fields. Hybrid modes cannot possess axial symmetry, and the modes shown in Table IV appear to be the lowest order hybrid mode for which k = 1. Determining the radial mode

TABLE IV. MODE CHARACTERISTICS OF A DCR EMPLOYING SINGLE CRYSTAL SAPPHIRE TUBING

ν_o(GHz)	β	Q_L	Q_O	$E_\theta = 0$ at centerline	$H_z = 0$ at centerline	Tentative Mode Identification
8.959	0.827	2861	5227	Yes	No	TE_{0p3}
8.975	0.413	4290	6062	Yes	No	TE_{0p3}
9.258	0.474	3392	5000	Yes	No	TE_{014}
9.564	0.151	1428	1644	Yes	Yes	HE_{1p4}
9.749	0.543	781	1205	Yes	Yes	HE_{1p4}
10.263	0.675	779	1305	Yes	Yes	HE_{1p5}
10.296	0.383	1227	1697	Yes	Yes	HE_{1p5}
9.526*	0.417	1732	2518			TE_{012}

*Varian TE_{012} Waveguide Cavity equipped with radiation window

number, m, was not attempted because of the difficulty involved with implementing a radial electric field probe. It was determined that both the electric and magnetic fields are equal to zero on the cavity axis for the four hybrid modes shown in Table IV, whereas both field components were definitely non-zero near the walls of the dielectric tube.

The existence of an off axis symmetry direction for the sapphire tube was confirmed by noting the behavior of the mode spectrum as the sapphire tube was rotated about its own axis. A ruled alignment plate was constructed to hold the sapphire tube in precise axial alignment and to permit indexing of the angular position of the tube with respect to its own axis. The sapphire DCR, its coupling plate, and the alignment plate are shown in Figure 10. It was found that rotation of the sapphire tube caused changes in both the coupling coefficient and resonant frequency of the cavity modes. Mode amplitudes were observed to grow and then recede with closely spaced pairs exhibiting an "out of phase" relationship. It is very likely that the difference in the measured TE_{014} mode resonant frequency (9.258 GHz), and the design resonant frequency (9.500 GHz) can be attributed to an effective dielectric constant that lies somewhere between the values $\epsilon_r = 8.6$, and $\epsilon_r = 10.6$. Computer calculations predict an effective dielectric constant of $\epsilon_r = 9.2$ for an equivalent isotropic dielectric tube with the sapphire tube's dimensions and a resonant frequency of 9.258 GHz. It must be remembered, however, that the field configurations are not known for an anisotropic material, and the isotropic model used in the above calculation may not be valid.

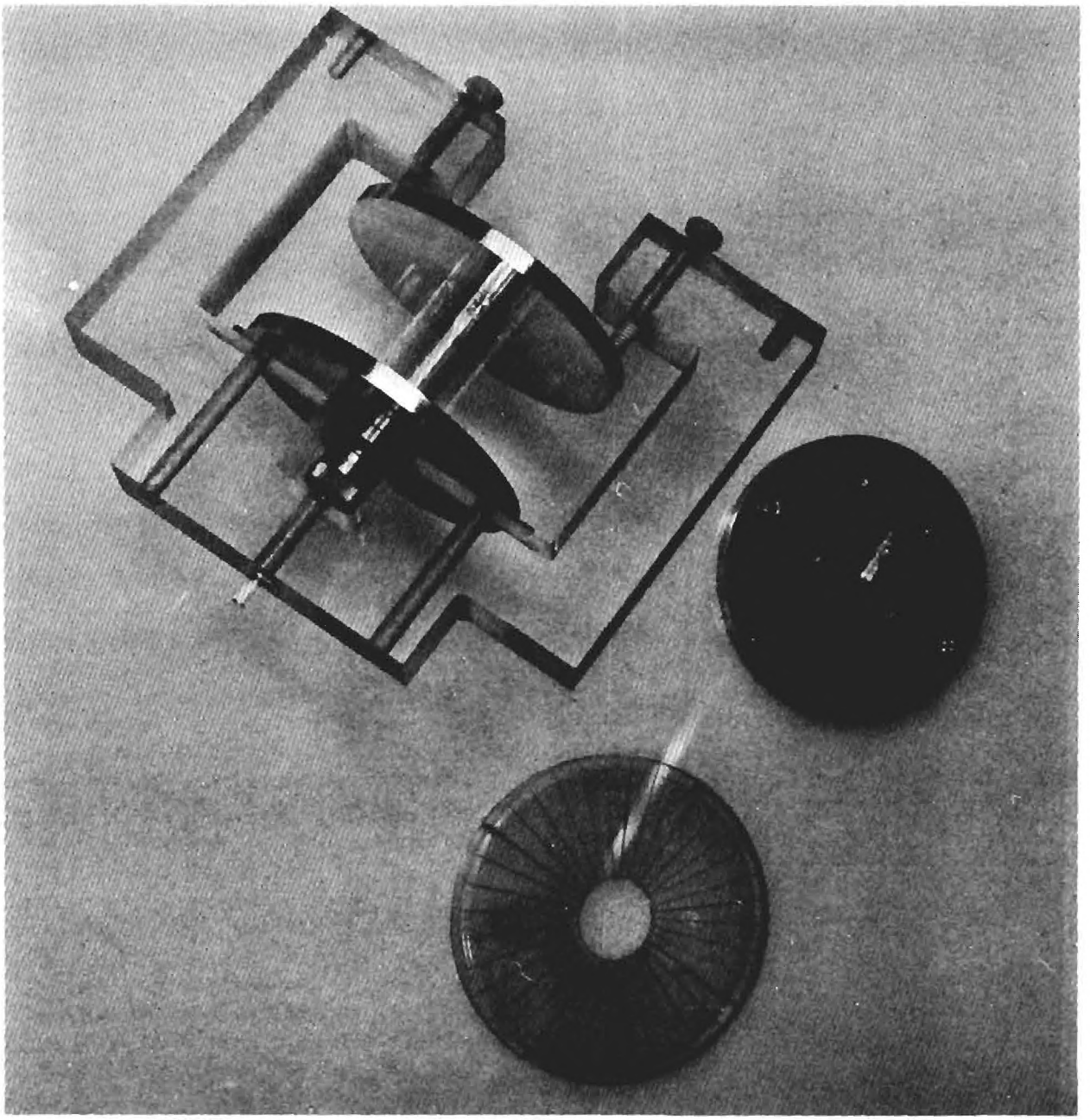

Figure 10. Photograph of the Sapphire DCR

The detailed behavior of the TE_{014} mode is shown in Figure 11. In this figure, the microwave coupling coefficient, the deviation in resonant frequency, and the ESR coupling strength have been plotted as functions of the rotational position of the sapphire tube. It can be seen that the non-zero axial magnetic field necessary for ESR coupling is present only for limited angular regions over one full revolution of the tube. It is possible that this behavior is the result of two or more distinct modes being combined with smoothly varying amplitude functions. Although the exact form of mode coupling is not as yet understood, it is clear that the coupling mechanism depends on the anisotropic dielectric properties of the single crystal sapphire. One would not, for example, expect any variation for an amorphous material or a crystalline material whose microwave transmission properties possessed axial symmetry. This experiment was repeated with the Spectrosil tubing and no variations were observed.

For the TE_{014} mode, the sapphire DCR exhibited an unloaded Q of 5000. Two other TE modes at 8.98 and 8.96 GHz exhibited unloaded Q's of 6152 and 4992 respectively. All three modes coupled strongly to the DPPH sample, but the TE_{014} mode was chosen for the ESR experiments because of its resonant frequency is closer to the Varian waveguide cavity which is designed for operation at 9.5 GHz. As shown in Table IV, the Q of the sapphire DCR is higher than the Q of the Varian TE_{012} waveguide cavity by about a factor of two.

An important measure of performance for an ESR cavity is the degradation in Q caused by lossy samples. Since many ESR samples are more conveniently

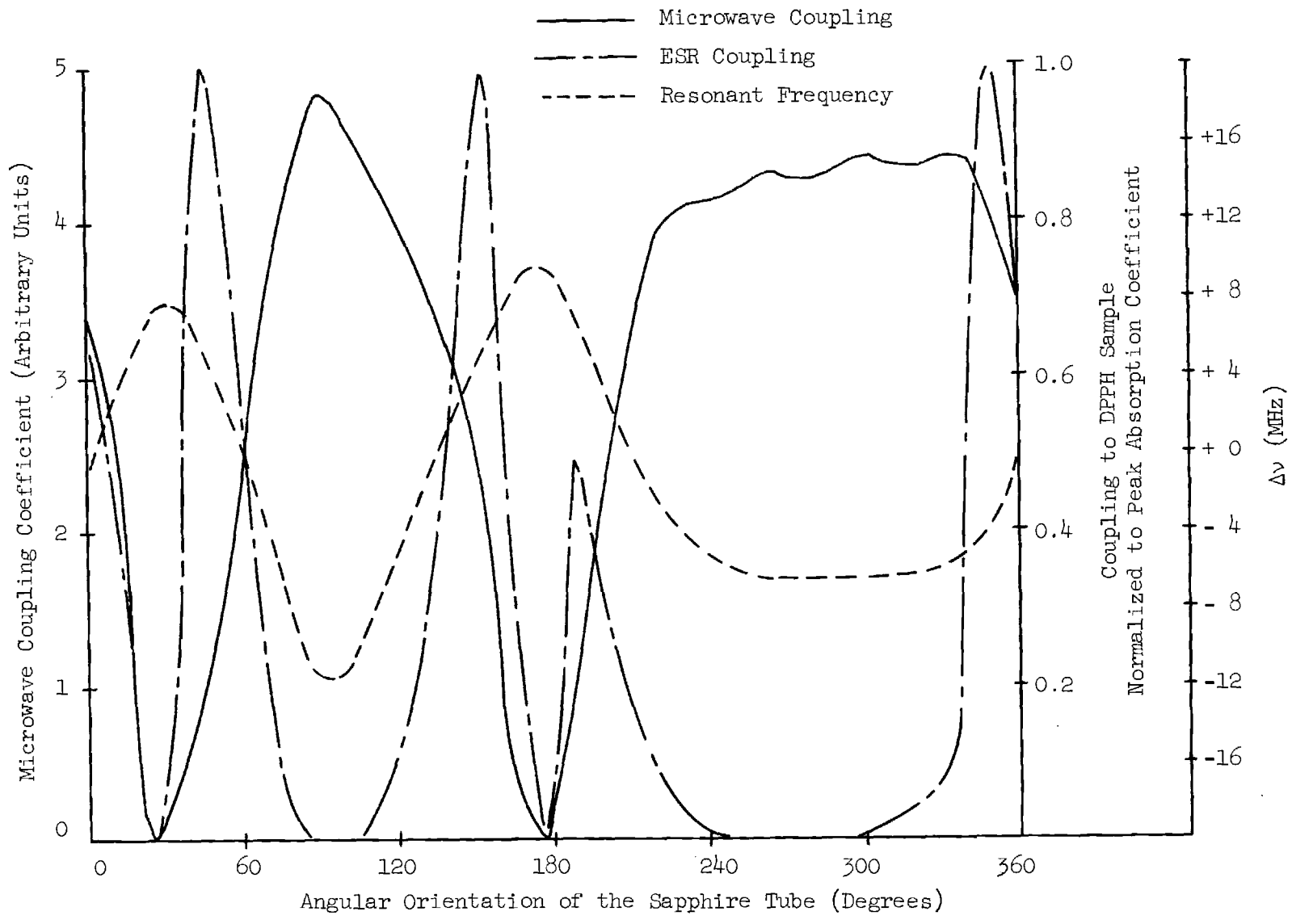

Figure 11. Dependence of the DCR Coupling Characteristics on the Angular Position of the Sapphire Tube About Its Axis

prepared by dissolution in one of the common solvents, measurements were made to determine the degradation in Q caused by placing a 3 mm bore capillary tube containing a lossy solvent on the DCR axis. Various solvents were chosen to cover a range of dielectric constants between 1.7 and 55.

The resonant frequency, coupling coefficient, and loaded Q were measured for each solvent, and are summarized in Table V. In each case the dielectric loading caused the coupling coefficient to change slightly, hence the degrading effect of the solvent is represented by the unloaded quality factor, Q_0, and not by Q_L. Of all the solvents tested, toluene had the least effect on Q_0 while dimethyl sulfoxide had the greatest. Water, with its high dielectric constant and loss tangent, completely quenched the cavity Q. It was interesting to note that hexafluoroisopropanol, a protein solvent, reduced the Q only by a factor of two.

B. Microwave Characteristics of the Fabry-Perot Resonator

Two Fabry-Perot resonators were constructed during this research program. The initial prototype employed eight-inch diameter spherical reflectors with nearly confocal spacing. The reflectors were mounted on a precision bed so that the spacing could be varied while maintaining the proper alignment. The frequency interval between resonant modes for a Fabry-Perot cavity is approximately given by

$$\Delta\nu \simeq \frac{C}{2d} \quad ,$$

provided the axial mode number n is large with respect to unity. Thus for a reflector spacing of 11.8 inches, one would expect axial modes to occur

TABLE V. PROPERTIES OF THE SAPPHIRE DCR WITH LOSSY SAMPLE LOADING

Sample[1]	ϵ_r	tan δ	ν_o (GHz)	Mode	β	Q_L	Q_o
Reference[2]			9.256	TE_{014}	0.474	3392	5000
DPPH[3]			9.251	TE_{014}	0.454	3425	4980
10^{-4} Molar[4] DPPH	2.28[+]		9.250	TE_{014}			
Ethanol	1.7[*]	0.068[*]	9.252	TE_{014}	0.143	2020	2309
Toluene	2.44[+]		9.254	TE_{014}	0.426	3018	4304
Methanol	8.9[*]	0.810[*]	9.248	TE_{014}	0.143	1505	1720
Acetone	20.7[†]		9.244	TE_{014}	0.186	2015	2390
Nitro-benzene	31.1	0.166	9.249	TE_{014}	0.085	1413	1533
Dimethyl Sulfoxide			9.246	TE_{014}	0.260	1090	1373
Hexafluora-isopropanol			9.253	TE_{014}	0.141	2020	2305
Water	55[*]	0.540[*]	--	TE_{014}	0.001	--	--

1. Sample volume = 0.313 cm^3

2. Reference sample contained empty Spectrosil tube (3 mm bore x 0.6 mm wall) on cavity centerline

3. 0.387 grams 2,2-Diphenyl-1-Picrylhydrazl (Free Radical)

4. 10^{-4} solution of DPPH in benzene

[*] A. R. VonHippel, Dielectric Materials and Applications, The M.I.T. Press, Cambridge, Mass., 1954

[+] Handbook of Chemistry and Physics, The Chemical Rubber Co., 47th Edition, 1967

[†] American Institute of Physics Handbook, McGraw-Hill, New York, 1957

at intervals of 0.501 GHz. Using the sweep generator, modes were observed at 9.5 GHz (n = 19), and at intervals of approximately 0.5 GHz over the range 8.0 to 12.4 GHz. The resonator Q of any mode in this range was so high that one could not observe the true line shape using the sweep generator because of its residual FM noise spectrum. This became apparent when no changes were observed in the Q for resonances between 8.0 and 12.4 GHz although the Fresnel number changed from N = 0.92 at 8.0 GHz to N = 1.38 at 12.0 GHz.

Calibration of the sweep generator using a cavity wavemeter provided a means of estimating the Q of the Fabry-Perot resonator. The width of the resonance curve indicated a Q of about 40,000 for all modes between 8.0 and 12.0 GHz. Although the Q could have been measured with greater accuracy using a synchronized klystron oscillator, the measurement would have been unprofitable since the final cavity design was restricted to reflectors of no greater than 5.5 inches in diameter.

A second cavity, whose design parameters were discussed in Section II was constructed with dimensions compatible with the Varian six-inch magnet which was employed in the ESR measurements reported herein. Axial modes were observed at 8.65 GHz (n = 12), 9.35 GHz (n = 13), 10.11 GHz (n = 14), 10.79 GHz (n = 15), 11.54 GHz (n = 16), and 12.27 GHz (n = 17). Coupling to the cavity was achieved with a 0.438-inch diameter circular iris with a thickness of 0.025 inch which was located in the center of the reflectors. A rectangular to square waveguide transition was employed to feed the reflector since the iris diameter was larger than the narrow wall dimension of the rectangular X-band waveguide. A photograph of the Fabry-Perot

resonator and the waveguide coupling transition is shown in Figure 12. The field configuration at the coupling hole will excite the TE_{11} mode in the short section of the square waveguide which feeds the coupling iris and it was found necessary to install H-plane fins in order to reduce the gain of trapped resonant modes in the waveguide transition.

The measured resonance characteristic which is shown in Figure 13 for the TEM_{0013} (9.35 GHz) mode, reveals an unloaded Q of 5180. The diffraction losses were predictably high since the reflectors employed in this cavity were the original eight-inch reflectors which had been turned down to a diameter of 5.5 inches. With a twelve-inch radius of curvature, the g parameter for this cavity is 0.34 and the Fresnel number, N, is 0.98. From Li's[12] calculations the diffraction loss would be about 0.6 per cent, and the unloaded Q would be about 6500. For the same cavity with confocal geometry ($g = 0$), the estimated Q would be about 39,000.

The effects of sample loading on microwave characteristics were investigated by measuring the change in ν_o, β, and Q, as a thin sheet of DPPH was moved along the cavity axis from an electric field maximum to an electric field minimum. The DPPH was allowed to absorb water before the measurements were performed in order to increase its interaction with the electric field. No changes in Q were observed; however, the coupling coefficient decreased from 0.250 at the electric field minimum to 0.136 at the electric field maximum, while the resonant frequency decreased by 2.5 MHz between the same two points.

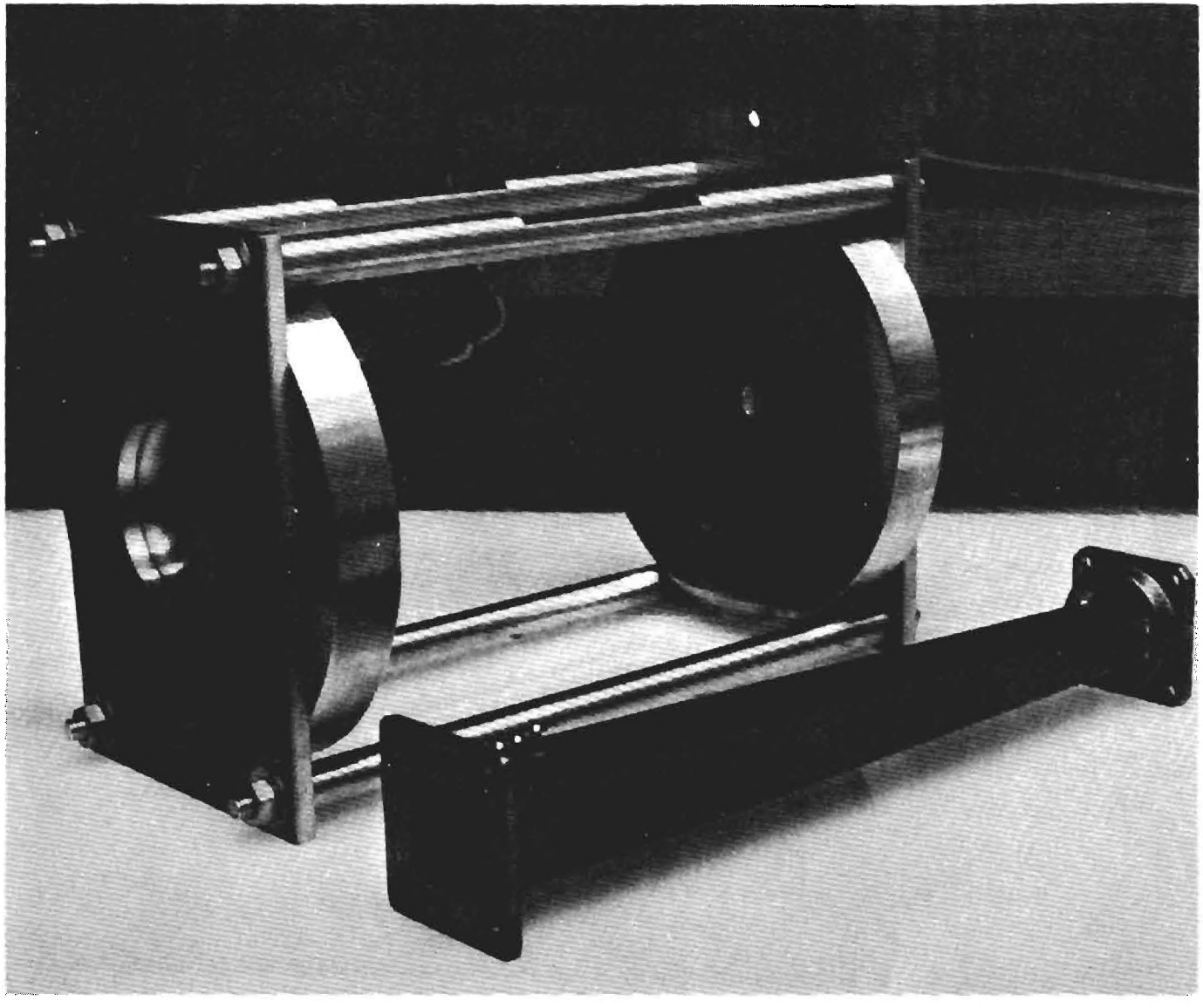

Figure 12. Photograph of the Fabry-Perot Resonator and the Waveguide Coupling Transition

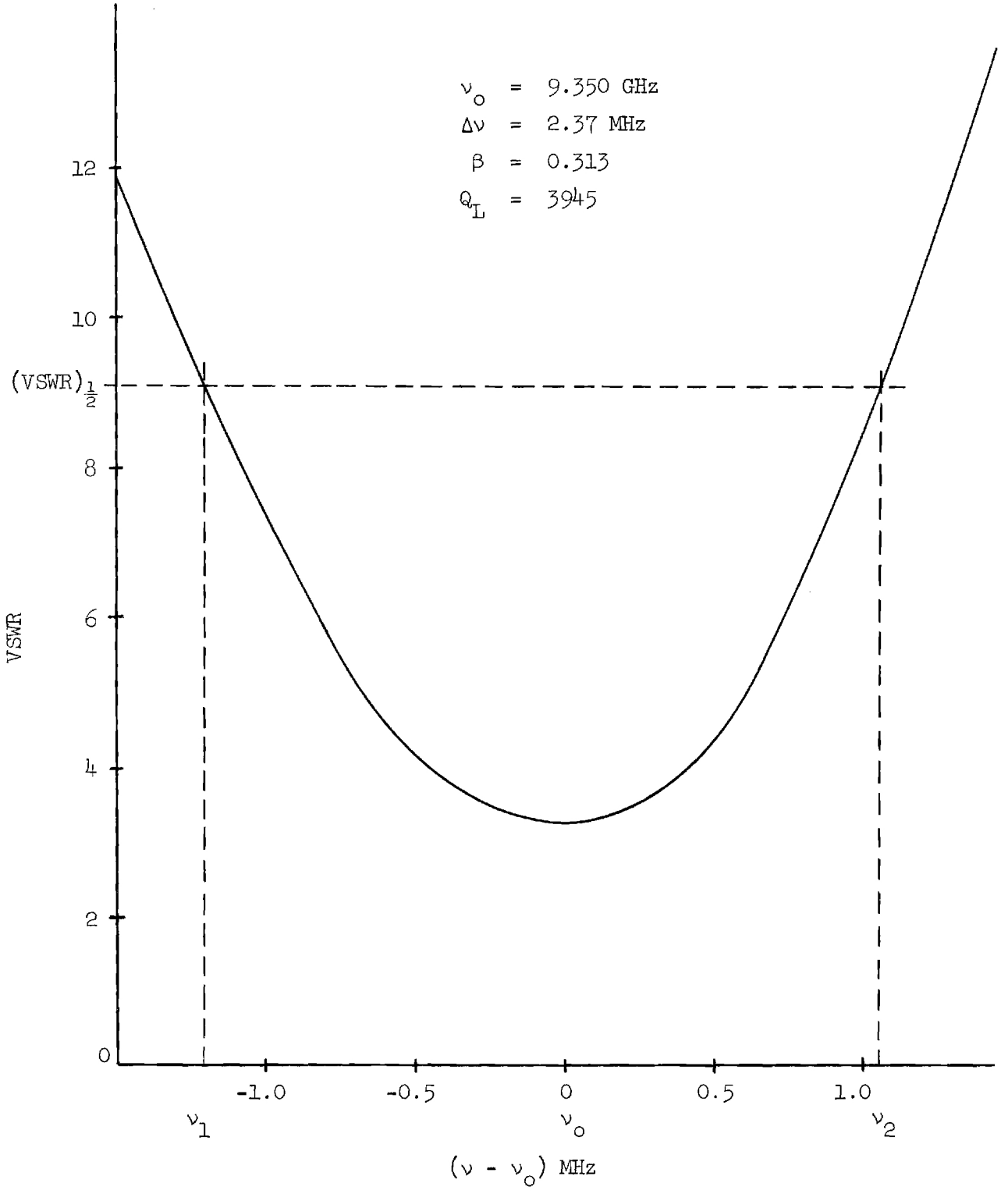

Figure 13. Resonance Characteristics of a Fabry-Perot Resonator in the TEM_{0013} Mode

When the Fabry-Perot cavity was installed between the pole pieces of the six-inch Varian Magnet, it was found that the extension of the pole pieces into the resonator volume caused a severe degradation of the cavity Q and prevented any further ESR measurements with this cavity. Time did not permit the fabrication of another Fabry-Perot resonator; however, it is felt that a comparable Q could be obtained by reducing the reflector diameter to about 4.5 inches and remachining the reflector curvature for a confocal spacing of about 7 inches. As noted earlier, it appears that the Fabry-Perot resonator would best be suited to a larger magnet structure, where the reflector diameter could be made at least six to eight wavelengths at the design frequency. For 9.5 GHz, a pole gap of about seven inches would be required.

IV. ESR MEASUREMENTS ON THE OPEN BOUNDARY RESONATOR

An ESR spectrometer incorporating a Varian Model V-3700 six-inch magnet with a Varian Model VFR-2903 Mark I power supply and field dial control unit was assembled from available microwave and electronic components. The block diagram of this spectrometer, which is shown in Figure 14, illustrates its basic mode of operation. A synchronized klystron oscillator is employed to provide a frequency stability of one part in 10^7. The klystron oscillator is mechanically tuned to the resonant frequency of the ESR cavity, and the magnetic field, which is modulated at a 6 kHz rate, is slowly swept through an amplitude range which includes the sample resonance value. The change in cavity reflection coefficient caused by absorption of power in the ESR sample at resonance is detected in a 6 kHz synchronous detector. The dc output of the synchronous detector provides the input to a chart recorder whose speed is calibrated in terms of the magnetic field sweep.

A photograph of the laboratory installation of the six-inch magnet and the ESR spectrometer is shown in Figure 15. The first prototype Fabry-Perot resonator, with eight-inch reflectors, can also be seen in the background. Details of the mounting assembly for the DCR are shown in Figure 16. The DCR is suspended between the magnet pole pieces by a plexiglass bracket which is mounted to the magnet's yoke assembly. A flexible waveguide section is employed to connect the resonator to the spectrometer's microwave instrumentation. One can easily envision the possibilities for sample illumination which are afforded by this type of cavity installation.

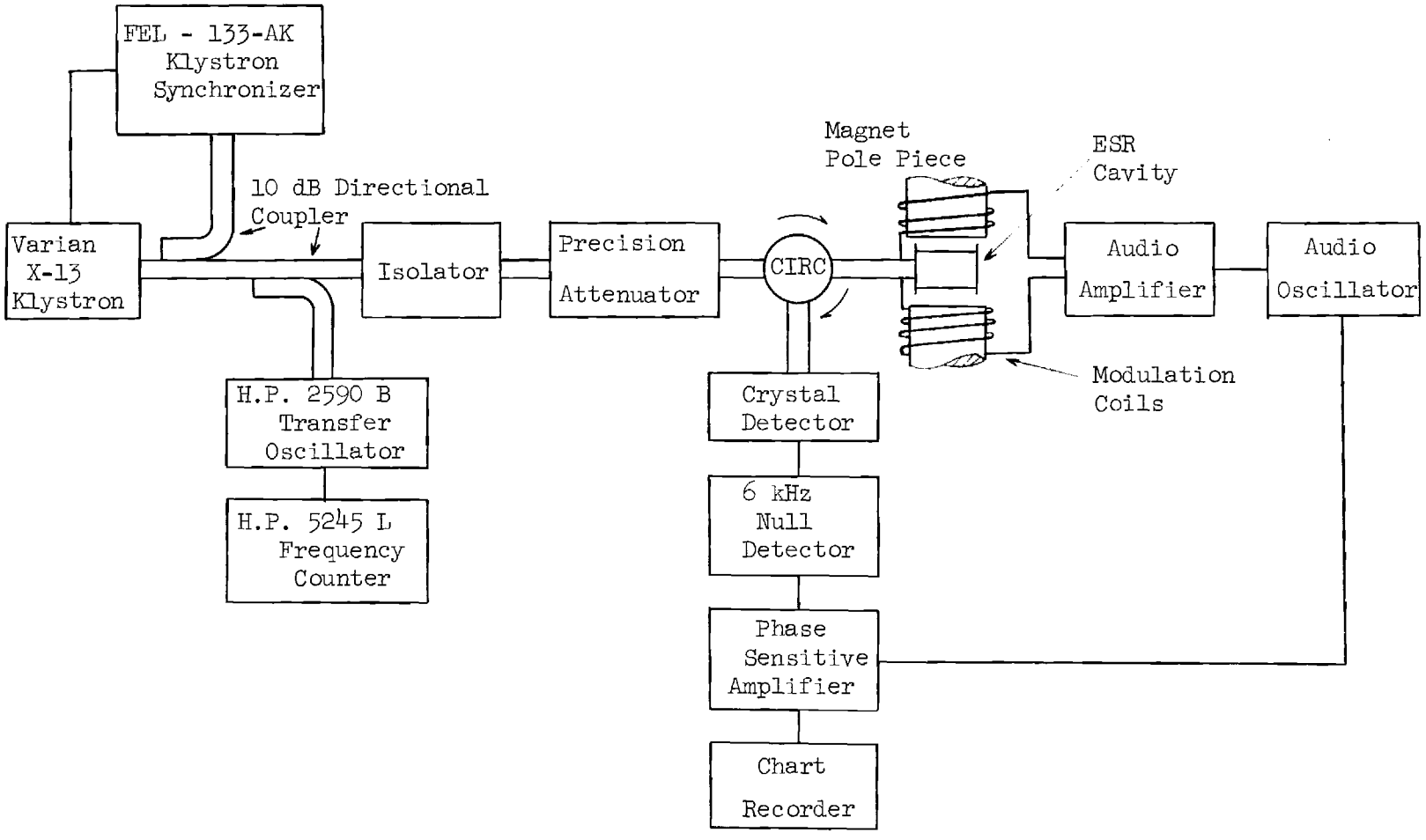

Figure 14. Block Diagram of the ESR Spectrometer

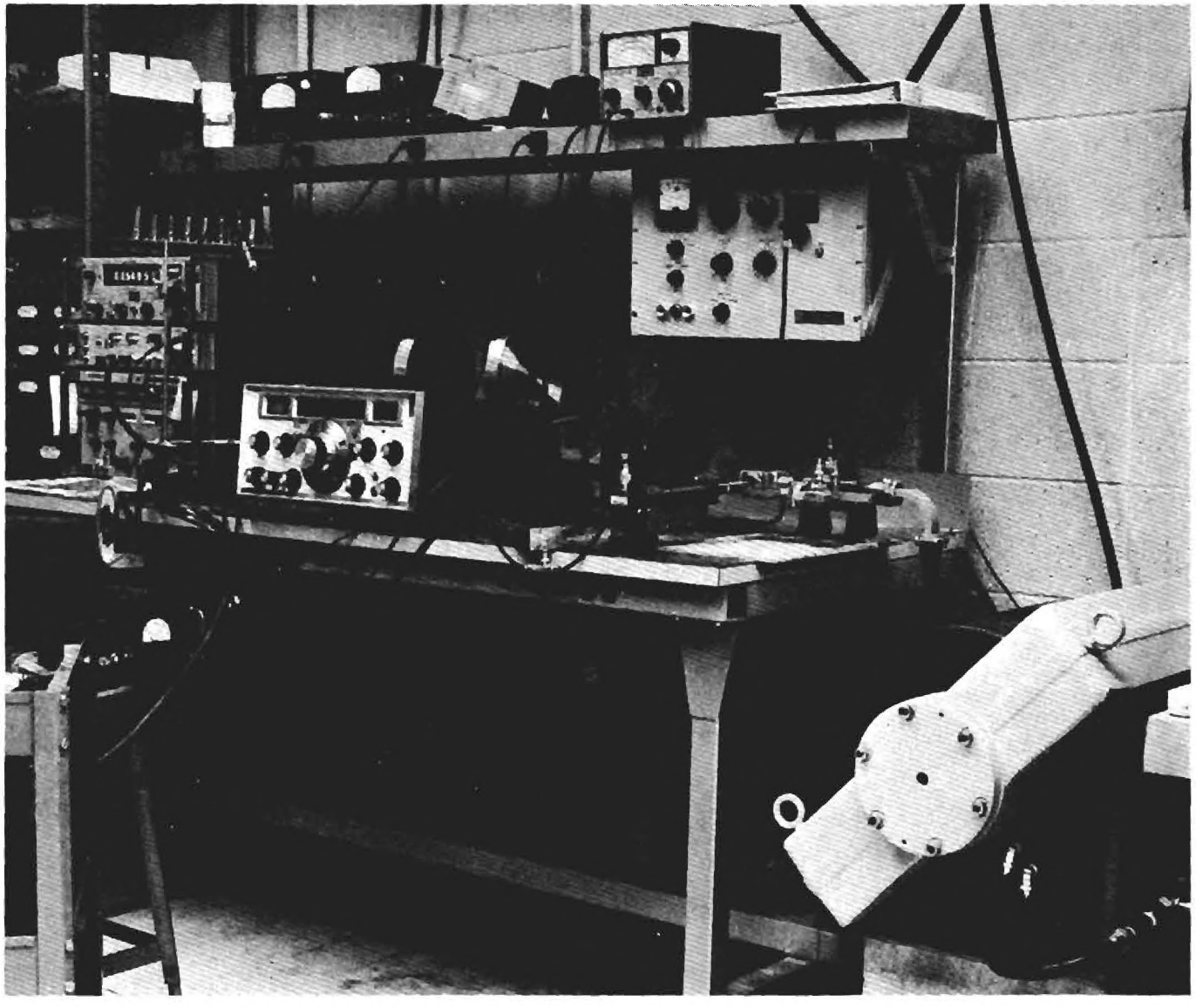

Figure 15. Photograph of the ESR Magnet Installation

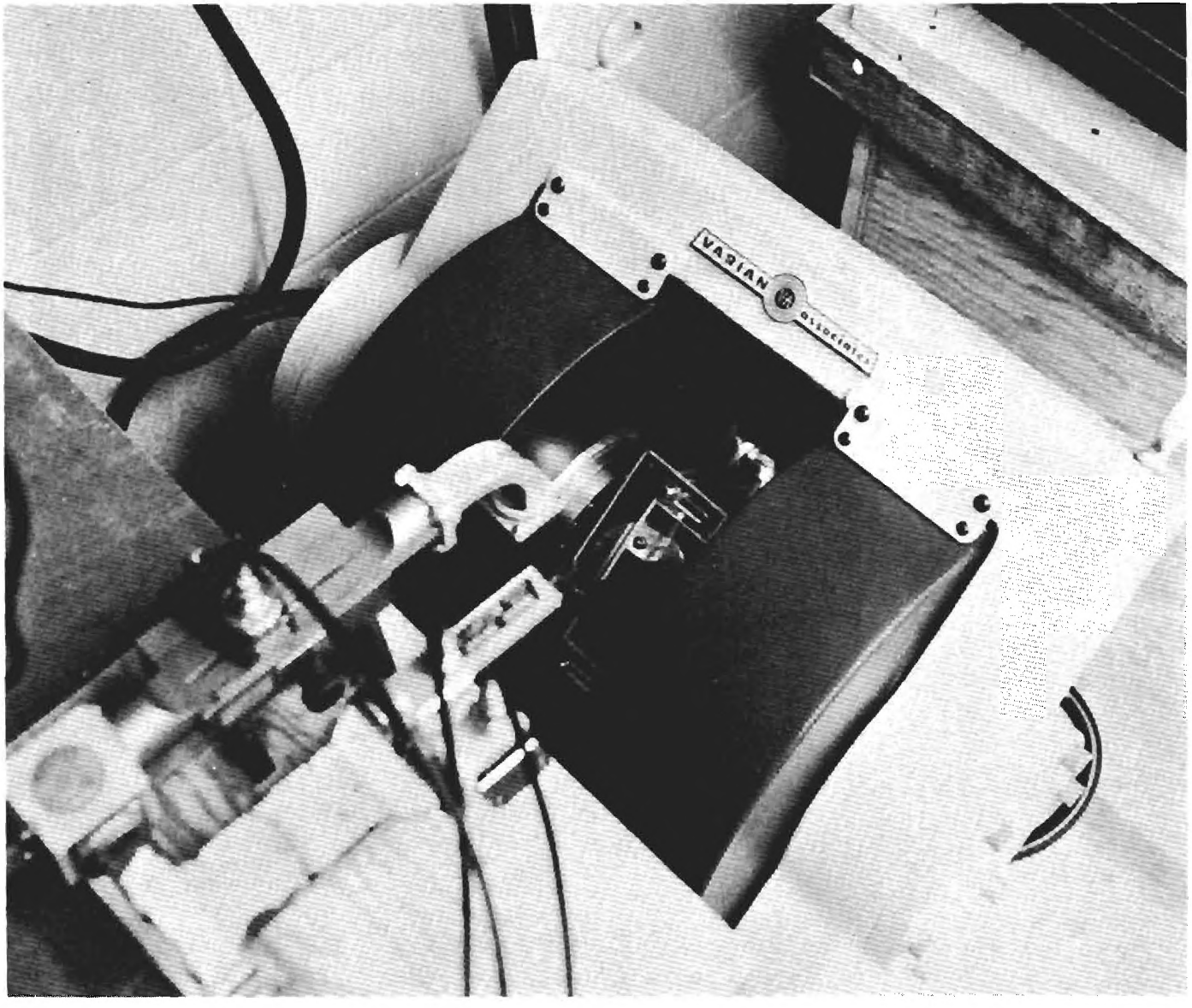

Figure 16. Photograph Showing Details of the Mounting Assembly for the DCR

The spectrometer's measurement capabilities are illustrated in Figure 17, which shows the ESR characteristics of DPPH in a standard Varian TE_{012} waveguide cavity. Figure 17(a) is the ESR absorption characteristic for DPPH and was obtained by connecting a high gain differential amplifier directly to the receiver crystal detector and then recording the microwave power level reflected from the cavity as a function of magnetic field strength. Modulation of the slowly varying magnetic field at a 6 kHz rate produces the modulated absorption characteristic shown in Figure 17(b). This trace was obtained by connecting the chart recorder directly to the output of the 6 GHz receiver amplifier. The modulation amplitude was set approximately equal to the measured absorption linewidth in DPPH (3.53 Gauss), and the level varied over a wide range to insure linearity of the absorption characteristic. The resonance characteristic most often used in the ESR literature is the derivative of the absorption characteristic and is obtained by demodulating the 6 kHz reflected signal in a phase sensitive detector whose reference is derived from the modulation oscillator. Figure 17(c) is the derivative of the absorption characteristics shown in Figure 17(a), and was obtained by connecting the output of the 6 kHz receiver amplifier to a phase sensitive detector and chart recorder as shown in Figure 14.

The absorption characteristics of DPPH in the sapphire DCR are shown in Figure 18. The relative performance of the sapphire DCR was determined by comparing its measured signal-to-noise ratio for detection of electron spin resonance in DPPH with that for the reference Varian TE_{012} waveguide

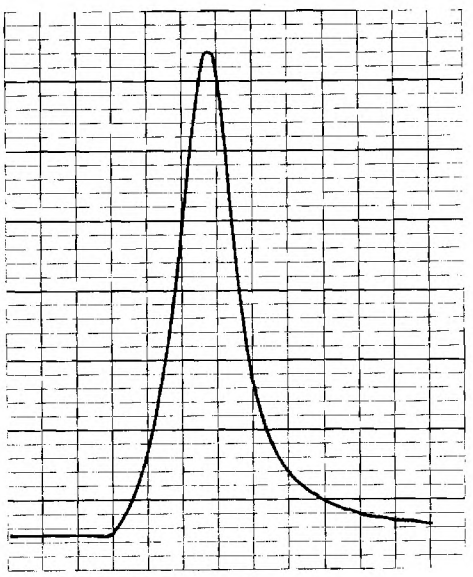

4.0 Gauss/div.

(a) Absorption Characteristic

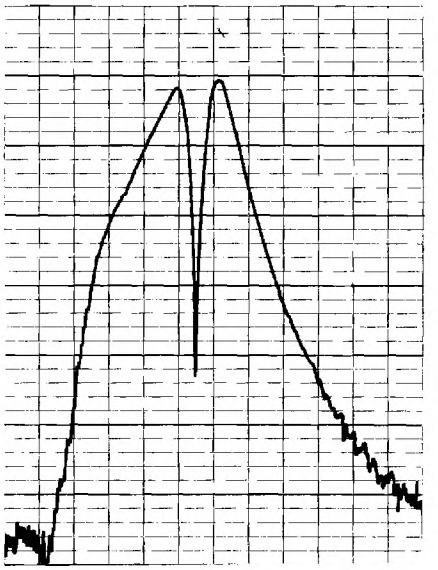

4.0 Gauss/div.

(b) Modulated Absorption Characteristic

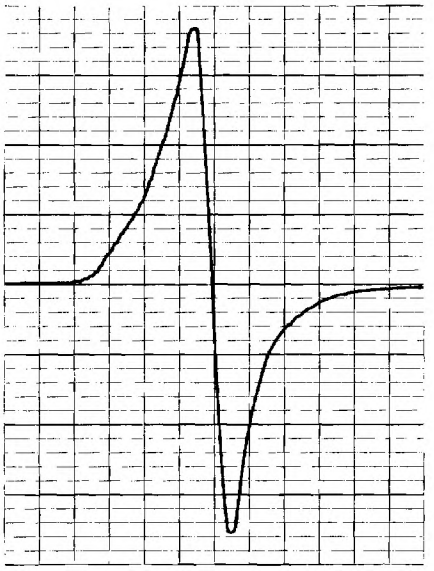

4.0 Gauss/div.

(c) Derivative of Absorption Characteristic

H_o = 3.430 kG

ν_o = 9.526 GHz

Sweep Magnitude = 50 G

Sweep Time = 2.5 min.

Modulation = 5 G at 6 kHz

Figure 17. ESR Characteristics of DPPH in a TE_{012} Waveguide Cavity

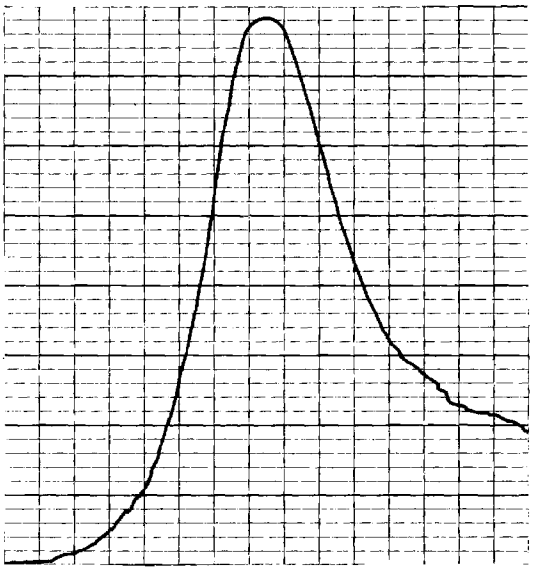

1.0 Gauss/div.

(a) Absorption Characteristic

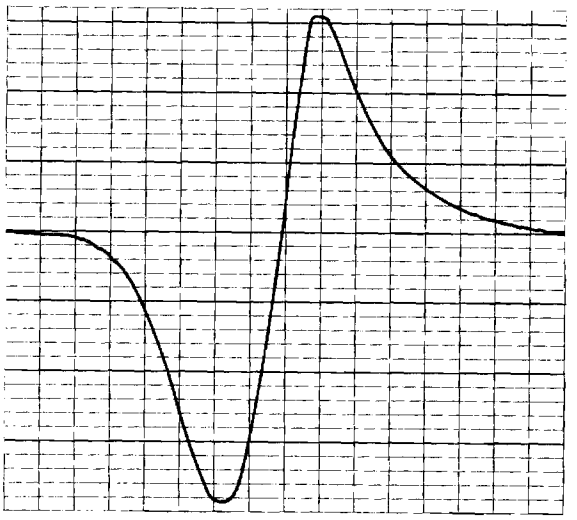

1.0 Gauss/div.

(b) Derivative of Absorption Characteristic

H_o = 3.323 kG

ν_o = 9.258 GHz

Sweep Magnitude = 25 G

Sweep Time = 10.0 min.

Modulation = 5 G at 6 kHz

Figure 18. ESR Characteristics of DPPH in a Sapphire DCR

cavity. The Varian cavity was equipped with a radiation window which degraded its normal Q, but this was considered necessary in view of the design objectives of the DCR in order to afford a fair standard for comparison. For an arbitrary microwave input power level, the relative performance of the two cavities was as follows:

Cavity	ν_0 (GHz)	P_0 (mW)	S/N (dB)	Sample Volume (cc)
Sapphire DCR	9.258	1.0	34	0.32
Varian	9.526	1.0	24	0.16

At resonance, the change in reflected power is equal to the change in power absorbed by the sample in the cavity. Since the power absorbed in the sample is proportional to the sample volume, the net improvement in sensitivity for the DCR would be the increase in S/N given in dB minus the increase in sample volume in dB. Thus, the sapphire DCR would provide an improvement of approximately 7 dB in sensitivity over the Varian cavity equipped with a radiation window. One can convert the increase in sensitivity to the effective increase in minimum detectable spins for any detection scheme by employing the results of Feher's[16] analysis.

Although time did not permit optimization of the ESR spectrometer for detecting low spin samples, an attempt was made to estimate the minimum detectable spins for this instrument. The weight of DPPH in the 3 mm bore sample tube was determined by subtracting the weight of the empty sample tube from the weight of the tube containing the volume of DPPH. Using the measured weight of 0.387 mg, and the molecular weight of DPPH, the DCR

sample volume is found to contain 0.98×10^{-3} moles. The signal-to-noise ratio for the maximum available microwave input power (80 mW) is 44 dB; thus the minimum detectable number of spins should be approximately 2.4×10^{16}. Because of the priority attached to other measurements, this figure was not confirmed by successive dilutions of DPPH in an appropriate solvent. A single test was run, however, with a 10^{-4} molar solution of DPPH in benzene, and ESR detection was not obtained. For the DCR sample volume (0.32 cc) a 10^{-4} molar solution contains approximately 1.9×10^{16} spins.

The principle limitation on sensitivity for the ESR spectrometer under discussion stems from the relatively high noise figure of the 6 kHz receiver amplifier which employs transistorized circuitry throughout. Since the poor signal-to-noise ratio at 6 kHz is caused by the flicker noise mechanism, which is inversely proportional to frequency, this problem could be circumvented if the modulation circuits were redesigned for 100 kHz. The design of a receiver for minimum noise figure is a formidable task and would have consumed a disproportionately large share of the time available without contributing significantly to the primary goal of optimization of open boundary resonators for use in ESR systems.

V. CONCLUSIONS

The applicability of the open boundary resonator as a tool for the investigation of ESR phenomena has been the subject of a one-year research program at Georgia Tech. Two open boundary resonator types, a dielectric cavity resonator (DCR), and a Fabry-Perot resonator (FPR), have been studied. Both types have been shown to possess a high microwave quality factor, Q, and a favorable geometry for applications involving the study of radiation induced transient radicals.

Prototype dielectric tube resonators were fabricated from two highly dissimilar materials. One, an amorphous synthetic quartz (Spectrosil®), was shown to have a loss tangent which prohibited its use in ESR applications, while the other, a single-crystal synthetic sapphire, exhibited extremely low loss characteristics at the microwave operating frequency. Comparative tests in an ESR spectrometer revealed a 10 dB improvement in signal-to-noise ratio for the sapphire DCR over a commercial Varian TE_{012} waveguide ESR cavity equipped with a radiation window. The applicability of the sapphire DCR to ESR measurements was further demonstrated by measuring the degradation in Q caused by loading the sample holder with a number of different organic solvents. In all cases, the loaded Q was shown to be adequate for the detection of free radical materials which could be dissolved in these solvents.

Tests performed with the Fabry-Perot structure demonstrated its high Q microwave properties and adaptability to ESR sample loading. It was

found, however, that the dimensions of the prototype cavity were such that the pole pieces of the ESR magnet caused perturbations of the cavity field structure which prevented further ESR testing. The microwave tests indicate that this prototype could probably be used with a six-inch pole gap or, alternatively, it is possible that a new set of reflectors could be machined for compatible operation with the four-inch pole gap of the Varian magnet which was employed in the ESR measurements.

These preliminary tests performed during the one-year research program have shown that the open boundary resonator is competitive with the standard closed boundary resonator, and, in addition, possesses a superior geometry for the illumination of ESR samples with electromagnetic radiation extending into the near-ultraviolet. The application of open boundary resonators is a relatively new concept in ESR instrumentation, and the wide variety of sample holding configurations which exist for the closed boundary resonator have not as yet been developed for the open boundary resonator. For example, since cryogenic techniques play such an important role in biological ESR applications, there is an urgent need for the design and development of a cryogenic sample holder for the open boundary resonator. Similarly, the importance of information which can be obtained from the ESR characteristics of functional tissue samples justifies the development of sample holders whose configuration has been optimized to provide the maximum ESR sensitivity for lossy sample-loading. Only through a research program designed to exploit the field configurations of the open boundary resonator in the development of specialized sample holders can the open boundary resonator achieve its full potential.

VI. ACKNOWLEDGMENTS

The work reported herein was made possible by the combined efforts of several key personnel in the Electronics Division. The author is grateful to Mr. J. B. Langley II and Mr. H. L. Bassett for their assistance in performing the microwave and ESR measurements, and to Mr. C. H. Bonham who performed the computer calculations on the dielectric cavity resonator. The efforts of Mr. W. D. Fife, Jr., in the construction of the prototype open boundary resonators and the design of the cavity supporting structure are also gratefully acknowledged.

The interesting and helpful discussions with Dr. J. E. Rhodes on the field configurations and anisotropic behavior of the sapphire tube resonator were of great value. Dr. A. P. Sheppard's continuing interest and technical suggestions on the measurement of cavity Q were also appreciated. Dr. J. J. Heise, of the School of Biology, was instrumental in pointing out the application of microwave technology to the instrumentation needs in ESR spectroscopy and maintained interest in the course of research throughout the project.

Respectfully submitted,

R. G. Shackelford
Project Director

Approved:

A. P. Sheppard, Head
Special Techniques Branch

REFERENCES

1. Zavoisky, E., J. Phys. SSSR 9, 211 (1945)

2. Commoner, B., J. Townsend, and G. E. Pake, Nature 174, 689 (1954)

3. Beinert, H. and G. Palmer, Adv. Enzymol. 27, 105 (1965)

4. Hollocher, T. C., Jr., and B. Commoner, Proc. Nat. Acad. Sci. (U.S.) 47, 1355 (1961)

5. Nebert, D. W., and H. S. Mason, Cancer Res. 23, 833 (1963)

6. Commoner, B., Acad. Roy. Belg., Classe Sci., Mem., Collection in 8°, 33, 114 (1961)

7. Androes, G. M. and M. Calvin, Biophys. J. 2, 217 (1962)

8. Rosenbaum, F. J., Rev. Sci. Inst. 35, 1550 (1964)

9. Boyd, G. D. and J. P. Gordon, B.S.T.J. 40, 489 (1961)

10. Becker, R. C. and Coleman, P. D., Proceedings of the Symposium on Millimeter Waves, Vol. 9, pp. 191-222, Polytechnic Press, New York (1959)

11. Becker, R. C., Technical Report No. 2, Contract No. AT(11-1)-392, Electrical Engineering Research Laboratory, University of Illinois, (1959)

12. Li, T., B.S. T. J., 44, 923, (1965)

13. Goubau, G., and Schwering, F., IRE Trans. Ant. and Prop., AP-9, 248, (1961)

14. Ginzton, E. L., Microwave Measurements, McGraw Hill, New York, N. Y., (1957)

15. VonHippel, A., Dielectric Materials and Applications, The M.I.T. Press, Cambridge, Mass. (1954)

16. Feher, G., B.S.T.J., 36, 449 (1957)

APPENDIX

COMPUTER PROGRAM FOR CALCULATION OF THE DIELECTRIC CAVITY RESONATOR CHARACTERISTIC EQUATION

```
@FOR,IS MAIN
CYCLE 000 COMPILED BY 1201 0057C ON 29 OCT 69 AT 23:26:31.


   MAIN PROGRAM

   STORAGE USED (BLOCK, NAME, LENGTH)

        0001   *CODE   000370
        0000   *DATA   000405
        0002   *BLANK  000000


   EXTERNAL REFERENCES (BLOCK, NAME)

        0003   BESL
        0004   MBSLK
        0005   MBSLI
        0006   NINTR$
        0007   NRDU$
        0010   NIO1$
        0011   NIO2$
        0012   NWDU$
        0013   SQRT
        0014   NSTOP$


   STORAGE ASSIGNMENT  (BLOCK, TYPE, RELATIVE LOCATION, NAME)

    0001   000002 1L        0001   000355 100L      0001   000024 113G      0001   000046 125G      0001   000302 15L
    0001   000320 20L       0000   000517 200F      0000   000340 201F      0000   000345 203F      0000   000365 204F
    0000   000357 205F      0001   000075 3L        0001   000340 30L       0001   000101 4L        0001   000165 5L
    0000 R 000275 A         0000 R 000313 AI0       0000 R 000314 AI1       0000 R 000303 AJ0       0000 R 000304 AJ1
    0000 R 000307 AK0       0000 R 000310 AK1       0000 R 000003 B         0000 R 000301 C         0000 R 000316 DIFF
    0000 R 000273 ED        0000 I 000276 ICOUNT    0000 I 000274 K         0000 R 000000 K1        0000 R 000001 K2
    0000 I 000272 M         0000 I 000270 MN        0000 I 000271 NN        0000 L 000002 PREVLO    0000 R 000135 R
    0000 R 000315 TERM1     0000 R 000311 TERM2     0000 R 000277 TOPI      0000 R 000267 V         0000 R 000300 VIS
    0000 R 000302 W         0000 R 000305 Y0        0000 R 000306 Y1        0000 R 000312 Z


00100     1*   C   THIS PROGRAM EVALUATES THE DESIGN EQUATIONS FOR A DIELECTRIC CAVITY.
00100     2*   C         THE INPUT PARAMETERS ARE:
00100     3*   C              A: THE INSISIDE RADIUS OF THE DIELECTRIC CYLINDER PER
00100     4*   C                 WAVELENGTH
00100     5*   C              B: THE OUTSIDE RADIUS
00100     6*   C              ED: RELATIVE DIELECTRIC CONSTANT
00100     7*   C              V: RATIO OF PROPAGATION VELOCITY TO SPEED OF LIGHT
00100     8*   C              MN: NUMBER OF VALUES OF ED USED
00100     9*   C              NN: NUMBER OF VALUES OF V REMAINING
00100    10*   C         SAMPLE DATA CARDS FOR TWO VALUES OF V AND TWO VALUES OF ED:
00100    11*   C              .95  2  1
00100    12*   C              10.
```

```
00100    13*   C              11.
00100    14*   C              .85  2  0
00100    15*   C              10.
00100    16*   C              11.
00101    17*         REAL K1, K2
00103    18*         LOGICAL PREVLO
00104    19*         DIMENSION B(90), R(90)
00105    20*       1 READ(5,204) V, MN, NN
00112    21*         DO 150 M=1,MN
00115    22*         READ(5,205) ED
00120    23*         WRITE(6,200) ED, V
00124    24*         DO 100 K=1,90
00127    25*         B(K) = .1 + .01*K
00130    26*         IF (R(K) .GT. 90. .AND. K .GT. 1) GO TO 3
00132    27*         A = B(K)
00133    28*         GO TO 4
00134    29*       3 A = B(K-1)*R(K-1) + .01
00135    30*       4 ICOUNT = 0
00136    31*         PREVLO = .FALSE.
00137    32*         TOPI = 6.2831853
00140    33*         VIS = (1./V)**2
00141    34*         K1 = TOPI * SQRT(VIS-1)
00142    35*         K2 = TOPI * SQRT(ED-VIS)
00143    36*         C = K2/K1
00144    37*         W = K2*B(K)
00145    38*         CALL BESL(W, AJ0, AJ1, Y0, Y1)
00146    39*         CALL MBSLK(W, AK0, AK1)
00147    40*         TERM2 = (C * AJ0 * AK1 + AJ1 * AK0)/(C * Y0 * AK1 + Y1 * AK0)
00150    41*       5 R(K) = A/B(K)
00151    42*         ICOUNT = ICOUNT + 1
00152    43*         IF (ICOUNT .GT. 2500) GO TO 30
00154    44*         IF (1./R(K) .LT. .95) A = B(K)-.009
00156    45*         Z = K2*A
00157    46*          CALL BESL(Z, AJ0, AJ1, Y0, Y1)
00160    47*         CALL MBSLI(Z, AI0, AI1)
00161    48*         TERM1 = (C * AJ0 * AI1 - AJ1 * AI0)/(C * Y0 * AI1 - Y1 * AI0)
00162    49*         DIFF = (TERM1 - TERM2)/ABS(TERM2)
00163    50*         IF (ABS(DIFF) .LT. 3.E-2) GO TO 20
00165    51*         IF (DIFF) 10, 20, 15
00170    52*      10 IF (A .LT. .087) A= B(K)-.009
00172    53*         A = A - 0.0005
00173    54*         IF (PREVLO) A = A + 0.0003
00175    55*         GO TO 5
00176    56*      15 IF (A .GT. 1.1) A = B(K)-.009
00200    57*         A = A + 0.00009
00201    58*         PREVLO = .TRUE.
00202    59*         GO TO 5
00203    60*      20 WRITE(6,201) A, B(K), R(K), TERM1, TERM2
00212    61*         GO TO 100
00213    62*      30 R(K) = 100.
00214    63*         WRITE(6,203) A, B(K), R(K)
00221    64*     100 CONTINUE
00223    65*     150 CONTINUE
00225    66*         IF (NN .GT. 0) GO TO 1
00227    67*         STOP
00230    68*     200 FORMAT(1H1, 10X, 3HE =, F6.2, 10X, 5HV/C =, F5.3 /// 11X, 5HA/LAM,
00230    69*       1         10X, 5HB/LAM, 12X, 3HA/B, 19X, 5HTERM1, 15X, 5HTERM2 /)
```

```
00231     70*      201 FORMAT(1H , 3(9X, F7.5), 15X, E10.5, 10X, E10.5)
00232     71*      203 FORMAT(1H , 3(9X, F7.5), 16X, 17HNO SOLUTION FOUND)
00233     72*      204 FORMAT (F6.0, 2I3)
00234     73*      205 FORMAT (F6.0)
00235     74*          END

      END OF COMPILATION:        NO  DIAGNOSTICS.
```

```
@FOR,IS BESL
CYCLE 000 COMPILED BY 1201 08576 ON 29 OCT 69 AT 23:26:39.


   SUBROUTINE BESL      ENTRY POINT 00037B

   STORAGE USED (BLOCK, NAME, LENGTH)

        0001   *CODE   000422
        0000   *DATA   000124
        0002   *BLANK  000000


   EXTERNAL REFERENCES (BLOCK, NAME)

        0003   ALOG
        0004   SQRT
        0005   COS
        0006   SIN
        0007   NERR3$


   STORAGE ASSIGNMENT  (BLOCK, TYPE, RELATIVE LOCATION, NAME)

    0001  000165 20L       0001  000357 30L       0003 R 000000 ALOG      0000 R 000013 CON       0000 R 000016 CON1
    0000 R 000011 F0       0000 R 000014 F1       0000   000111 INJP$     0000 R 000000 PI        0000 R 000012 THT0
    0000 R 000015 THT1     0000 R 000007 TJ       0000 R 000010 TY        0000 R 000001 T1        0000 R 000002 T2
    0000 R 000003 T3       0000 R 000004 T4       0000 R 000005 T5        0000 R 000006 T6


00101    1*          SUBROUTINE BESL(X, AJ0, AJ1, Y0, Y1)
00103    2*          PI = 3.1415927
00104    3*          IF (X .GT. 3.0) GO TO 20
00106    4*          T1 = (X/3.0)**2
00107    5*          T2 = T1*T1
00110    6*          T3 = T2*T1
00111    7*          T4 = T2*T2
00112    8*          T5 = T4*T1
00113    9*          T6 = T3*T3
00114   10*          AJ0 = 1.- 2.2499997*T1 + 1.2656208*T2 - .3163866*T3 + .0444479*T4
00114   11*         1      - .0039444*T5 + .00021*T6
00115   12*          Y0 = (2./PI) * ALOG(0.5*X) * AJ0 + .36746691 + .60559366*T1
00115   13*         1      - .74350384*T2 + .25300117*T3 - .04261214*T4 + .00427916*T5
00115   14*         2      - .00024846*T6
00116   15*          TJ = 0.5 - .56249985*T1 + .21093573*T2 - .03954289*T3 +
00116   16*         1      .00443319*T4 - .00031761*T5 + .00001109*T6
00117   17*          AJ1 = X * TJ
00120   18*          TY = (2./PI) * ALOG(0.5*X) * AJ1 - .6366198 + .2212091*T1 +
00120   19*         1      2.1682709*T2 - 1.3164827*T3 + .3123951*T4 - .0400976*T5 +
00120   20*         2      .0027873*T6
00121   21*          GO TO 30
00122   22*       20 T1 = (3./X)
```

```
00123     23*          T2 = T1*T1
00124     24*          T3 = T2*T1
00125     25*          T4 = T3*T1
00126     26*          T5 = T4*T1
00127     27*          T6 = T5*T1
00130     28*          F0 = .79788456 - .00000077*T1 - .0055274*T2 - .00009512*T3 +
00130     29*         1       .00137237*T4 - .00072805*T5 + .00014476*T6
00131     30*          THT0 = X - .78539816 - .04166397*T1 - .00003954*T2 + .00262573*T3
00131     31*         1       -.00054125*T4 - .00029333*T5 + .00013558*T6
00132     32*          CON = (1./SQRT(X)) * F0
00133     33*          AJ0 = CON * COS(THT0)
00134     34*          Y0 = CON * SIN(THT0)
00135     35*          F1 = .79788456 + .00000156*T1 + .01659667*T2 + .00017105*T3 -
00135     36*         1       .00249511*T4 + .00113653*T5 - .00020033*T6
00136     37*          THT1 = X - 2.35619449 + .12499612*T1 + .0000565*T2 - .00637879*T3
00136     38*         1       + .00074348*T4 + .00079824*T5 - .00029166*T6
00137     39*          CON1 = CON * F1/F0
00140     40*          AJ1 = CON1 * COS(THT1)
00141     41*          Y1 = CON1 * SIN(THT1)
00142     42*       30 RETURN
00143     43*          END

      END OF COMPILATION:        NO  DIAGNOSTICS.
```

```
@FOR,IS MBSLI
CYCLE 000 COMPILED BY 1201 0857C ON 29 OCT 69 AT 23126:45.


   SUBROUTINE MBSLI     ENTRY POINT 000226

   STORAGE USED (BLOCK, NAME, LENGTH)

        0001   *CODE   000246
        0000   *DATA   000064
        0002   *BLANK  000080


   EXTERNAL REFERENCES (BLOCK, NAME)

        0003   EXP
        0004   SQRT
        0005   NERR3$


   STORAGE ASSIGNMENT  (BLOCK, TYPE, RELATIVE LOCATION, NAME)

    0001   000073 10L        0001   000216 20L        0000 R 000011 CON        0000   000054 INJP$      0000 R 000006 T1
    0000 R 000012 TI0        0000 R 000013 TI1        0000 R 000000 T1         0000 R 000001 T2        0000 R 000002 T3
    0000 R 000003 T4         0000 R 000004 T5         0000 R 000005 T6         0000 R 000007 T7        0000 R 000010 T8


00101     1*          SUBROUTINE MBSLI(X, AI0, AI1)
00103     2*          IF (X .GT. 3.75) GO TO 10
00105     3*          T1 = (X/3.75)**2
00106     4*          T2 = T1*T1
00107     5*          T3 = T2*T1
00110     6*          T4 = T2*T2
00111     7*          T5 = T4*T1
00112     8*          T6 = T3*T3
00113     9*          AI0 = 1. + 3.5156229*T1 + 3.0899424*T2 + 1.2067492*T3 +
00113    10*         1       .2659732*T4 + .0360768*T5 + .0045813*T6
00114    11*          TI = 0.5 + .87890594*T1 + .51498869*T2 + .15084934*T3 +
00114    12*         1       .02658733*T4 + .00301532*T5 + .00032411*T6
00115    13*          AI1 = X * TI
00116    14*          GO TO 20
00117    15*       10 T1 = (3.75/X)
00120    16*          T2 = T1*T1
00121    17*          T3 = T2*T1
00122    18*          T4 = T2*T2
00123    19*          T5 = T4*T1
00124    20*          T6 = T3*T3
00125    21*          T7 = T6*T1
00126    22*          T8 = T7*T1
00127    23*          CON = (1./SQRT(X)) * EXP(X)
00130    24*          TI0 = .39894228 + .01328592*T1 + .00225319*T2 - .00157565*T3 +
00130    25*         1       .00916281*T4 - .02057706*T5 + .02635537*T6 - .01647633*T7 +
```

```
00130    26*          2       .00392377*T8
00131    27*           TI1 = .39894228 - .03988024*T1 - .00362018*T2 + .00163801*T3
00131    28*          1       - .01031555*T4 + .02282967*T5  - .02895312* T6
00131    29*          2       + .01787654*T7 - .00420059*T8
00132    30*           AI0 = CON * TI0
00133    31*           AI1 = CON * TI1
00134    32*       20 RETURN
00135    33*           END

      END OF COMPILATION:       NO  DIAGNOSTICS.
```

```
@FOR,IS MBSLK
CYCLE 000 COMPILED BY 1201 0857C ON 29 OCT 69 AT 23:26:52.


   SUBROUTINE MBSLK     ENTRY POINT 000235

   STORAGE USED (BLOCK, NAME, LENGTH)

        0001   *CODE    000287
        0000   *DATA    000063
        0002   *BLANK   000000


   EXTERNAL REFERENCES (BLOCK, NAME)

        0003   MBSLI
        0004   ALOG
        0005   EXP
        0006   SQRT
        0007   NERR3$


   STORAGE ASSIGNMENT  (BLOCK, TYPE, RELATIVE LOCATION, NAME)

    0001   000107 10L        0001   000225 20L        0000 R 000013 A         0000 R 000011 AI0       0000 R 000012 AI1
    0004 R 000000 ALOG       0000 R 000014 B          0000 R 000006 CON       0000   000052 INJP$     0000 R 000007 TK0
    0000 R 000010 TK1        0000 R 000000 T1         0000 R 000001 T2        0000 R 000002 T3        0000 R 000003 T4
    0000 R 000004 T5         0000 R 000005 T6


00101     1*          SUBROUTINE MBSLK(X, AK0, AK1)
00103     2*          IF (X .LT. 2) GO TO 10
00105     3*          T1 = 2./X
00106     4*          T2 = T1*T1
00107     5*          T3 = T2*T1
00110     6*          T4 = T3*T1
00111     7*          T5 = T4*T1
00112     8*          T6 = T5*T1
00113     9*          CON = (1./SQRT(X)) * EXP(X)
00114    10*          TK0 = 1.25331414 - .07832358*T1 + .02189568*T2 - .01062446*T3
00114    11*         1      + .00587872*T4 - .0025154*T5 + .00053208*T6
00115    12*          TK1 = 1.25331414 + .23498619*T1 - .0365562*T2 + .01504268*T3
00115    13*         1      - .00780353*T4 + .00325614*T5 - .00068245*T6
00116    14*          AK0 = CON * TK0
00117    15*          AK1 = CON * TK1
00120    16*          GO TO 20
00121    17*       10 CALL MBSLI(X, AI0, AI1)
00122    18*          A = AI0
00123    19*          B = AI1
00124    20*          T1 = (X/2.)**2
00125    21*          T2 = T1*T1
00126    22*          T3 = T2*T1
```

```
00127    23*          T4 = T3*T1
00130    24*          T5 = T4*T1
00131    25*          T6 = T5*T1
00132    26*          AK0 = - ALOG(0.5*X) * A - .57721566 + .4227842*T1 + .23069756*T2
00132    27*        1       + .0348859*T3 + .00262698*T4 + .0001075*T5 + .0000074*T6
00133    28*          TK1 = X * ALOG(0.5*X) * B + 1. + .1544314*T1 - .67278579*T2
00133    29*        1       - .18156897*T3 - .01919402*T4 - .00110404*T5 - .00004686*T6
00134    30*          AK1 = (1./X) * TK1
00135    31*       20 RETURN
00136    32*          END

      END OF COMPILATION:       NO  DIAGNOSTICS.
```

```
@XQT
29 OCT 69 AT 23:26:58   THE COLLECTOR 1100-0012


ADDRESS LIMITS    001000 011402      040000 044535
STARTING ADDRESS  011013

WORDS DECIMAL      4355 IBANK         2398 DBANK

                SEGMENT MAIN          001000 011402      040000 044535

NSWTC$/FOR          1   001000 001021
NRBLK$/FOR          1   001022 001047
NRWND$/FOR          1   001050 001126      2   040000 040011
NWEF$/FOR           1   001127 001272      2   040012 040031
NBDCV$/FOR                                 0   040032 040226
NFTCH$/FOR          1   001273 001566      2   040227 040265
NFTV$/FOR           1   001567 001611
NCNVT$/FOR          1   001612 002057      2   040266 040352
NCLOS$/FOR          1   002060 002213      2   040353 040377
NWBLK$/FOR          1   002214 002337
NBSBL$/FOR          1   002340 002375
NUPDA$/FOR          1   002376 002402
NBF00$/FOR                                 2   040400 042601
NCBD$/FOR           1   002423 002506      2   042602 042612
NOTIN$/FOR          1   002507 003023      2   042613 042617
NOUT$/FOR           1   003024 003756      2   042620 042647
NININ$/FOR          1   003757 004174      2   042650 042670
NINPT$/FOR          1   004175 005047      2   042671 042711
NFMT$/FOR           1   005050 005753      2   042712 042730
NIOER$/FOR          1   005754 006031      2   042731 043005
NFCHK$/FOR          1   006032 006620      2   043006 043135
                                           4   043136 043206
NTAB$/FOR                                  2   043207 043245
ERU$
NSTOP$/FOR          1   006621 006643      2   043246 043253
NOBUF$/FOR          1   006644 006706
NIER$/FOR           1   006707 006770      2   043254 043401
NIBUF$/FOR          1   006771 007042
NINTR$/FOR          1   007043 007077      2   043402 043420
SINCOS$/FOR         1   007100 007156      2   043421 043437
NERR$/FOR           1   007157 007503      2   043440 043557
SQRT$/FOR           1   007504 007546      2   043560 043566
EXP$/FOR            1   007547 007614      2   043567 043607
ALOG$/FOR           1   007615 007643      2   043610 043635
BLANK$COMMON (COMMON BLOCK)
MBSLK               1   007644 010122      0   043636 043720
                                           2   BLANK$COMMON
MBSLI               1   010123 010370      0   043721 044004
                                           2   BLANK$COMMON
```

```
BESL                    1   010371 011012      0   044005 044130
                                               2   BLANK$COMMON
MAIN                    1   011013 011402      0   044131 044535
                                               2   BLANK$COMMON

SYS$*RLIB$. LEVEL 33
END OF COLLECTION - TIME 0.946 SECONDS
```